Diabetes-Associated Metabolic Stress on the Regulation of Endothelial Nitric Oxide Synthase Content and Mitochondrial Function

By

Manoj Mohan Mohanan Nair

A thesis submitted to the Faculty of Graduate Studies of
The University of Manitoba
in partial fulfillment of the requirements for the degree of

MASTER OF SCIENCE

Department of Physiology& Pathophysiology
Faculty of Health Sciences
University of Manitoba
Winnipeg, Canada

Abstract

Nitric oxide (NO), a vasoprotective and ubiquitous signaling molecule generated from the endothelial cells (EC) by the enzyme endothelial nitric oxide synthase (eNOS) have a vital role in regulation of vascular function and integrity. However, a significant attenuation of eNOS and NO leads to endothelial dysfunction (ED) and increased risk of cardiovascular disease (CVD) in diabetes. Lipoproteins particularly LDL, undergo glycation in diabetic patients and turns it into pro-atherogenic glycated LDL (glyLDL). However, the impact of glyLDL on eNOS, the transmembrane signalling events, involvement of mitochondrial and endoplasmic reticulum (ER) stress in EC remains unclear. Also, literatures reveal impaired platelet mitochondrial function in diabetes patients; however, the impact of family history of diabetes on platelet mitochondrial bioenergetics still remains unknown. In the present study, we had provided the evidence for diabetes-associated metabolic stress involving glyLDL can attenuate eNOS protein, gene and activity in EC, as well as glyLDL and high glucose attenuates eNOS content in EC. Receptor of advanced glycation end products (RAGE) and H-Ras pathway are implicated in the upstream signalling events in the downregulation of eNOS in EC. In addition, ER stress, impaired mitochondrial function due to significant reduction of complex-specific oxygen consumption and bioenergetics were identified in glyLDL-treated EC. Further, we have also detected significant impairment in platelet mitochondrial bioenergetics in healthy individuals with familial history of diabetes. Identifying the mechanisms involved in diabetes associated metabolic stress induced signaling in EC and early detection of mitochondrial impairment in healthy individuals will help to find new targets for the prevention and treatment of diabetic cardiovascular complications and improve quality of life in diabetic patients.

Acknowledgements

First and foremost, I would like to thank Almighty GOD for his blessings, wisdom, peace of mind, good health and gift of life. Next, I sincerely express my gratitude and thanks to my supervisor, Dr. Garry X Shen for his encouragement, guidance, insightful criticisms and support from the initial to the final level which enabled me to successfully complete my Master degree in Physiology and Pathophysiology at the University of Manitoba. This work would not have been possible without his keen interest in the experimental design, attention to detail and enthusiasm for research. In addition, he is approachable and willing to help his student with research.

I owe my deepest gratitude and thanks towards the distinguished members of my advisory committee, Dr. Mohammed Moghadasian, Dr. Suresh Mishra and Dr. Jiuyong Xie for their valuable guidance, support, incisive criticism, thoughtful discussions and approval of my work. I thank Dr. Peter A Cattini, Head of the Department, Physiology and Pathophysiology for his advice and direction throughout the program. I would like to thank my labmates and collaborators for their help throughout this work, Dr. Rouzhi Zhao, Dr. Xueping Xie, Dr. Subir Roy Chowdhury and Dr. Paul Fernyhough. I would like to thank the members of Diabetes Research Group including, Dr. Nyomba, Dr. Sudharshana Rao Ande, Dr. Hoa Nguyen, Dr. Xing-Hai Yao, Dr. Pauline Padilla-Meier, Ms. Lori Berard and Ms. Teresa Anderlic for their valuable support, technical help and love. Moreover, I express my sincere gratitude to Ms. Gail McIndless and Ms. Judith Olfert for their administrative support.

I am thankful to Dr. Preshan Chelikani, Dr. Rajinder Bhullar for their helpful discussions in certain stages of my research. I deeply acknowledge and sincerely thank Dr. Asok Kumar K,

Dr. Uma Maheshwari, Dr. Manjula Devi, Dr. Manoj Kumar P, Dr. Prasanth Puthenveetil, Dr. Thanga Mariappan, Dr. Geetha Thanga, Dr. T.K Ravi and my friends in Winnipeg and from India for their valuable support and love throughout my duration of study.

I am indebted to my father, Mr. Mohanan Nair and my mother, Mrs. Nalina Kumari (retired teachers) for their unconditional love, care and inseparable support throughout my life that helped me to be what I am now. I am ever grateful to my younger brother Mr. Krishna Mohan for his support, love, and confidence in me. I also sincerely thank my parents-in-law Prof. Somasekharan Unnithan and Usha Devi for their constant support and love during the course of my study. Last but not the least; I wholeheartedly express my appreciation to my wife, Rakendu Ushadevi for her dedication, love, persistent confidence and support through out my studies in University of Manitoba.

I am grateful to the financial support from International Graduate Student Entrance Scholarship (IGSES), International Graduate Student Scholarship (IGSS), Section of Endocrinology & Metabolism (University of Manitoba). I am thankful to the Canadian Diabetes Association (CDA) for providing me the travel grant to attend the 2014 CDA conference.

DEDICATION

I dedicate this thesis work

to my dear grandparents, dad, mom, and brother

to my family members

moreover, to my beloved wife

For all their constant support and unconditional love

Table of Contents

List of Tables

List of Figures

List of Abbreviations

AA	antimycin A
ADP	Adenosine monophosphate
AGEs	advanced glycation end products
ANOVA	analysis of variance
Apo-B	apolipoprotein B-100
ATP	adenosine triphosphate
ATCC	American Type Culture Collection
BMI	body mass index
BSA	bovine serum albumin
CAD	coronary artery disease
CVD	Cardiovascular disease
cAMP	cyclic adenosine monophosphate
cGMP	Cyclic guanosine monophosphate
CPDA 1	Citrate phosphate dextrose adenine 1
C_T	cycle threshold
cyt *c*	cytochrome *c*
°C	degree centigrade
cDNA	complementary deoxyribonucleic acid
Dig	digitonin
DM	diabetes mellitus
DMEM	Dulbecco's modified eagle medium
DMSO	dimethyl sulfoxide
EtOH	ethanol
EC	endothelial cells
ED	endothelial dysfunction
ECL	enhanced chemical luminescence
EDRF	endothelial derived relaxing factor
EDTA	ethylenediamino-tetra-acetic acid
eNOS	endothelial nitric oxide synthase

ER	endoplasmic reticulum
ETS	electron transport system
ETC	electron transport chain
ERK-1/2	extracellular signal-regulated kinase-1/2
EPC	endothelial progenitor cell
FAD	flavoprotein or Flavin adenine dinucleotide
$FADH_2$	substrates from citric acid cycle
FBS	fetal bovine serum
FCCP	carbonylcyanidep-trifluoromethoxyphenylhydrazone
FTI	farnesyltransferase inhibitors
GDP	guanine dinucleotide phosphate
glyLDL	glycated LDL
GTP	guanine trinucleotide phosphate
HDL	high-density lipoprotein
H-Ras	Harvey rat sarcoma
HRP	horseradish peroxidase
h	hour
Hsp	heat shock proteins
HUVEC	human umbilical vein endothelial cell
HCl	hydrochloride
IgG	immunoglobin G
IM	inner membrane
JNK	c-Jun-N-terminal kinase
KCl	potassium chloride
KCN	potassium cyanide
KLF	Krupple like factor
kDa	kilo-dalton
LDL	low-density lipoprotein
LDLR	LDL receptor
LP(a)	lipoprotein (a)
MAPK	mitogen-activated protein kinase

MEK	MAP kinase kinases ½
MiR medium	mitochondrial respiratory medium
mg/ml	miligram per mililitre
ml	millilitre
mM	milimolar
mmol/L	millimolar per liter
min	minute
mtDNA	mitochondrial DNA
mETC	mitochondrial electron transport chain
mRNA	messenger ribonucleic acid
NAD^+	nicotinamide adenine dinucleotide
NADPH	reduced nicotinamide adenine dinucleotide phosphate
NF-κB	nuclear factor κB
NO	nitric oxide
NOS	Nitric oxide synthase
OCR	oxygen consumption rate
OM	outer membrane
O_2	oxygen
oxLDL	Oxidized LDL
PAEC	porcine aortic EC
PAGE	polyacrylamide gel electrophoresis
PAI-1	plasminogen activator inhibitor-1
4-PBA	4-phenylbutyric acid
PCR	polymerase chain reaction
pERK-1/2	phosphorylated extracellular-signal regulated kinase-1/2
PI3K	phosphatidylinositol 3-kinase
PKC	protein kinase c
PRP	platelet rich plasma
PVDF	polyvinylidene fluoride
P value	probability value
PBMC	Peripheral blood mononuclear cells

RAGE	receptor for advanced glycation end products
RCI	respiratory control index
RNA	Ribonucleic acid
RNS	reactive nitrogen species
ROS	reactive oxygen species
SD	standard deviation
rpm	revolutions per minute
SDS	sodium dodecyl sulphate
SR	scavenger receptors
SMC	smooth muscle cells
SDS	sodium dodecyl sulphate
T2DM	type 2 diabetes mellitus
TBS-T	tris-buffered saline with Tween 20
TMPD	N,N,N',N'-tetra methyl-p-phenylenediamine dihydrochloride
TNBS	2,4,6-trinitrobenzenesulfonic acid
Tris HCL	tris hydrochloride
TLR	toll like receptor
tPA	tissue-plasminogen activator
UCPs	uncoupling proteins
uPA	urokinase-plasminogen activator
UPR	Unfolded protein response
µg/ml	microgram per mililitre
µl	microlitre
µM	micro-molar
µmol/l	micro molar per litre
VLDL	very low-density lipoprotein
VSMC	vascular smooth muscle cell
WHO	world health organization

Chapter 1

Introduction

Cardiovascular disease complications are the primary cause of deaths in diabetes patients (Warboys et al., 2011). In Canada, cardiovascular complications account for one-third of the mortality of the individuals (Genest et al., 2009). World Health Organization (WHO) estimates about 17.3 million people died due to cardiovascular disorders (CVDs) in year 2008, among which, 7.3 million were due to atherosclerotic coronary artery diseases (CAD). It is predicted that the cardiovascular mortality will alarmingly rise to 25 million by year 2030. Diabetes alone has contributed to 1.3 million deaths (WHO., 2011). Diabetes increases the risk for cardiovascular disease for 2-4 times. CVD complications can be reduced by 20-50% by tight control of low-density lipoprotein (LDL)-cholesterol (CDCP., 2011).

Glycation and oxidation increase the atherogenic potential of lipoproteins (Bierman, 1992). LDL glycation is associated with the acceleration of atherosclerosis in diabetes. Elevated levels of glycated LDL (glyLDL) can be detected in diabetic patients (Lyons, 1993). Endothelium produces the regulatory mediators related to vascular function such as nitric oxide (NO), adhesion molecules, plasminogen activator inhibitor-1 (PAI-1) and cytokines. Endothelial nitric oxide synthase (eNOS) regulates the nitric oxide (NO) production from EC (Quyyumi, 1998). Oxidative stress is linked to impaired NO bioactivity and endothelial function (Stocker and Keaney, 2004).

Endothelial dysfunction detected in diabetic patients is diagnosed with reduced NO-mediated vasodilation (Wautier et al., 2001). GlyLDL attenuated shear stress induced NO production and impaired LDL clearance through the low density lipoprotein receptor (LDLR) on EC (Posch et al., 1999). Oxidized LDL (oxLDL) was observed to decrease eNOS protein and

increase reactive oxygen species (ROS) in EC (Luciano et al., 2000). Calpain activation by oxidized or glycated LDL raised eNOS degradation in EC (Dong et al., 2009). Glyco-oxidized LDL impaired endothelium more potently compared to oxLDL and reduced vasodilation due to increased superoxide formation (Chikani et al., 2004).

Glycated high density lipoprotein (HDL) was observed to induce apoptosis in EC due to mitochondrial dysfunction (Matsunaga et al., 2001). Damage or reduced mitochondrial DNA or copy number is related to mitochondrial dysfunction in diabetes (Rolo and Palmeira, 2006). Alterations in the endoplasmic reticulum (ER) Ca^{2+} cause ER stress leading to ROS formation and reduced mitochondrial electron chain (mETC) transport proteins that are the primary enzymatic components of ROS production (Leem and Koh, 2012). ER stress in EC may be an significant contributor to diabetes-associated vascular complications (Basha et al., 2012).

Relationships between endothelial dysfunction and mitochondrial dysfunction remain largely unexplored. This thesis work aims to investigate and to understand the mechanism for diabetes associated metabolic stress-induced cardiovascular complications. The translational studies involving human platelets from healthy subjects were carried out to determine the feasibility and potential application of a clinically feasible method to detect early abnormalities in mitochondrial function in the platelets of individuals with risk of diabetes.

Chapter 2

Literature review

2.1 Atherosclerosis

Atherosclerosis is characterized by the cholesterol accumulation in the macrophages of medium-sized and large arteries and is considered as the major cause for mortality in diabetes. The risk of coronary atherosclerosis is 3-5 folds greater in the diabetes patients than non-diabetics. Diabetes is a major factor contributing to the development of atherosclerosis. Atherosclerosis is stimulated by the genetics and environmental factors. The events associated with the pathogenesis of the atherosclerosis are complex (Stocker and Keaney, 2004). Loss of bioactivity of NO and ROS is the principal feature of atherosclerosis. Endothelial dysfunction directly contributes to atherosclerosis and a lower level of cofactor tetrahydrobiopterin (BH_4) is often detected in atherosclerosis (Alp et al., 2004). Increased levels of LDL in the plasma promote deposition of cholesterol in the arteries, which forms the principal risk factor for atherosclerosis (White et al., 2008). Endothelial dysfunction including impaired endothelium-derived vasodilation initiates the vascular inflammation and atherogenesis process. The lipoprotein retention in the arterial wall is linked to the modified apolipoprotein B-100 (apoB)-100 derived lipoproteins. Proteoglycans have an important role in retaining the apoB lipoproteins in initial phase of atherosclerosis (Stocker and Keaney, 2004). Atherosclerosis is considered as a lipid driven chronic inflammatory disease with the accumulation of lipids and inflammatory mediators in the arteries (Warboys et al., 2011). The disrupted integrity of EC has a significant role in the atherosclerosis progression (Hamuro et al., 2002). Accelerated atherosclerosis in diabetes is due to alteration in the vascular cell function and a response to the interaction with glycated lipids and proteins in plasma. ApoB is a specific protein which is mostly prone to

undergo glycation in diabetes (Toma et al., 2011). NO, is the primary contributor and regulator of vascular tone, and is also involved in different pathways in atherogenesis and vascular dysfunction. The anti-atherogenic and vascular protective effects of eNOS are deteriorated by OxLDL. OxLDL amplifies the glyco-oxidation and facilitates the atherogenesis and affecting the vascular function. Glycation enhances oxidation and accelerates atherosclerosis (Napoli et al., 2002). Accumulated lines of evidence suggest endothelial dysfunction as an initial event in the atherosclerosis progression (Sitia et al., 2010).

2.2 Diabetes

Diabetes mellitus (DM) is a metabolic disorder characterized with hyperglycemia and reduced secretion or insulin receptor insensitivity. DM is broadly classified as type 1 DM, characterized by diminished production of insulin; type 2 DM characterized by impaired β-cell function and insulin resistance and finally diabetes occurring first time during pregnancy known as gestational diabetes. Type 1 DM accounts only 10 % of DM, and type 2 DM represents vast majority of diabetes with explosively increasing prevalence during last 30 years (Rolo and Palmeira, 2006).

Diabetes is linked with increased macrovascular complications and microvascular complications. CAD, cerebrovascular and peripheral vascular diseases are included in macro vascular complications. Nephropathy, retinopathy and neuropathy are included in the microvascular complications in diabetes (Beckman et al., 2002). Diabetes damages normal cellular functions in EC, smooth muscle cells (SMC), and platelets. Endothelial dysfunction has been detected in diabetes patients (Beckman et al., 2002; Schmidt and Stern, 2000)

Hyperglycemia is an important factor for the progression of endothelial dysfunction in diabetes. Several markers of endothelial impairment have been detected in type 2 DM. Type 2

DM is independently linked with the flow-mediated vasodilation (Hadi and Suwaidi, 2007). Diabetic dyslipidemia is associated with raised triglycerides (TG), chylomicrons, very low-density lipoproteins (VLDL), or LDL and low levels of HDL-cholesterol (Shen, 2003). Atherogenic mechanisms in diabetes include, dyslipidemia (apoprotein and lipoprotein abnormality), glycation and advanced glycation of proteins, oxidation and glycooxidation, foam cell formation and the procoagulant state (Bierman, 1992).

2.3 LDL and glyLDL

The LDL-cholesterol levels in plasma and the accelerated atherosclerosis is positively co-related. LDL transports the cholesterol in the blood. Cholesterol, triglyceride, phospholipids and apoB are the major components in LDL. Impaired LDLR restricts the LDL clearance from the circulation and results in increased LDL in circulation. Deposition of LDL on the arterial walls is the major factor for the atherosclerosis development (Stocker and Keaney, 2004).

The apoB, recognition site on LDL surface supports the interactions with receptors on the cell membrane. Abnormalities in the LDL structure due to oxidation or glycation decreases its uptake by the LDLR (Tozer and Carew, 1997). Increased levels of glyLDL detected in circulation enhance the complications in CVD (Steinberg, 1987).

Hyperglycemia increased the non-enzymatic glycation in apoB of LDL and amino acid, lysine undergoes major glycation. Glycated apoB levels are significantly found increased in diabetic patients. Glycation of LDL turns it atherogenic. Small dense LDL was noted to be more susceptible to glycation than buoyant LDL (Younis et al., 2009). Glycation can be induced by reactive sugars, and LDL is observed to contain rich in glycated apoB. GlyLDL prepared *in-vitro* and glyLDL obtained from diabetic patients attenuated the eNOS expression and triggered apoptosis in EC. Also circulating glyLDL levels in the healthy subjects were relatively higher

than oxLDL (Soran and Durrington, 2011). LDL is also observed to undergo glycation in the vessel intima and accumulates in the sub-endothelial layer (Sima and Stancu, 2002). Glycation is the non-enzymatic irreversible reaction, where the susceptible amino acid lysine interacts with glucose and forms stable products termed "Maillard" reaction or browning. Metabolic abnormalities due to glyLDL accelerate the atherosclerosis process in diabetes. Glycation and oxidation increase collagen cross linking and cause abnormal vascular tone and rigidity that leads to endothelial injury (Lyons, 1993; Tames et al., 1992).

Proteins and DNA are glycated *in-vitro* and *in-vivo* to form AGEs. Diabetic plasma contains increased glucose that over time reacts with the amino group of proteins, mostly in arginine and lysine residue to form glycated intermediates. These intermediates are collectively known as AGEs. The first glycation product determined clinically was glycated hemoglobin (HbA_1c); which is an established marker for diabetes (Akhter et al., 2013). Hyperglycemia promotes formation of AGEs by the non-enzymatic glycation of lipids and proteins (Ramasamy et al., 2005). The glycation can cause secondary damage to the biomolecules like lipids, nicotinamide adenine dinucleotide hydrogen phosphate (NADPH), and enzymes and has a vital role in the progression of diabetes associated complications (Morgan et al., 2002).

Glycooxidation of LDL stimulates atherogenesis in DM through MAPK-ERK/JNK pathway (de Nigris et al., 2012). Diabetic LDL from diabetic patients reduced the shear stress mediated NO production and glyLDL is a major risk factor for endothelial dysfunction and atherosclerosis in diabetes (Posch et al., 1999). Study from our lab and others have previously shown that glyLDL stimulated superoxide release from the endothelium or from EC (Posch et al., 1999; Zhao and Shen, 2005). This evidence indicates that the lipoprotein glycation has a significant role in the development of diabetes-associated cardiovascular complications.

2.4 CVD

Cardiovascular disease is identified as the major cause of deaths among diabetics. Raised glyLDL levels are commonly detected in uncontrolled diabetic patients, and the risk of developing cardiovascular complications is 2-6 folds higher in diabetes (Ren et al., 2002; Zhang et al., 1998). Plaques formed in arteries are the major pathological cause of CAD (Warboys et al., 2011). Diabetic coronary arteries show a significant reduction of the relaxation response to acetylcholine and the hyperglycemic condition predisposes to atherosclerotic CAD. The impaired endothelial function and inability to produce NO has been implicated as an early event in CAD risk. Increased oxidative and nitrosative stress has been associated with decreased NO and peroxynitrite generation in aortic and coronary vessels (El-Remessy et al., 2010). Mechanisms involved in diabetes-associated impairment in vascular relaxation remains unclear.

2.5 NO and eNOS

NO was discovered in early 1772 by Joseph Priestly. It was found *in vivo* as a transparent gas with a lifetime of 6-10 seconds. Exposure of NO to the bovine aortic coronary artery strips led to the discovery of vascular smooth muscle relaxation property of NO in 1979. Later during 1980, Furchgott has discovered the endothelium-derived relaxing factor (EDRF) response to acetylcholine in EC. In 1987, in a separate study by Ignarro *et.al* and Moncada *et.al* proved that EDRF is NO (Yetik-Anacak and Catravas, 2006). The role of NO as EDRF was the topic for 1998 Nobel Prize in Physiology or Medicine (Huang, 2009).

The endothelium due to its unique location in the internal lining of entire blood vessels acts as a selective barrier between blood and the SMC. It controls the nutrients, hormones and macromolecules transport into the underlying tissue. Intact endothelium ensures fluidity of blood and limits blood coagulation. It helps in vascular tone regulation by producing both vasodilators

and vasoconstrictors like NO and endothelin-1 (Bakker et al., 2009). In addition to vasodilation, NO prevents platelet aggregation, SMC proliferation and inflammation (Schalkwijk and Stehouwer, 2005). eNOS, also suppress SMC proliferation, modulates leukocyte-endothelial interaction and thrombosis (Huang, 2009).

Chromosome 7 encodes the eNOS gene and it contains 26 exons that encode a mature mRNA with 4052 nucleotides that further get translated to 1,203 amino acids (140 kDa) and 25 introns. eNOS is an oxidoreductase which catalyzes the reaction between L-arginine and NADPH to form NO and NADP+. Dimeric form is the active form of eNOS, and its enzyme activity is activated by shear stress and receptor-mediated signaling. Calcium/calmodulin and heat shock protein (hsp90) mediate the eNOS activation while caveolin-1, nitric oxide synthase interacting protein, nitric oxide synthase trafficking inducer inhibits the eNOS activation (Jamaluddin et al., 2014). Multiple splice variants and isoforms exist for NOS in different cellular compartments for performing different cellular functions. eNOS localized at the cell membrane enables the β-adrenergic mediated force production. NO produced endogenously from the endothelium influences the tissue oxygen consumption and controls the respiration at the level of cytochrome *c* oxidase. Peroxynitrite irreversibly reduced the mitochondrial respiration by release of iron from iron-sulfur centers. NO in sarcoplasmic reticulum performs the calcium homeostasis that ultimately controls the cardiac contractility (Stocker and Keaney, 2004).

eNOS requires the dimerization and intracellular caveolae localization. eNOS can undergo phosphorylation at Ser-1177 by Akt kinase and other kinases. NO can be inactivated by the interaction of superoxide to form peroxynitrite. Superoxide is formed from the uncoupling of eNOS or by NADPH oxidase. Thus, multiple mechanism simultaneously can cause endothelial dysfunction, causing a reduction of bioavailable NO, which otherwise safeguards the vessels

from molecular events leading to atherosclerosis (Huang, 2009). Human eNOS activity is controlled at multiple phosphorylation sites such as Ser-1177 which activates eNOS and Thr-495 inhibits eNOS activity (Jamaluddin et al., 2014).

eNOS is predominant isoform of NOS which is accountable for the production of vasoprotective molecule NO (Forstermann and Munzel, 2006). It helps in maintaining the vascular tone & integrity. This gaseous radical diffuses into the extracellular compartments and targets its action in the underlying SMC and circulating blood platelets (Wu, 2002). This vascular NO activates the soluble form of guanylyl cyclase, which subsequently activates the cyclic guanosine monophosphate (cGMP) in SMC. NO has a vital role as an anti-platelet aggregator, inhibitor of adhesion, DNA synthesis, mitogenesis and SMC proliferation. Hence, it acts as an essential anti-atherogenic molecule in multiple aspects (Forstermann and Munzel, 2006). NO activates the soluble guanylate cyclase and elevated cGMP level that accounts for the vascular smooth muscle relaxation effects. NO binds with its receptor heme group of the guanylate cyclase to promote enzyme activation and stimulation of cGMP (Ignarro, 1989). The enzymatic cofactors for eNOS include flavine adenine dinucleotide (FAD), flavin mononucleotide (FMN), and tetrahydrobiopterin (BH_4). The BH_4 synthesis is rate limited by guanosine 5'- triphosphate cyclohydrolase. The absence of this enzyme can cause uncoupled eNOS producing more superoxide anions (Huang, 2009). These evidence specify that, eNOS is a crucial factor involved in endothelial dysfunction and pathogenesis of cardiovascular diseases.

NO has a vital role in vascular homeostasis. EC are paracrine organs that regulate vascular contractions and relaxations, apoptosis or cell proliferation, platelet and leukocyte functions. Among the various endothelial-derived factors, NO and prostacyclin are studied extensively due to their crucial role in vascular physiology as vasodilators that maintain vascular

homeostasis. However, their regulation in vascular physiology in diabetes remains unclear. NO prevents constriction of the coronary arteries, inhibits platelet aggregation, expression of adhesion molecules and the release/action of vasoconstrictor, endothelin-1 (Michel and Vanhoutte, 2010). The transcription factor, Krupple like factor 2 (KLF-2), is considered as a vital factor which regulates the eNOS promoter that inhibits the endothelin-1 (Martínez-Fernández et al., 2014). KLF-2 is claimed to have a significant role in maintaining the vascular homeostasis. KLF-2 regulates eNOS and PAI-1, and is expressed highly in the endothelium. LDL down-regulates the KLF-2 expression by DNA and histone methylation, leading to dysfunctional and hypercoagulable endothelium. KLF-2 plays a critical role in maintaining an anti-inflammatory and anti-thrombotic endothelial surface by upregulating eNOS and down-regulating PAI-1 transcriptionally. Recent reports suggest LDL exposure down-regulates KLF-2 in EC (Kumar et al., 2013).

NO-dependent vasodilation is the primary mechanism by which the vascular tone and integrity is regulated. Impairment of eNOS activity leads to the pathophysiological alterations in the vascular homeostasis causing diabetic vascular complications, atherosclerosis and hypertension (Rafikov et al., 2014). Uncoupling of eNOS has been clinically associated with diabetes, hypertension and atherosclerosis (Li et al., 2014). Impairment of endothelial NO production may lead to insulin resistance in type 2 DM. Oxidative stress and diabetes is likely to have a genetic correlation. The eNOS gene at chromosome 7q36 was reported to exhibit polymorphism. The eNOS Glu298Asp polymorphism was associated with attenuated basal NO production (Banerjee and Vats, 2013). Clinical studies have shown that, supplementing BH_4 could improve endothelium-dependent vasodilation in Type 2 DM (Heitzer et al., 2000).

Endothelial dysfunction broadly implies the attenuated nitric oxide and the imbalance of the relaxing and contracting factors in endothelium. It is an important factor involved in the abnormalities associated with atherosclerosis, diabetes, hypertension and aging (Wautier and Schmidt, 2004). eNOS uncoupling is accountable for the endothelial dysfunction, reduced function and number of endothelial progenitor cells (EPC) in diabetes. Attenuated NO production in EPC is due to AGEs-induced apoptosis mediated by MAPK signaling (Shen et al., 2010).

2.6 RAGE

Increased glucose cause non-enzymatic glycation of proteins, lipids, and nucleic acids. Proteins that contain more lysine and arginine are prone to modification (Rabbani et al., 2010; Ramasamy et al., 2005). RAGE was observed on the surface of vascular cells. Studies in our lab have previously shown an increased RAGE expression in porcine aortic EC (PAEC) due to treatment with glyLDL (Sangle, Zhao, et al., 2010). RAGE is a receptor on the cell surface (Neeper et al., 1992). RAGE was observed as a signal transduction receptor which regulates production of ROS (Ramasamy et al., 2005).

RAGE is involved in catabolism or excretion of damaged, senescent tissue and in the regulation of signal transduction pathways. RAGE is observed to be upregulated in diabetic lesions (Cipollone et al., 2003). RAGE activation leads to a cascade of intracellular signaling pathways. RAGE is observed to activate PI3K/Akt and MAP kinases (Stern et al., 2002). RAGE overexpression is associated with the increased inflammation in human diabetic atherosclerotic plaques. RAGE inhibition can prevent diabetes-associated vascular dysfunction (Wautier and Schmidt, 2004). The significance of RAGE in glyLDL-stimulated eNOS downregulation in EC remains unclear.

2.7 Small G-proteins

The small G-proteins are the biological switches acting as major signaling molecules for various cellular processes. It can be broadly classified into five families based on their structure and functions as Ras, Rho, Rab, Sar1/Arf, and Ran (Takai et al., 2001). Ras has isoforms, such as H-Ras, N-Ras and K-Ras. H-Ras is widely distributed in tissues modulating signals through membrane receptors and signal transduction pathways. Ras is regulated by the guanine-nucleotide-exchange factors by post-translational modification of Ras proteins in presence of farnesyltransferase as a catalyst (Stephens et al., 2001; Takai et al., 2001). The translocation of Ras to the plasma membrane from cytosol depends on the farnesylation (Zhang and Casey, 1996). Studies previously conducted have shown that H-Ras activates intracellular ROS production in EC. Small G-proteins are considered as therapeutic targets in cardiovascular diseases (Ohtsu et al., 2006).

Small G-proteins, Ras and Rho mediate the membrane receptor activation (Puddu et al., 2005; Ruiz-Velasco et al., 2004). H-Ras activation was observed in oxidative stress in EC treated with glucose (Kowluru et al., 2004). Activation of H-Ras and translocation of membrane was observed on human EC treated with LDL (Zhu et al., 2001). H-Ras activation regulates and activates transcription factor, NF-κB. Studies in our lab have shown that glyLDL significantly raised the abundance of H-Ras in the membrane fraction in EC (Sangle, Zhao, et al., 2010). The significance of H-Ras translocation and related signaling in glyLDL-stimulated downregulation of eNOS required to be further investigated.

2.8 ER stress

ER is a significant cellular organelle responsible for the function of biosynthesis and protein folding. The pathological and physiological factors may hinder the function of ER to

elicit ER stress in the cells. Unfolded protein response (UPR) constitutes a signaling cascade due to ER stress. ER helps the protein to become functional by proper folding and rendering it active, which is essential for cell survival (Fonseca et al., 2009).

ER stress is detected in dead retinal EC, experimental diabetic retinopathy and on exposure of the retinal EC with heavily oxidized glycated LDL (HOG-LDL). HOG-LDL induced the phosphorylation of eIF2α, nuclear translocation of ATF6 and increased GRP78. Moreover, mRNA levels of XBP-1 and CHOP were found to be increased in pericytes incubated with HOG-LDL. Similarly oxLDL is also observed to induce ER stress in retinal EC. ER is a sensor for cellular stresses (Fu.; et al., 2012). UPR has four distinct responses:

1) molecular chaperones upregulation 2) translational attenuation 3) ER-associated protein degradation and 4) apoptosis. The three important regulators involved are inositol requiring 1 (IRE1), PKR-like kinase (PERK), and activating transcription factor 6 (ATF6). Other components like IRE1-JNK, CHOP, and GSK3β also contribute to ER stress signaling (Fonseca et al., 2009). An increased ER stress due to glyLDL exposure on HUVEC increased the accumulation of misfolded proteins and UPR mediators, GRP78/94, XBP-1 and CHOP in EC (Xie and Shen, 2014). The role of ER stress and related signaling mechanism in glyLDL-stimulated reduction of eNOS further remains to be determined.

2.9. Mitochondrial electron transport function/activity

Mitochondrial dysfunction has a vital role in the diabetes pathogenesis. Increased ROS production and mitochondrial dysfunction has been associated with diabetes and CAD (Xie et al., 2010). Mitochondria forms the primary source of energy in cells through the oxidative phosphorylation in the ETC. ATP is the primary source of energy in the cells. Mitochondrion has an extrenal membrane and internal membrane. ETC is composed of 4 types of enzymatic complexes present at the inner mitochondrial membrane. Complex I is the NADH-ubiquinone dehydrogenase, Complex II is the succinate cytochrome *c* reductase, Complex III is the ubiquinone cytochrome *c* reductase, Complex IV is the cytochrome c oxidase and Complex V is the ATP synthase (Madamanchi et al., 2005).

Complex I and Complex III are the major source for production of ROS in ETC (Turrens, 2003). The electron formed from FADH2 by Complex II passes through the reverse electron transport into the Complex I and generates ROS in mitochondra (Liu et al., 2002). NO and superoxide interaction produces peroxynitrite, which may cause enzyme inactivation, DNA damage, and mitochondrial dysfunction (Ballinger et al., 2000). Mitochondrial superoxide generation occurs mostly in Complex I and III. Increased superoxide production has been associated with the glycosylation in vascular cells (Stocker and Keaney, 2004). The dysfunction in Complex IV affects ATP production and stimulate ROS production (Atamna et al., 2001).

Increased ROS production in mitochondria, mitochondrial DNA damage, respiratory chain dysfunction, proliferation and apoptosis of vascular smooth muscle cells are associated with atherosclerosis and dysfunction in endothelial cells (Madamanchi and Runge, 2007). However, mitochondrial dysfunction in EC treated with glyLDL requires further investigation.

2.10 Diabetes and assessment of mitochondrial bioenergetics

High-resolution respirometry can be used as a sensitive diagnostic test for assessing mitochondrial function in intact cells. Multiple substrate uncoupler-inhibitor titration protocols can be used to detect the oxidative phosphorylation and can help to understand the mitochondrial function and diseases (Pesta and Gnaiger, 2012). Mitochondrial dysfunction is detected as a significant contributing factor to β-cell failure in type 2 DM. Metabolic stress activates the ROS production in the mitochondria of β-cell and affects the mitochondrial structure and function. ROS production also activates the proton leak, uncoupled protein-2 (UCP-2), ATP synthesis, impair integrity of mitochondrial membrane and releases the cytochrome *c* to the cytosol. Also, mitochondria in β-cell from type 2 DM exhibit morphological and functional abnormalities. ROS also promotes the mitochondrial DNA fragmentation, protein cross-linking, and further activates stress pathways (Ma et al., 2012).

Exploring the mitochondrial function in type 2 DM is a interesting area of research work. Various *in-vitro, in-vivo* and *in-situ* experiments are available to determine the mitochondrial function. Mitochondrial bioenergetics determines ATP synthesis and ion homeostasis in cells. ATP synthesis through oxidative phosphorylation is the principal function of mitochondria. ATP synthesis can be assessed through measuring mitochondrial oxygen consumption or respiration. Mitochondria play a central role in regulating the cellular redox homeostasis. The mitochondrial respiration can be evaluated through the respirometric oxygen flux by different methods using amperometric oxygen sensors or phosphorescent probes. Amperometric measurements using Clark electrode are commonly used to measure respiration (Perry et al., 2013). Mitochondrial dysfunction is detected in type 2 DM. Mitochondrial dysfunction contributes to raised lipid storage in the skeletal muscle, heart, and liver. The skeletal muscle biopsy of the offspring of

type 2 DM showed an impairment in mitochondrial function and a tendency of reduced *in-vivo* mitochondrial function in first degree relative suggesting a compromised mitochondrial defect can occour earlier in type 2 DM (Phielix et al., 2008). Mitochondria are involved in the physiological signaling that, regulates energy and redox metabolism. They are dynamic organelles with two membranes, is the site of the redox reaction, electron transfer, and nutrient oxidation. The free energy transferred from electron transfer generates the proton motive force, resulting in ATP production (Garcia-Souza and Oliveira, 2014). Dysfunction in platelets has a significant role in type 2 DM and its associated vascular complication. Higher content of ATP and lower membrane potential in mitochondria are observed in type 2 DM (Guo et al., 2009). The oxygen consumption measurements in the peripheral blood mono-nuclear cells (PBMC) obtained from diabetic patients were detected with an increased basal, maximal and uncoupled respiration (Hartman et al., 2014).

Platelets are derived from megakaryocytes, and they are anucleate with functionally active mitochondria. During quiescent state, platelets have higher ATP turnover, and its respiration is coupled to ATP production. Mitochondrial disorders are usually incurable and caused by nuclear or mitochondrial DNA mutations. The classical method of measuring mitochondria function is by muscle biopsy, which is invasive and has risk for infections. The alternative methods for assessing mitochondrial function using blood cells possess several advantages over the classical method (Garcia-Souza and Oliveira, 2014), which avoid biopsy and is more acceptable by patients. Platelets isolated from peripheral blood samples are an appropriate model for the clinical assessment of mitochondrial respiration activity (Hroudova et al., 2013; Sjovall et al., 2013; Sjovall et al., 2010). In this study, we propose to evaluate the

potential application of platelet mitochondrial function assay in healthy subjects with and without family history of heart disease or diabetes.

2.11 Research questions

1. What is the impact of glyLDL on eNOS in cultured HUVEC and related transmembrane signaling pathway?
2. How does glyLDL influence the mitochondrial function in cultured HUVEC?
3. Do gender, age, body mass index and family history of chronic metabolic diseases influence the platelet mitochondrial bioenergetics in healthy subjects?

2.12. Hypothesis

1. GlyLDL may inhibit eNOS expression in HUVEC by activation of membrane receptor and small G protein.
2. GlyLDL may impair mitochondrial function by impairing the respiratory chain activity and mitochondrial bioenergetics profile in cultured HUVEC.
3. Abnormalities may exist in platelet mitochondrial bioenergetics of healthy human subjects with variation in gender, age, body mass index and family history of chronic metabolic diseases.

2.13. Objectives

1. To examine transmembrane upstream signaling events in glyLDL-stimulated expression of eNOS in cultured HUVEC.
2. To determine the effect of glyLDL on mitochondrial complex activity and bioenergetics profile in cultured HUVEC.
3. To assess the impact of variation in gender, age, body mass index and family history of chronic metabolic diseases on the platelet mitochondrial bioenergetics in healthy subjects.

Chapter 3

Materials and Methods

3.1 Chemicals

Acrylamide, Bis-acrylamide, Tween-20, Sodium dodecyl sulfate (SDS), Tris-Base, Sodium Chloride, Dimethyl sulfoxide (DMSO) and Fetal Bovine Serum (FBS) were obtained from Fisher Scientific® ON, Canada. F-12K Nutrient mixture was obtained from Gibco® Life Technologies Inc. ON, Canada. Primary and secondary antibodies (RAGE, H-Ras, goat-anti mouse IgG HRP, control goat IgG, goat-anti rabbit used in protein detection were obtained from Santa Cruz Biotechnology Inc. Santa Cruz, U.S.A. eNOS antibody was procured from BD Biosciences ON, Canada and Cell Signaling Technology® Inc. Denver, USA. Beta actin antibody was obtained from Abcam® Inc. Cambridge, U.S.A. H-Ras siRNA and control siRNA were obtained from Santa Cruz Biotechnology Inc. Santa Cruz, USA. Farnesyltransferase inhibitor, FTI-276 was obtained from Calbiochem® Millipore, Canada. Ultrasensitive nitric oxide synthase assay kit–NB78 was obtained from Oxford Biomedical Research® Oxford, UK, Trizol reagent and real-time polymerase chain reaction kit was obtained from Invitrogen, Inc. Canada. eNOS custom oligonucleotides and power SYBR® green dye were obtained from Applied Bio-Systems® Inc., USA. Beta actin custom oligonucleotides were obtained from ACGT Corp, ON, Canada. ECL Prime detection solution was obtained from Amersham® Inc, GE Healthcare USA, SiLentFect® Lipid for Transfection studies were obtained from Bio-Rad Laboratories Inc, USA. Western Blotting PVDF membrane was obtained from Roche Diagnostics Inc, USA. 4-phenylbutyric acid (4-PBA), an ER stress inhibitor and all other chemicals used throughout the experiments were of standard reagent grade and are obtained from Sigma-Aldrich® Inc, ON, Canada unless otherwise indicated.

3.2 Equipments

Class IIA/B3 biological safety cabinet, water-jacketed CO_2 incubator used were from Forma Scientific Inc., Canada. Chemical weighing balance was from Denver Instruments Inc., USA. Haemocytometer was from (Spencer ® Bright light Improved Neubauer, Sahli Adams, USA). Analytical weighing balance was from Sartorius Research, Germany. Benchtop pH Meter Orion® was from Thermo Scientific Inc, Canada. Nikon TMS inverted microscope was from Nikon Instruments, USA and Olympus Infinity 2-BX-40 microscope was from Carson Group Inc. ON, Canada. Titre-plate shaker was from Lab Line Instruments Inc., USA. 3D-Rotator mixer was from Southwest Science Inc, New Mexico. Magnetic stirrer/hot plate was from Thermo Scientific Inc., Canada. Electrophoresis and electric transfer power supply was from Fisher Biotech Inc., Canada. Bio-Rad mini protean tetra cell was from Bio-Rad Laboratories Inc, USA. Oroboros Oxygraph-2k was from Oroboros, Austria. Digital vortex-VersaMix®, Vortex Genei-2 Isotemp-210 temperature controlled water bath, digital vortex mixer were from Fisher Scientific. Eppendorf centrifuge-5424 was from Eppendorf, ON, Canada. Optima TLX-Ultracentrifuge, Beckman LE-80 Ultracentrifuge Optima, Allegra X-12R Centrifuge were from Beckman Coulter Inc., USA. IEC Centra GP-8R Centrifuge was from DJB Labcare Ltd, England. Fluostar Optima 96 well plate fluorimeter was from BMG LabTech®, Germany. Ultrospec 2000 UV-VIS spectrophotometer was from Pharmacia Biotech-Scinteck Instruments Inc, USA. NaNopure Infinity® Ultra-pure water systems were from Barnstead Thermolyne Inc, USA.

3.3 Cell culture

Seed cells of human umbilical vein EC (HUVEC) were obtained from American Type Culture Collection® (ATCC-Manassas, USA). The cells were grown in supplemented F12K medium as described previously (Ren and Shen, 2000). HUVEC medium was prepared by supplementing 500 ml of F12K nutrient mixture with the following supplements. 10% heat-inactivated FBS, 1% penicillin/streptomycin (Life Technologies Inc, Canada), 30 µg/ml EC growth factor and 0.1 mg/ml of heparin (Sigma-Aldrich® Inc, Canada). The cells were grown in a humidified incubator with 95% air, 5% CO_2, and 37 ºC with supplemented F12K media and used within 3-7 passages from seed cells. The cells were cultured in a 100mm polypropylene cell culture dish (Corning Incorporated Inc, USA). During each sub-culture, confluent cells were cultured at 1:2 or 1:3 ratios by using cell dissociation agents, Trypsin/EDTA. HUVEC cultures were monitered for appropriate morphology under microscopy.

3.4 LDL isolation

LDL (density 1.019-1.063 g/ml) was isolated from freshly collected blood from healthy human volunteers. After collection of 250 ml of blood aseptically in a Teruflex® blood bag containing anticoagulant citrate phosphate, dextrose, and adenine solution, blood was centrifuged at 2000 rpm for 30 min at 4 °C to separate plasma. This plasma obtained was adjusted for the appropriate density (double distilled water and potassium bromide solution) using a digital density meter DMA-35 (PAAR Instruments Inc., Austria). The plasma was the filled into polyallomer Quick Seal® centrifuges tubes (Beckman Instruments Inc., Canada). Sequential floating ultracentrifugation at 40,000 rpm was performed using Beckman LE-80 Ultracentrifuge Optima (Beckman Coulter Inc., Canada) for 48 h. After ultracentrifugation, 2-3 ml of pale yellow layer on the top of Beckman tubes were collected. This LDL fraction is dialyzed using

the dialyzing buffer containing EDTA in a sealed dialyzing tube overnight to remove potassium bromide and prevent auto-oxidation of LDL (Ren et al., 1997). This purified and concentrated LDL preparations were collected in sterile corning tubes, sealed with para film and stored at 4 °C in the dark with nitrogen gas incubated over the LDL to avoid oxidation. Blood was withdrawn from the healthy donors for LDL isolation after obtaining informed consent signed from all donors. The studies conducted were in accordance with the Helsinki Declaration and the protocol and consent form were approved by the Research Ethics Board, University of Manitoba.

3.5 LDL glycation

GlyLDL was prepared from LDL by incubation with 50 mM glucose and 50 mM sodium cyanoborohydride in the presence of 0.01% EDTA for 14 days at 37 °C as described (Zhang et al., 1998). After two weeks of incubation, glyLDL preparations were dialyzed thoroughly using dialyzing buffer containing EDTA to eliminate free glucose or any chemicals in the preparation. Dialyzing helps in concentrating or purifying the glyLDL preparation. The glycation of lysine in glyLDL was analyzed using 2, 4, 6-trinitrobenzenesulfonic acid (TNBS) assay (Duell et al., 1990). Approximately 30% of lysine residues glycated in the preparations were used in the experiments. The glyLDL prepared are stored at 4 °C in the dark in Corning tubes sealed under a layer of nitrogen.

3.6 Protein estimation by Lowry assay

The protein concentrations of the lipoproteins and modified lipoproteins stimulated, and non-stimulated HUVECs were estimated from aliquots of their corresponding samples by Lowry assay. Bovine serum albumin (BSA, 1mg/ml) was used as standard and the absorbance was read using UV-VIS spectrophotometer at 650 nm. The concentration of the aliquot was calculated and reported in µg/µl of the protein in the sample.

3.7 Measurement of non-enzymatic glycation (TNBSA Assay)

The extent of protein glycation occurred in modified lipoproteins were measured from aliquots of their samples by TNBSA (2, 4, 6-Trinitrobenzene sulfonic acid) assay (Duell et al., 1990). Aliquots of the lipoprotein was mixed with 4 % sodium bicarbonate and 0.1% TNBSA for one hour at 37 °C and the absorbance was noted at 340 nm using Ultrospec-2000 UV-VIS spectrophotometer. The percentage of glycation of lysine was calculated from their absorbance value compared to that of LDL and greater than 30% is considered for glycated LDL to be appropriate to use in experiments to treat HUVEC.

3.8 Experimental incubation

GlyLDL and LDL were used in physiological concentrations to stimulate HUVECs. LDL (100 µg/ml) or glyLDL (0-150 µg/ml) were treated with HUVEC for 24 h or as indicated in experiments. Equivalent volume of the vehicle (control) was used for equivalent time of stimulation. 8-10 % SDS-PAGE was used in separating the proteins by Western Blotting. Polyclonal RAGE-blocking antibody (10 µg/ml) was gifted by Dr. A.M. Schmidt, Columbia University, USA) was pre-incubated for 30 min. Also, FTI-276 (farnesyltransferase inhibitor) H-Ras inhibitor and 4-PBA, an ER stress inhibitor were used in experiments with a pre-incubation of 30 minutes. Substrates and inhibitors for mitochondrial respiratory chain complexes were used in mitochondrial function studies using Oxygraph. The complex specific substrate, inhibitors and uncouplers were used in Oxygraph studies to evaluate the mitochondrial respiratory chain activities and the mitochondrial bioenergetics in HUVEC.

3.9 Protein separation using Western blotting

After experimental incubation, cells were lysed using ice-cold lysis buffer and cellular proteins were extracted. Cell lysate was mixed with equal quantity of 2X SDS loading dye and heated for 5 minutes at boiling temperature. The protein extracted (40 µg) was separated on an 8-12 % SDS-PAGE gel using a mini protean tetra cell depending on the molecular weights of protein. Further, it is electrotransferred to methanol activated PVDF membrane using a mini protean cell transfer apparatus for 1h at a constant current of 100 V. These membranes were then blocked with 5% non-fat dry milk in Tris-buffered saline with 0.25% v/v Tween-20 (TBS-T) for 1h at room temperature. Blocked membrane was incubated for 1h with appropriate primary antibody. After appropriate incubation period, the membranes are cleaned three times for 5 minutes in 1X TBS-T and further incubated with secondary antibody with horseradish peroxidase (HRP) for appropriate time and temperature. Again after secondary antibody incubation for an hour, the membranes were cleaned three times for 5 minutes in 1X TBS-T buffer. The primary antibodies and the secondary antibodies used were listed in **(Table: 1).** The proteins precisely bounded on the membrane are detected by enhanced chemiluminescence (ECL) detecting reagent. The relative intensity of protein band in the electrotransferred PVDF membranes were detected on a Chemi-Doc system (BioRad Laboratories Inc, USA) or by autoradiography on a transparent blue X-ray film (Thermo Scientific Inc, USA). The band intensities were normalized with the level of beta-actin, a house-keeping protein and detected by Quantity One software from Bio-Rad® Laboratories Inc. U.S.A.

S.No	Antibody	Dilution used	Incubation	Obtained from
Primary antibody				
1	Anti-eNOS polyclonal mouse IgG	1:500	Room temperature for 2 h	BD Transduction laboratories, Inc Cat.No. 610296
2	Anti-H-Ras polyclonal rabbit IgG	1:200	Room temperature for 1 h	Santa cruz Biotechnology, Inc Cat: No.SC-520
3	Anti-β-actin monoclonal mouse IgG	1:20,000	Room temperature for 1 h	Abcam laboraories Inc Cat.No. 49900
Secondary antibody				
1	Goat anti-mouse IgG HRP	1:1000	Room temperature for 1 h	Santa cruz Biotechnology, Inc Cat: No.SC-2005
2	Goat anti-rabbit IgG HRP	1:1000	Room temperature for 1 h	Santa cruz Biotechnology, Inc Cat: No.SC-2004

Table: 1 Primary and secondary antobodies used in the Western blotting experiments to detect the expression of specific proteins.

3.10 Detection of H-Ras translocation

After treatment of HUVECs with glyLDL for 24 h, the cells were collected and homogenized in a dounce homogenizer (Fisher scientific Inc., Canada). The membrane and cytosolic fractions were separated in Optima TLX ultracentrifuge at 100,000×g at 4 °C for 1h as described (Sangle, Zhao, et al., 2010). The expression of H-Ras in membrane fraction and cytosolic fraction separated in the PVDF membrane were detected by Western blotting technique using antibody against human polyclonal H-Ras antibody. The relative intensity of protein band in the electrotransferred PVDF membrane was determined by Chemi-Doc and Quantity One software from Bio-Rad Inc. USA.

3.11 Quantitative real time-polymerase chain reaction (Real Time-PCR)

The levels of human eNOS mRNA gene were quantified using the Real Time-PCR (Applied Bio-systems or ABI, TX) and ABI 7500 Real-Time PCR system using previously described protocol (Nguyen et al., 2011; Saluja et al., 2011; Zhao et al., 2009). Total RNA was extracted from cultured HUVECs (stimulated versus control) using Trizol Reagent (Invitrogen Inc, Canada). cDNA were synthesized from 5µg of total RNA using reverse transcriptase and oligo (dt) primer. The eNOS and β-actin mRNA gene expressions were amplified by using primer sequences as mentioned below;

eNOS mRNA Forward: 5'- GTT TGT CTG CGG CGA TGT -3.'

eNOS mRNA Reverse: 5'- GTG CGT ATG CGG CTT GTC -3'

β-actin mRNA Forward: 5'- ATT GCC GAC AGG ATG CAG GAA -3.'

β-actin mRNA Reverse: 5'- GCT GAT CCA CAT CTG CTG GAA -3'

The primers were synthesized and obtained from AGCT Corp, Canada and Applied Biosystems Inc, USA as performed in (Chen et al., 2009). Real Time-PCR was performed using

fluorescent dye Power SYBR® Green PCR Master Mix. The conditions used were following; (95 °C for 5 min, 95 °C for 15s, 60 °C for 20s, and 72 °C for 40s for 40 cycles). Relative quantification of eNOS mRNA levels was determined from the cycle threshold (C_T) and normalized to the β-actin mRNA levels obtained simultaneously in the samples. The C_T and melting curve analysis were performed to verify the consistency of results obtained.

3.12 NO synthase (NOS) Assay

The NOS activity was performed by using ultrasensitive colorimetric assay kit obtained from Oxford Biomedical Research Inc, UK. The assay utilizes the NADPH recycling system to measure the nitric oxide derived from nitrate and nitrite linearly. NO, rapidly degrades to nitrate and nitrite. This assay involves the enzymatic conversion of nitrate to nitrite by enzyme nitrate reductase and quantification of nitrite using Griess Reagent. The reaction absorbance was read spectrophotometrically at 540 nm using 96 well flat bottom microtiter plate readers in Fluostar-Optima (BMG LabTech®, Germany). Cultured HUVECs were plated in a 100 cm culture dish and treated with glyLDL (100 µg/ml) and control vehicle for 24 h. Following stimulation, the cells are homogenized, and the cell homogenates were prepared. The cell homogenates were incubated in 96 well microtiter plates for estimating the NOS activity. 100 µg of the protein from the cell homogenates were used in the assay and performed as described in the protocol (Oxford Biomedical Research® Inc, Oxford, UK).

3.13 Assessment of mitochondrial respiratory chain complexes in permeabilized HUVEC using Oxygraph-2k

The oxygen consumption rate in permeabilized HUVEC mitochondria was determined using a highly resolution respirometer with Clark-type oxygen electrode, Oxygraph-2k (Oroboros Instruments, Innsbruck, Austria). The permeabilized cells were used to measure the activities of the individual respiratory chain complexes as described in (Roy Chowdhury et al., 2010; Sangle, Chowdhury, et al., 2010).

After the treatment of the cultured HUVECs (75% confluent) with glyLDL for 24 h, the cells were trypsinized, washed with PBS and counted using hemocytometer. The freshly harvested cells were re-suspended in KCl medium (80 mM KCl, 10 mM Tris-HCl, 3 mM $MgCl_2$, 1 mM EDTA, 5 mM potassium phosphate, pH 7.4) (Sangle, Chowdhury, et al., 2010). HUVEC suspension (2 ml) in KCl medium was incubated at a concentration of 2.5 $x10^6$ cells/ml in each 2 ml glass chamber with a titanium stopper. The cells were continuously stirred in the KCl medium by magnetic stirrer bar at the bottom of the chamber. The air calibration of the polarographic oxygen sensors, cleaning of chambers, background correction and temperature setting at 37 °C was performed in a glass chamber before start of each experiment. After incubation, the cells were observed in the chamber to stabilize at a basal state (physiological coupling state-without any additions of substrate or inhibitor). The basal level of oxygen consumption rate denotes the normal cellular energy demands on oxidative phosphorylation.

HUVECs were permeabilized using digitonin, which keeps the mitochondrial outer membrane intact. The effect of glyLDL on individual complexes in mitochondrial ETC of HUVECs was studied in the presence of respiratory substrates and inhibitors of mitochondrial complexes. The manual titrations performed using mitochondrial substrates and inhibitors were

illustrated in **(Table: 2)** Glutamate (10 mM) combined with malate (5 mM), succinate (10 mM), ascorbate (5 mM) combined with N,N,N',N'-tetramethyl-p-phenylenediamine dihydrochloride (TMPD, 0.5 mM) are used as specific substrates for Complex I, Complex II/III and Complex IV respectively. Rotenone (1 µM), antimycin A (1 µg/mL) and potassium cyanide (KCN, 0.25 mM) were used as inhibitors for Complex I, Complex III and Complex IV respectively. DatLab-4 software from Oroboros was used for digital recording and analysis of the data obtained. Oxygen consumption rate was normalized using the cell number and expressed in pmol/sec/10^6 cells. Respiratory control index (RCI) was assessed from oxygen consumption rate induced by glutamate combined with malate and adenosine diphosphate (ADP, 2 mM) divided by the oxygen consumption rate after inhibited by rotenone.

Chemicals used	Abbreviated Event	Concentration (solvent used)	Final concentration of 2 ml $O_2$2k chamber	Titration (µl) into 2 ml chamber
Digitonin (mild detergent)	D	5 mg/ml (H_2O)	8 µg/10^6 cells	8
Substrates				
Glutamate (Complex I)	G	1 M (H_2O)	10 mM	20
Malate (Complex I)	M	1 M (H_2O)	5 mM	10
Adenosine-diphosphate (ATP synthase)	ADP	0.5 M (H_2O)	2 mM	8
Succinate (Complex II)	S	1 M (H_2O)	10 mM	20
Ascorbate (Complex IV)	A	1 M (H_2O)	5 mM	10
N,N,N',N'-tetra methyl-p-phenylenediamine-dihydrochloride (co-substrate for Complex IV)	TMPD	0.1 M (H_2O)	0.5 mM	10
Inhibitors				
Rotenone (Complex I)	R	One mM (EtOH)	1 µM	2
Antimycin-A (Complex III)	A	1 mg/ml (EtOH)	One µg/ml	2
Potassium cyanide (Complex IV)	KCN	0.1 M (H_2O)	0.25 mM	5

Table: 2 Oxygraph-2k manual titrations for determining the mitochondrial complex activity. The optimum concentrations of digitonin, all substrates and inhibitors were determined by titration.

3.14 Assessment of mitochondrial bioenergetics profile in intact non-permeabilized HUVECs using Oxygraph-2k

The mitochondrial bioenergetics profile in nonpermeabilized intact HUVECs was assessed using Oxygraph-2k (Oroboros, Austria) (Brand and Nicholls, 2011). The freshly harvested HUVECs were suspended in 2 ml of mitochondrial respiratory (MiR) medium 80 mM KCl, 10 mM Tris-HCl, 3 mM $MgCl_2$, 1 mM EDTA, 5 mM potassium phosphate, pH 7.4 (Sangle, Chowdhury, et al., 2010) supplemented with 1mM sodium pyruvate and 10mM D-Glucose. HUVEC suspension (2 ml) at a concentration of 2.5 $x10^6$ cells/ml were incubated glass chamber with continuous magnetic stirring.

The mitochondrial bioenergetics profile is measured from the oxygen consumption rate (control versus treated) in intact cells without permeabilization and in the absence of any substrates. The protocol initially measures the basal respiration, which indicates the resting state of cells. Then the cells were injected sequentially with oligomycin (1 µM), FCCP (1 µM) and rotenone (1 µM) combined with antimycin-A (1 µg/mL). The manual titrations performed using uncopler and inhibitors were illustrated in **(Table: 3)**. Oligomycin was used as an ATP synthase inhibitor to reveal the ADP phosphorylation independent of respiration. This reduced OCR indicate respiration maintained for ATP consumption. The Carbonyl cyanide p-trifluoro-methoxyphenyl hydrazone-FCCP was used as mitochondrial uncoupler (protonophore) to evaluate the maximal capacity of electron transfer system (ETS) to reduce oxygen by uncoupling of the respiratory chain and measure the raised ATP demand. Rotenone combined with antimycin-A was used as inhibitor of Complex I and III respectively to inhibit the electron flux. The non-mitochondrial oxygen consumption was substracted from other mitochondrial oxygen consumption rates to obtain their mitochondrial specific respiration. The residual

respiration is the proton leak which generates heat. Bioenergetics parameters including, basal respiration, maximal respiration, ATP linked respiration, non-mitochondrial respiration, coupling efficiency, respiratory control ratio and spare respiratory capacity were determined from the oxygen consumption rate obtained from Oxygraph-2k as previously described (Roy Chowdhury et al., 2012). Data obtained were collected, analyzed graphically presented using Oroboros DatLab-4 software. The oxygen consumption rate was normalized using the cell number and expressed as pmol O_2/sec/10^6 cells.

Chemicals used	Event	Concentration (solvent used)	Final concentration of 2 ml	Titration (µl)
Uncoupler				
Carbonyl cyanide p-trifluoro methoxy-phenyl hydrazone	FCCP	1 mM (EtOH)	0.5 µM	1-2
Inhibitors				
Oligomycin (ATP synthase inhibitor-Complex V)	O	5 mM (EtOH)	2.5 µM	1-2
Rotenone (Complex I inhibitor)	R	1 mM (EtOH)	0.5 µM	1-2
Antimycin-A (Complex III inhibitor)	AA	5 mM (EtOH)	2.5 µM	1-2

Table: 3 Oxygraph-2k manual titrations for determining the mitochondrial bioenergetics profile. Titration determined the optimum concentrations of uncoupler and inhibitors

3.15 Human donors

Peripheral blood was withdrawn from forty-eight Caucasian healthy blood donors at the Diabetic Research Clinic, University of Manitoba. This study was approved by the research ethics board of the University of Manitoba. Informed consent was signed by all participants before the withdrawal of blood by venipuncture. The donors in the study were not continuing any medications or smoking or alcohol one week prior to blood withdrawal.

3.16 Blood collection and platelet preparation

Blood (20-30 ml) was withdrawn from 48 healthy donors at 07:00-09:00 h after 12 h of overnight fasting at Diabetes Research Group Clinic, University of Manitoba. The blood were collected into BD vacutainer® blood collection tubes buffered with 3.2% sodium citrate (BD Franklin Lakes, USA). The platelets were freshly isolated by centrifugation at 200×g (Allegra X-12R Centrifuge, Beckman Coulter Inc, USA) for 15 minutes at room temperature to yield a platelet-rich plasma (PRP) as previously described (Sjovall et al., 2010). This PRP was further centrifuged at 2500×g for 10 minutes at room temperature (IEC Centra GP-8R centrifuge, DJB Labcare Ltd, England). The platelets obtained were washed with PBS and counted using a hemocytometer and microscope (Olympus Infinity 2-BX-40). The platelets were used immediately for measuring the mitochondrial oxygen consumption using Oxygraph-2k.

3.17 Assessment of mitochondrial bioenergetics profile in intact non-permeabilized human platelets using Oxygraph-2k

The mitochondrial bioenergetics in healthy human platelets were determined using Oxygraph-2K (Oroboros, Austria) as described in section 5.14. The freshly isolated platelets were resuspended in mitochondrial respiratory (MiR) medium. Platelet suspension (2 ml) in MiR medium at a concentration of 100 x 10^6 platelets/ml was incubated in each 2 ml glass chamber

with continuous magnetic stirring. The intact platelets were incubated in the chambers within 2-3 h of blood withdrawal as long hours may lead to platelet aggregation. Then platelets were sequentially injected with oligomycin (1 μM), FCCP (1 μM) and rotenone (1 μM) combined with antimycin-A (1 μM) to evaluate the mitochondrial bioenergetics profile as described previously in experimental section 5.14.

3.18 Statistics:

All the data obtained from experiments were expressed in mean ± standard deviation (SD). The differences between groups were evaluated by Student's t-test and among multiple groups were evaluated by one-way analysis of variance (ANOVA). All statistical analyzes were performed using GraphPad Prism-6 (GraphPad Software, San Diego, USA). The level of significance was defined as $p<0.05$.

Chapter 4

Results

The results of the present study are presented in following three sections**:**

1. Expression of eNOS and transmembrane upstream signaling events in HUVEC treated with glyLDL

2. Mitochondrial function in HUVEC treated with glyLDL

3. Platelet mitochondrial bioenergetics in healthy subjects

4.1 Expression of eNOS and transmembrane upstream signaling events in HUVEC treated with glyLDL.

4.1.1 Effect of glyLDL on eNOS protein in HUVEC

We examined the effects of physiological range of glyLDL (0-150 µg/ml) for 4-36 h on the content of eNOS protein in HUVEC using Western blotting. The results demonstrated that glyLDL (100 µg/ml) for 24 h down-regulated eNOS protein expression in a dose and time dependent manner in HUVECs compared to unstimulated HUVEC as control (EC medium at equivalent volume used as vehicle). Stimulation of HUVEC with glyLDL (100 µg/ml) for 24 h induced maximal downregulation of eNOS protein **($p<0.05$ or 0.01, Figure 1A, and 1B).** The band intensity of eNOS was normalized by β-actin as illustrated in **(Table: 4 and 5).**

The similar eNOS expression at 36 h control (without glyLDL incubated with equal volume of EC media at) and 36 h glyLDL may be due to the consequence of depleted basal eNOS in aged HUVEC or reduced eNOS due to endothelial apoptosis or arrest of cell growth at confluence (Artwohl et al., 2003; Rogers et al., 2013)

Normalised Control	25 µg	50 µg	100 µg	150 µg
1	0.6391	0.4008	0.1893	0.2352
1	0.6983	0.5811	0.761	0.6421
1	1.2054	0.9575	0.494	0.5622
Average	0.8476	0.646467	0.481433*	0.479833*
SD	0.311274	0.284048	0.286057	0.215592

Table: 4 Dose-dependence of glyLDL on eNOS protein expression in HUVEC in terms of normalized arbitrary value

HUVECs were treated with 25-150 µg/ml of glyLDL or vehicle (control) for 24 h for measurement of eNOS protein using Western blotting (Figure 1A). Data were expressed in the folds of control after normalization with β-actin (mean ± SD, n = 3 experiments) *, **: $p<0.05$ or 0.01 versus control (vehicle).

	4 h control	4 h glyLDL	12 h control	12 h glyLDL	24 h control	24 h glyLDL	36 h control	36 h glyLDL
	1	1.26	1.1	1.171	0.53	0.33	0.143	0.164
	1	1.03	0.84	0.87	0.61	0.39	0.103	0.091
	1	0.301	0.63	0.67	1.17	0.47	0.159	0.111
Average	1	0.86366	0.85666	0.90366	0.77	0.396**	0.135	0.122**
SD	0	0.50067	0.23544	0.25219	0.34871	0.07023	0.028844	0.037723

Table: 5 Time dependence of glyLDL on eNOS protein expression in HUVEC in terms of normalized arbitrary value.

HUVECs were treated with 100 µg/ml of glyLDL or vehicle (control) for (4-36) h for measurements of eNOS protein using Western blotting (Figure 1B). Data were expressed in the folds of control after normalization with β-actin (mean ± SD, n = 3 experiments) *, **: $p<0.05$ or 0.01 versus control (vehicle).

Figure 1 A

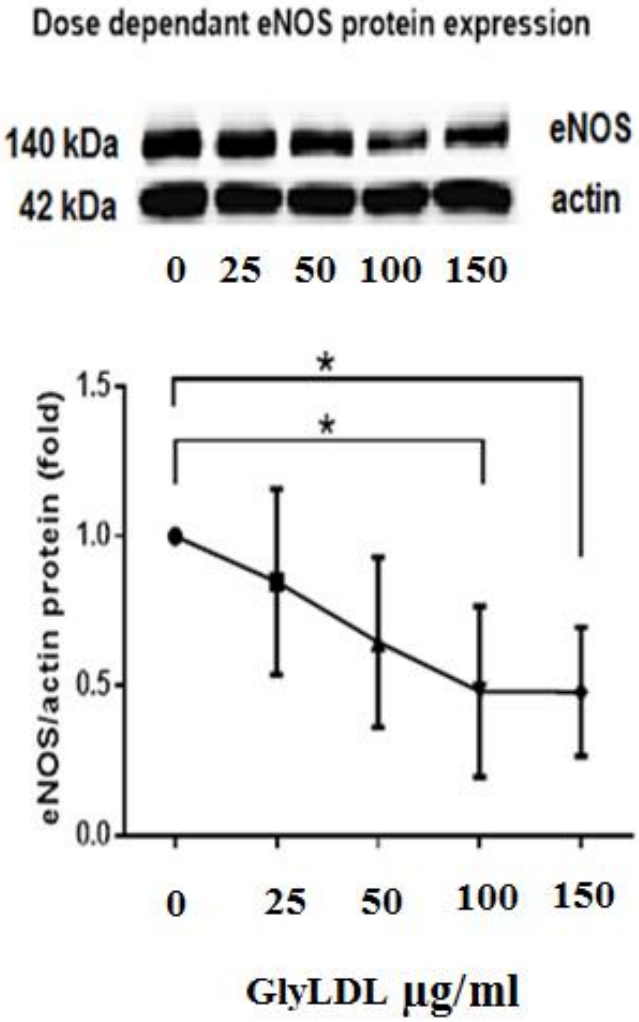

Figure 1 A: Dose dependence of glyLDL on eNOS protein expression in HUVEC.

Dose-dependence of glyLDL on eNOS protein in EC HUVECs were treated with 0-150 µg/ml of glyLDL or vehicle (control) for 24 h for measurements of eNOS protein. The protein expression of eNOS and β-actin were examined using Western blotting. Integrative data were expressed in folds of control after normalization with β-actin (mean ± SD, n = 3 experiments) *, **: $p<0.05$ or 0.01 versus control (vehicle).

Figure 1B

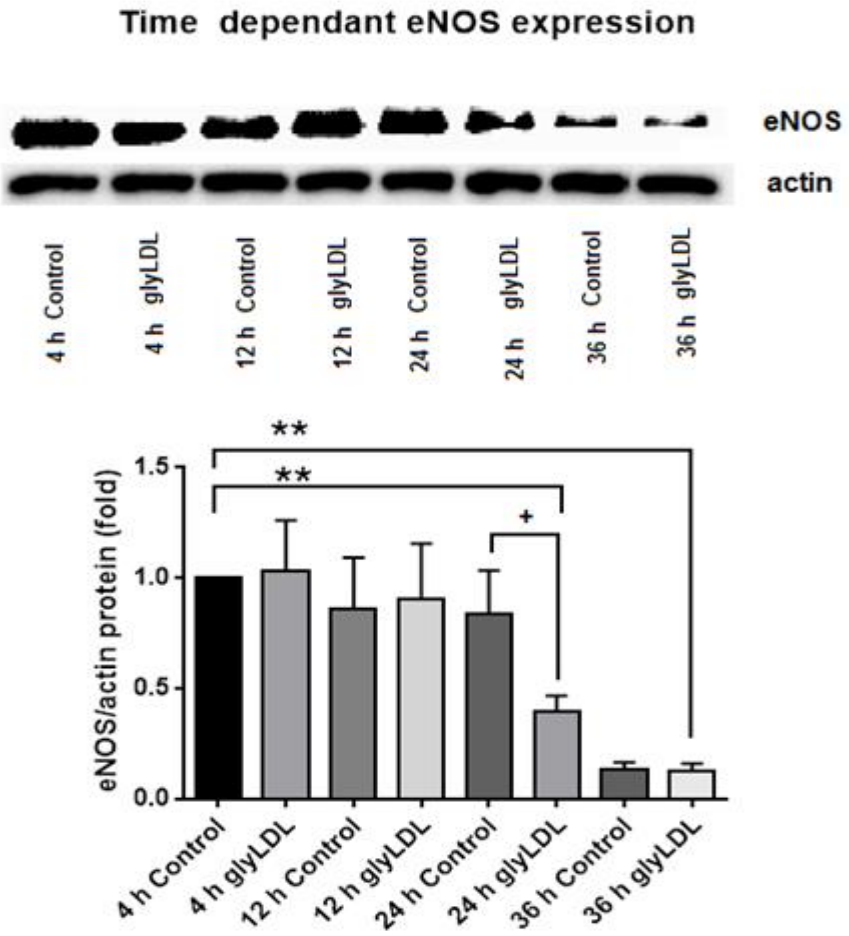

Figure 1 B: Time dependence of glyLDL on eNOS protein expression in HUVEC.

Time-dependence of glyLDL on eNOS protein in EC HUVECs were treated with 100 µg/ml of glyLDL or vehicle (control) for 4-36 h for measurement of eNOS protein. The protein expression of eNOS and β-actin were examined using Western blotting. Integrative data were expressed in folds of control after normalization with β-actin (mean ± SD, n = 3 experiments) *, **: $p<0.05$ or 0.01 versus 4 h control; +, ++: $p<0.05$ or 0.01 versus 24 h control (vehicle).

Further we examined the effects of glycation on LDL compared to unmodified LDL for 24 h at similar dose (100 µg/ml). GlyLDL enhanced the inhibition of eNOS protein in HUVEC compared to unmodified LDL or in unstimulated condition as control (vehicle) **(Figure 2 A).**

We also investigated the effects of low (5 mM) and high glucose (25 mM) in HUVEC for 24 h to observe the eNOS protein expression. High glucose exposure inhibited the eNOS protein more significantly than the low glucose in EC, which shows the downregulation of eNOS due to increased glucose stress in the cells as shown **(Figure 2 B).** These experiments indicate the impact of glucose and glycation independently in enhancing the eNOS downregulation in EC.

4.1.2 Effect of glyLDL on eNOS mRNA in HUVEC

We further investigated the effects of glyLDL (100 µg/ml) or vehicle for 24 h on steady levels of eNOS mRNA (gene expression) in HUVEC using quantitative real-time PCR **($p<0.05$, Figure 3)**. Total RNA were extracted from EC and real-time PCR was performed to measure the relative gene expression of eNOS in HUVEC. The results suggest that, stimulation of HUVECs with glyLDL significantly decreased eNOS mRNA level in EC **($p<0.01$, Table: 6).**

4.1.3 NOS activity in HUVEC treated with glyLDL

The impact of glyLDL (50-150 µg/ml) for 24 h on the activity of NOS in HUVECs was examined using ultrasensitive calorimetric NOS assay. The results suggest that, stimulation of HUVECs with glyLDL (100 µg/ml) for 24 h significantly attenuated the NOS activity in HUVECs **($p<0.05$, Figure 4)**, which supports the finding of glyLDL on eNOS protein and mRNA.

Real Time - PCR	mRNA level	
	Control	glyLDL
Trial 1	1	0.156
Trial 2	1	0.131
Trial 3	1	0.061
Average	1.0036	0.160333**
SD	0.131097	0.056181

Table: 6 Decreased eNOS gene (mRNA) expression in HUVEC treated with glyLDL in terms of normalized arbitrary value.

HUVECs were treated with 100 µg/ml glyLDL and vehicle for 24 h. The mRNA expression of eNOS and β-actin in total RNA from HUVEC were measured using quantitative real-time PCR. Integrative data were expressed in the fold of controls after normalization with β-actin (mean ± SD, n = 3 experiments). *, **: $p<0.05$ or 0.01 versus control (vehicle).

Figure 2 A

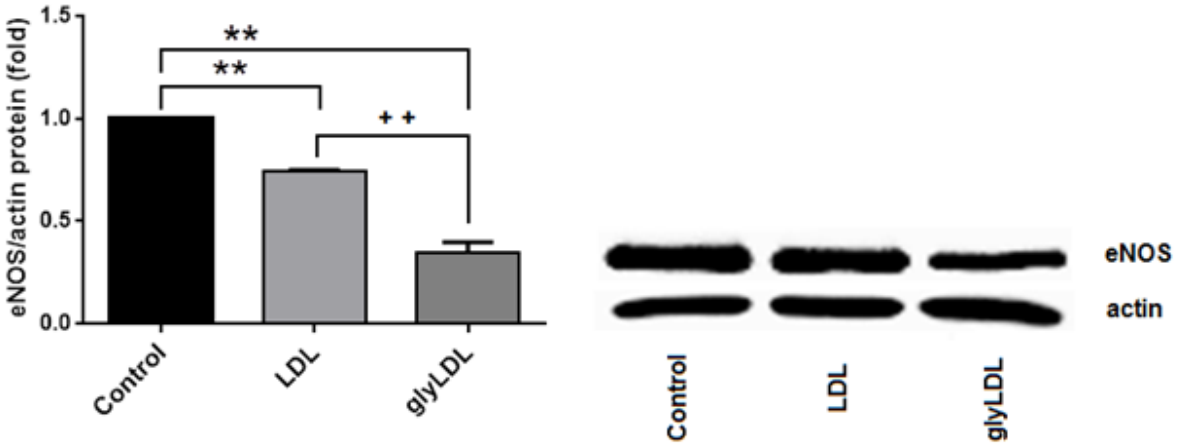

Figure 2 A: Effect of LDL and glyLDL on eNOS protein expression in HUVEC

HUVECs were treated with 100 µg/ml of LDL, glyLDL and vehicle (control) for 24 h. The protein expression of eNOS and β-actin in total cellular proteins were examined using Western blotting. Integrative data were expressed in folds of control after normalization with β-actin (mean ± SD, n = 3 experiments) *, **: $p<0.05$ or 0.01 versus control (vehicle); +, ++: $p<0.05$ or 0.01 versus LDL.

Figure 2 B

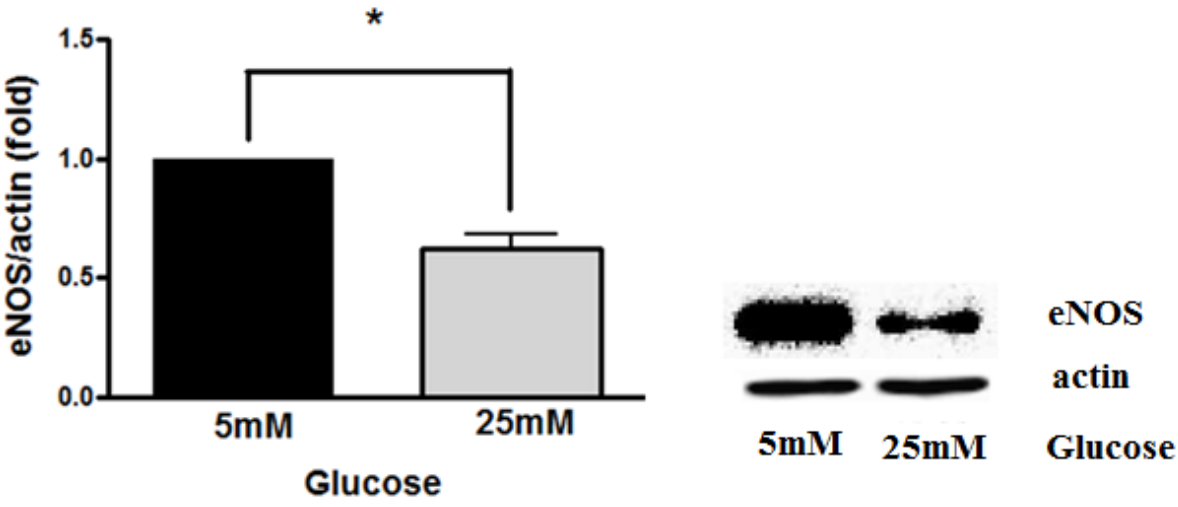

Figure 2 B: Effect of glucose on eNOS protein expression in HUVEC

HUVECs were treated with 5 mM glucose (control) and 25 mM of glucose for 24 h. The protein expression of eNOS and β-actin in total cellular proteins were examined using Western blotting.

Integrative data were expressed in folds of control after normalization with β-actin (mean ± SD, n = 3 experiments) *, **: p<0.05 or 0.01 versus 5mM glucose (control).

Figure 3

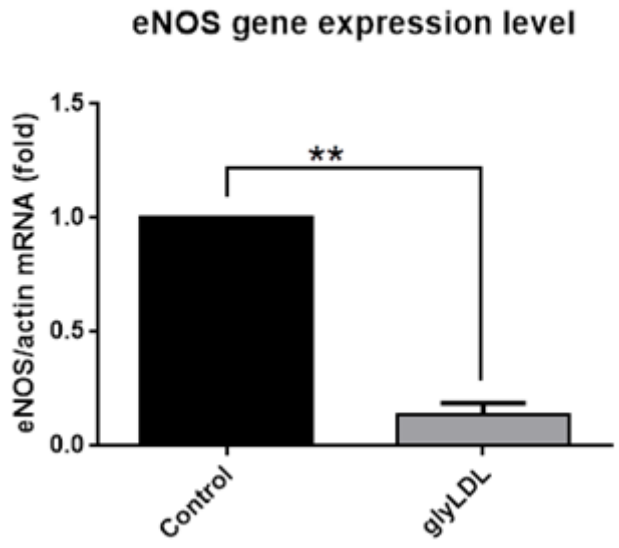

Figure 3: Decreased eNOS gene expression levels in HUVEC treated with glyLDL

HUVECs were treated with 100 µg/ml glyLDL and vehicle for 24 h. The mRNA expression of eNOS and β-actin in total RNA were examined using quantitative real-time PCR. Integrative data were expressed in the fold of controls after normalization with β-actin (mean ± SD, n = 3 experiments). *, **: p<0.05 or 0.01 versus control.

Figure 4

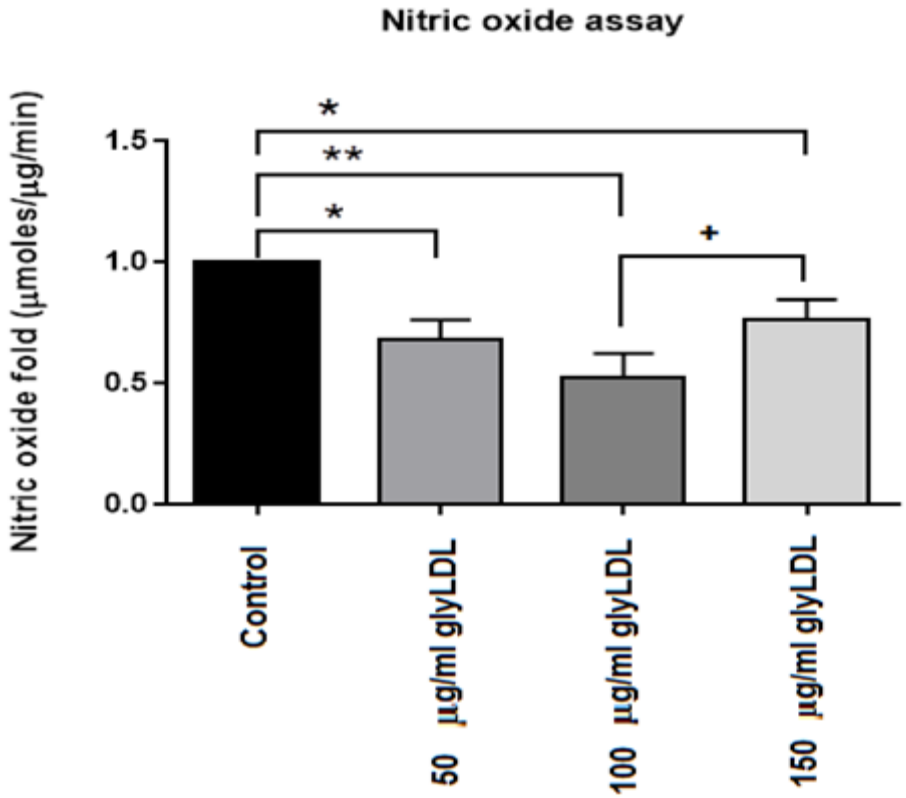

Figure 4: Effect of glyLDL on NOS activity in HUVEC

HUVEC were treated with glyLDL (50-150 µg/ml) or vehicle (control) for 24 h. Nitric oxide in cell lysate was measured using ultrasensitive calorimetric nitric oxide synthase (NOS) assay. Integrative data were expressed in folds of control as µmol/µg/min (mean ± SD; n = 3 experiments). *,** $p < 0.05$ or 0.01 versus control; +, ++: $p<0.05$ or 0.01 versus 100 µg/ml glyLDL.

4.1.4 RAGE involvement in the downregulation of eNOS in HUVEC treated with glyLDL

The participation of RAGE in glyLDL-stimulated downregulation of eNOS protein in HUVECs was investigated using blocking polyclonal antibody against RAGE. RAGE blocking antibody (10 μg/ml) as optimized in our lab (Sangle, Zhao, et al., 2010) prevented glyLDL-induced downregulation of eNOS protein in HUVEC. The results suggest that receptor, RAGE mediate glyLDL-induced transmembrane upstream signaling on the inhibition of eNOS in HUVECs **($p<0.01$, Figure 5)**.

4.1.5 H-Ras translocation and protein expression in HUVEC treated with glyLDL

The impact of glyLDL on translocation of H-Ras in from cytosol to cell membrane in HUVEC was examined at basal or glyLDL stimulated condition. HUVECs were treated with glyLDL (100 μg/ml) or vehicle for 24 h with or without the addition of 10 μM FTI-276, a farnesyltransferase inhibitor. The H-Ras protein in the membrane fraction was significantly upregulated with glyLDL treatment and FTI-276 prevented glyLDL-induced expression of H-Ras protein in HUVEC, but did not affect H-Ras in EC without exposure to glyLDL **($p<0.01$, Figure 6)**.

4.1.6 H-Ras involvement in glyLDL-stimulated downregulation of eNOS in HUVEC

The participation of H-Ras in glyLDL-induced inhibition in eNOS protein in HUVEC was studied using FTI-276. HUVECs were pre-incubated with FTI-276 (10 μM) for 30 min.

subsequently, HUVECs were exposed to glyLDL (100 µg/ml) for 24 h in an incubator. The protein levels of eNOS and β-actin were assessed using Western blotting. FTI-276 inhibited glyLDL-induced inhibition of eNOS in HUVEC. The results propose that glyLDL-induced eNOS downregulation in HUVEC is regulated by H-Ras protein **($p<0.01$, Figure 7**).

4.1.7 ER stress involvement in glyLDL-stimulated downregulation of eNOS in HUVEC

The ER stress involvement in glyLDL-stimulated downregulation of eNOS protein in HUVEC was determined using Western blotting. 4-PBA, an ER stress antagonist (2.5 mM), was used to verify the involvement of ER stress (Liu et al., 2015; Wiley et al., 2010). 4-PBA prevented glyLDL induced downregulation of eNOS protein in HUVECs **($p<0.01$, Figure 8**). The results indicate ER stress involvement in glyLDL-stimulated downregulation of eNOS in HUVEC.

Figure 5

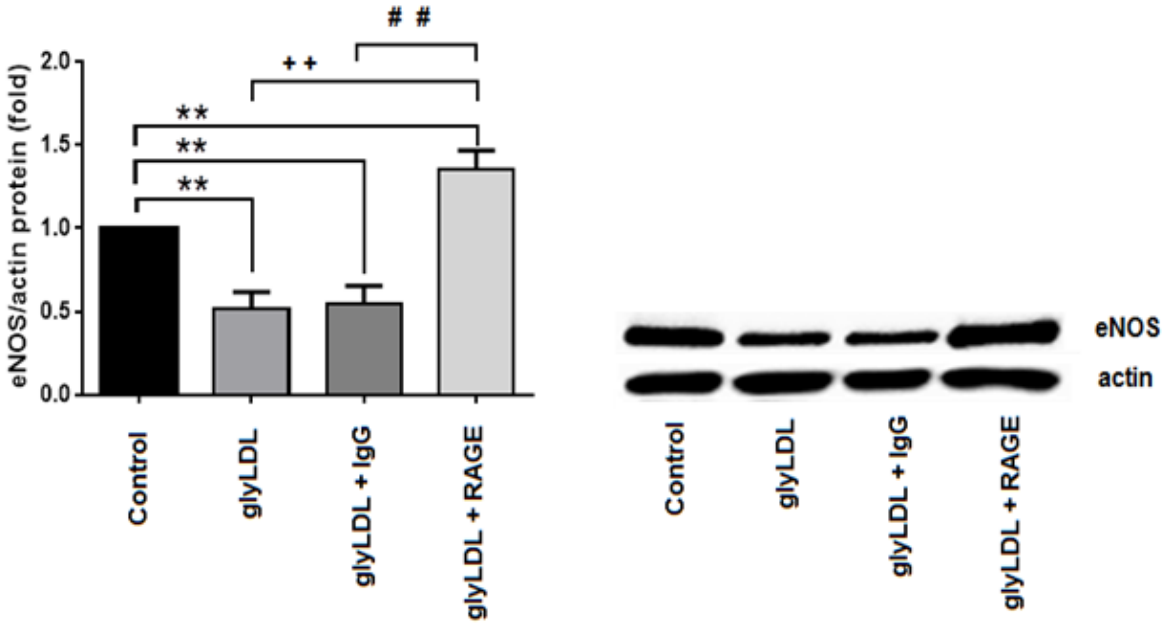

Figure 5: Receptor for advanced glycation end products (RAGE) mediates glyLDL-induced inhibition of eNOS in HUVEC

HUVECs were pre-incubated with 10 µg/ml RAGE blocking antibody for 30 minutes and then exposed to 100 µg/ml of glyLDL for 24 h. The protein expression of eNOS and β-actin were detected using Western blotting. Integrated data were expressed in folds of control after normalization with β-actin (mean ± SD, n = 3 experiments). *, **: $p<0.05$ or 0.01 versus control; +, ++: $p<0.05$ or 0.01 versus glyLDL; #, ##: $p<0.05$ or 0.01 versus glyLDL + IgG.

Figure 6

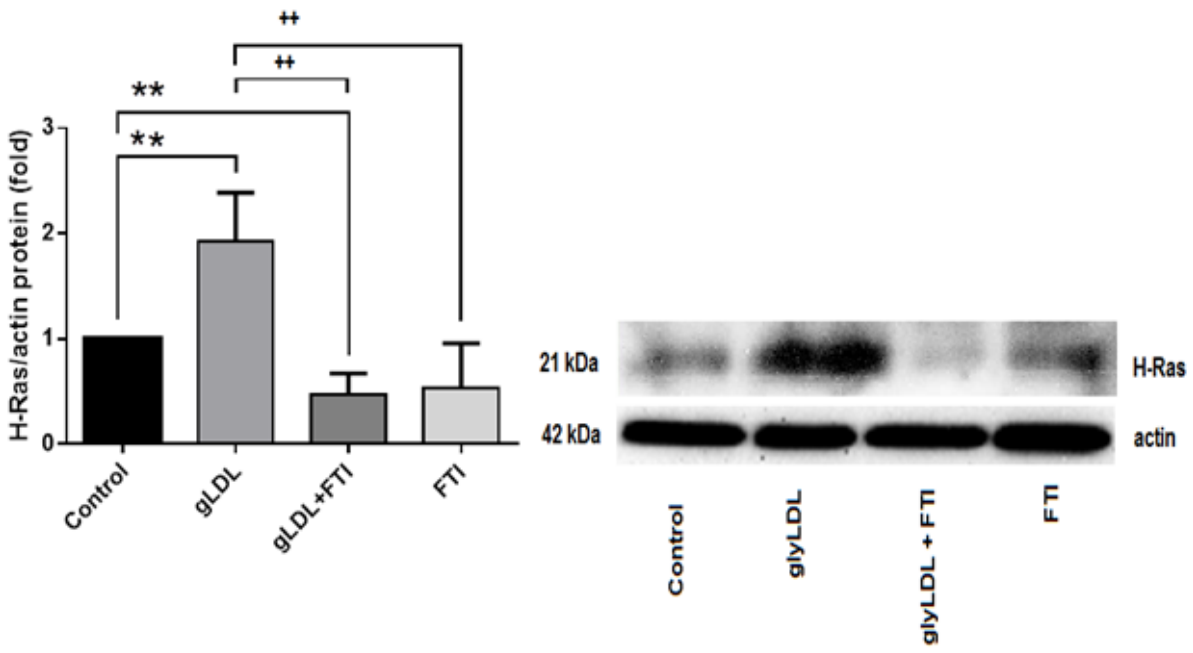

Figure 6: Effect of glyLDL on H-Ras translocation and protein expression in HUVEC

HUVECs were pretreated with vehicle (control) or FTI-276 (10 μM), an H-Ras inhibitor for 30 min and then treated with 100 μg/ml of glyLDL or vehicle for 24 h. The protein expressions of H-Ras and β-actin in membrane fractions were determined using Western blotting. Values are expressed in fold of controls after normalization with β-actin (mean ± SD n = 3 experiments). *, **: $p<0.05$ or 0.01 versus control; +, ++: $p<0.05$ or 0.01 versus glyLDL.

Figure 7

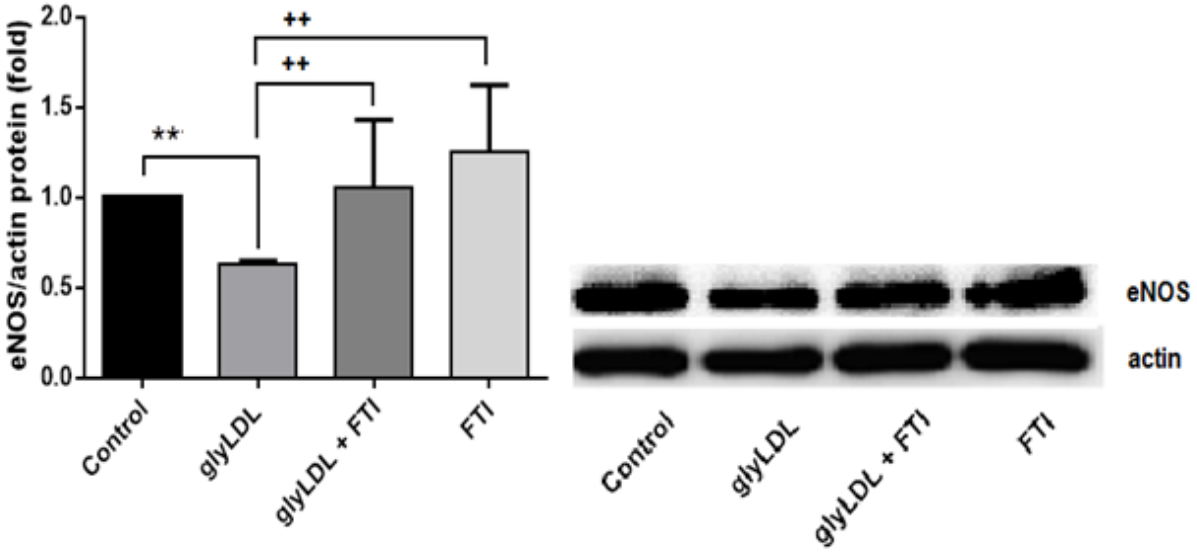

Figure 7: Involvement of H-Ras in glyLDL-induced eNOS downregulation in HUVEC

HUVECs were pre-treated with vehicle or FTI-276 (10 μM) for 30 min and then treated with vehicle (control) and 100 μg/ml of glyLDL for 24 h. eNOS and β-actin protein expressions in cellular proteins were detected using Western blotting. Integrated data were expressed in folds of control after normalization with β-actin (mean ± SD, n = 3 experiments). *, **: $p<0.05$ or 0.01 versus control; +, ++: $p<0.05$ or 0.01 versus glyLDL.

Figure 8

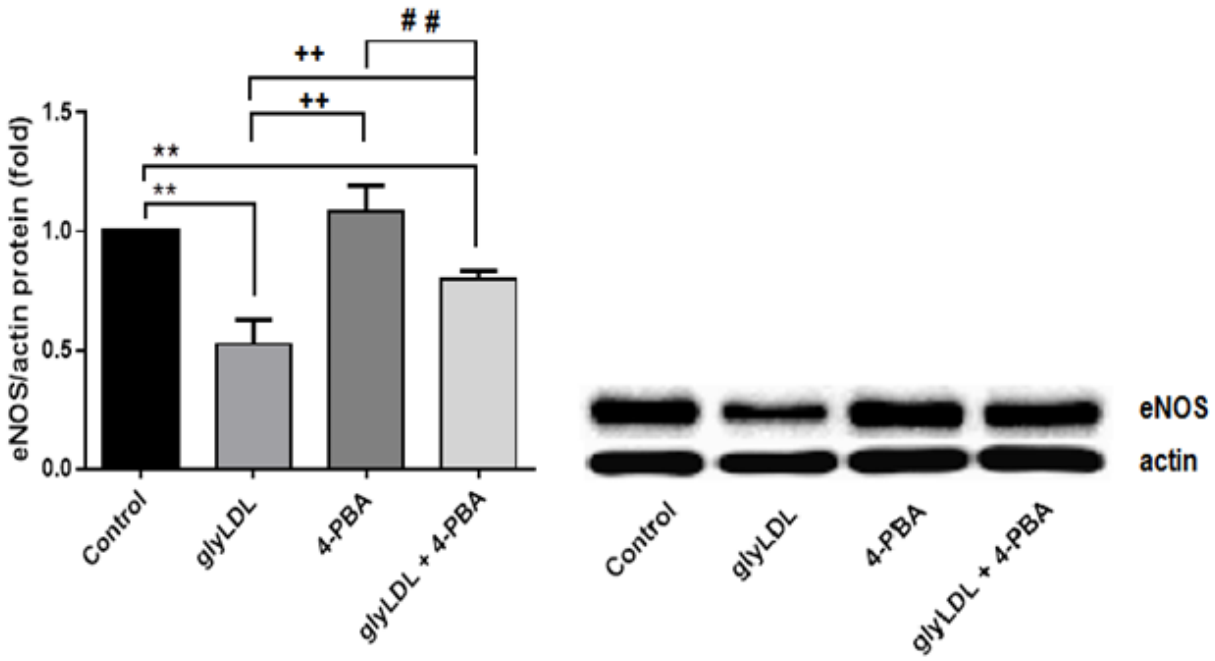

Figure 8: ER stress involvement in glyLDL-induced downregulation of eNOS protein in HUVEC

HUVEC's were pre-incubated with 4-PBA (2.5 mM) for 30 min with and then exposed to vehicle (control) or glyLDL for 24 h. The protein expression of eNOS and β-actin in total cellular proteins were examined using Western blotting. Integrative data were expressed in folds of control after normalization with β-actin (mean ± SD; n = 3 experiments). *, **: $p<0.05$ or 0.01 versus control; +, ++: $p<0.05$ or 0.01 versus glyLDL; #, ##: $p<0.05$ or 0.01 versus 4-PBA alone treated.

4.2 Mitochondrial function in HUVEC treated with glyLDL

4.2.1 Oxygen consumption in mitochondrial respiratory chain complexes in HUVEC treated with glyLDL

In this section of the study, the functionality of the individual mitochondrial respiratory chain complexes was determined from oxygen consumption rates in permeabilized HUVEC using Oxygraph-2k. Oxygen consumption rate is marker for mitochondrial respiration. Representative Oxygraph tracing of the mitochondrial oxygen consumption in permeabilized HUVEC is represented in **Figure 9**. HUVEC were treated with glyLDL (100 µg/ml) and control (vehicle) for 24 h. The cells were permeabilized using digitonin (2 µg/10^6 cells), a mild detergent which permeabilizes plasma membrane but keeps the mitochondrial membrane intact and expose to miotchomdrial inhibitors and substrates. The sequential addition of complex-specific substrates and inhibitors (Rotenone for Complex I, which inhibits NADH oxidation, antimycin A for Complex III and KCN, a competitive inhibitor of cytochrome c oxidase-Complex IV) were used as described in Methods. The results suggest that, treatment with glyLDL (100 µg/ml) for 24 h significantly reduced the specific oxygen consumption rate in Complex I, II/III and IV in HUVEC compared to that of oxygen consumption rate of control HUVEC **($p<0.05$ or <0.01, Figure 10 A-C)**.

4.2.2 Respiratory Control Index (RCI) in HUVEC mitochondria treated with glyLDL

RCI is determined from the oxygen consumption level in HUVEC while ADP is added to the glass chamber. RCI is the ratio of state 3 and state 4. The state 3 is the ADP excess and state 4 is ADP limited respiration. The results indicate that glyLDL (100µg/ml) treatment in HUVEC

for 24 h induce a significant decline of RCI in HUVEC compared to the control (vehicle) for equivalent time **(p<0.01, Figure 10. D**).

4.2.3 Mitochondrial bioenergetics profile in intact non-permeabilized HUVECs treated with glyLDL

The mitochondrial bioenergetics profile parameters used in our studies are detailed below.

Basal respiration indicates the minimal or baseline oxygen consumption/respiration to support essential cellular process before addition any substrates or inhibitors in the chamber. **Maximal respiration** is the respiration induced due to ADP or an uncoupler to estimate the maximal electron transport system (ETS) in the mitochondria of a cell. **ATP linked respiration** is the rate of mitochondrial ATP synthesis in a defined basal state after inhibition of ATP synthase by oligomycin. **Non-mitochondrial respiration** is the residual respiration rate obtained in presence of electron transport inhibitors. **Respiratory control ratio** is the ratio of the uncoupled state (state 3) to the state of oligomycin present (state 4) which is analogous to RCI in permeabilized mitochondria. **Spare respiratory capacity** is the response to ETC accelerator respiration and dividing it by the basal respiration that indicates the maximum ATP production in the mitochondria of the cells. It is the extra amount of ATP that can be produced in an increased energy demand (Desler et al., 2012). **Proton leak** is non phosphorylating resting state of the intrinsic uncoupled state of respiration, where heat production occurs and inhibition of the phosphorylation system. **Coupling efficiency** measures the ATP turnover in mitochondria. It is the fraction of basal respiration used for ATP synthesis.

The present study investigated the mitochondrial bioenergetics profile in intact non-permeabilized mitochondria of cultured HUVEC induced with of glyLDL (100 µg/ml) and vehicle (control) for 24 h. The representative Oxygraph tracing of the altered mitochondrial

bioenergetics profile in intact non-permeabilized HUVEC (Control versus glyLDL) obtained from Oxygraph-2k were represented in (**Figure 11).**

Mitochondrial bioenergetics measures the cellular respiration and the utilization of energy in the cells. Bioenergetics profile was assessed by quantifying the oxygen consumption from intact HUVEC using Oxygraph-2k without permeabilizing the cells. Oxygen consumption was determined in intact cells suspended in mitochondrial respiratory medium in order to simulate *in-vivo* condition at 37 °C in Oxygraph chambers. The bioenergetics parameters were assessed to characterize the cellular aerobic energy production in EC. In order to evaluate the bioenergetics parameters, HUVECs were sequentially treated with oligomycin, FCCP, and rotenone combined with antimycin-A as described previously (Roy Chowdhury et al., 2012).

The oxygen consumption without any addition of substrates or inhibitors reveals the physiological respiration in cells. Addition of oligomycin inhibits the ATP synthesis and shows the non-phosphorylating respiration in the inner mitochondrial membrane. FCCP stimulates the oxygen consumption by uncoupling the oxidative phosphorylation and measures the maximum electron transport system (ETS).

The effect of glyLDL on mitochondrial bioenergetics in EC has not been documented to our knowledge. The results indicate a significant reduction in bioenergetics parameters including basal, maximal and ATP linked respiration, coupling efficiency and spare respiratory capacity in glyLDL treated HUVECs compared to control HUVECs. However, no significant alterations in non-mitochondrial respiration and respiratory control ratio were detected. Impaired mitochondrial electron transport system in HUVECs exposed to glyLDL is represented in (**Figure 12. A-G)**.

Figure 9

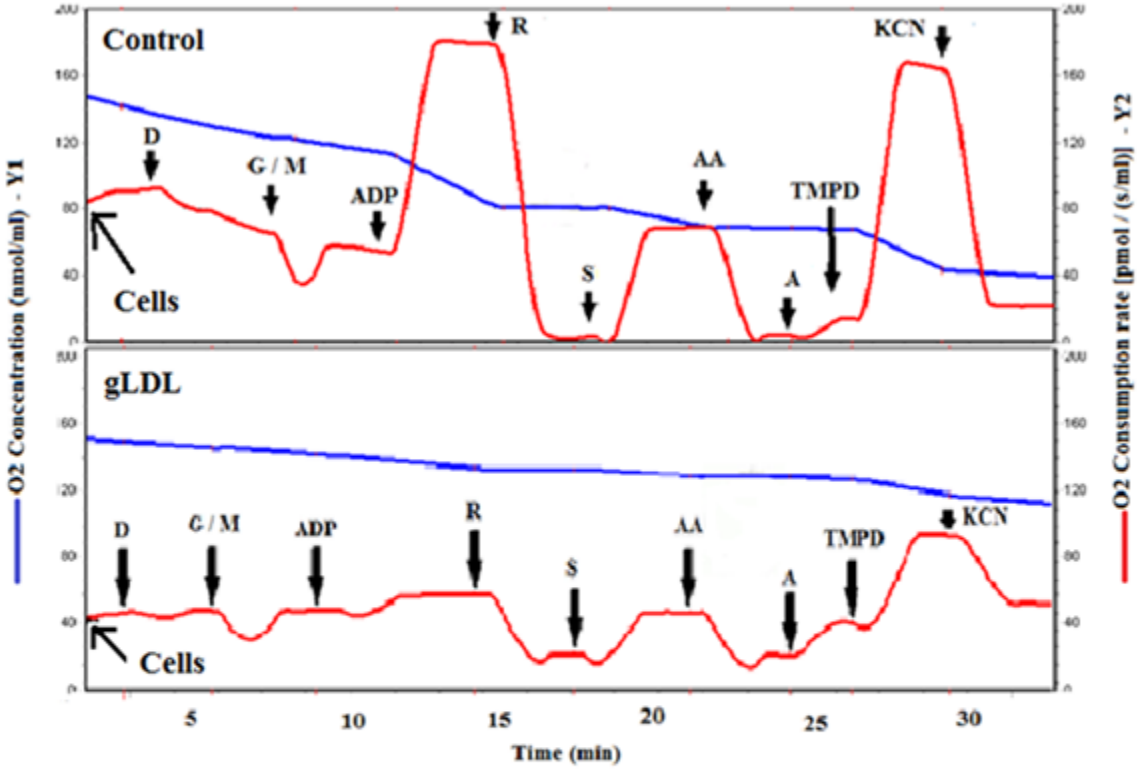

D-Digitonin
G-Glutamate
M-Malate
ADP-Adenosine diphosphate
R-Rotenone
S-Succinate
AA-Antimycin-A
A-Ascorbate
TMPD-N,N,N',N'-tetramethyl-1,4-benzenediamine, dihydrochloride
KCN-Potassium cyanide

Figure 9: Representative Oxygraph tracings of mitochondrial oxygen consumption in permeabilized HUVEC using complex specific substrates and inhibitors

The oxygen consumption in HUVEC was measured using oxygraph-2k. Arrows indicate addition of 2.5 x10^6 cells/ml and following substrates or inhibitors as abbreviated. D: digitonin (2 µg/10^6 cells); G: glutamate (10 mM); M: malate (5 mM); ADP: adenosine diphosphate (2 mM); R: rotenone (1 µM); S: succinate (10 mM); AA: antimycin A (1 µg/mL); A: ascorbate (5 mM);

TMPD: N,N,N',N'-tetramethyl-p-phenylenediamine dihydrochloride (0.5 mM); KCN: potassium cyanide (0.25 mM). Y1 (thin blue line): Decline of oxygen concentration in the chamber of Oxygraph containing live EC. Y2 (thick red line): Oxygen consumption rate in response to substrates and inhibitors for mitochondrial respiratory chain Complexes I-IV in HUVEC mitochondria.

Figure 10

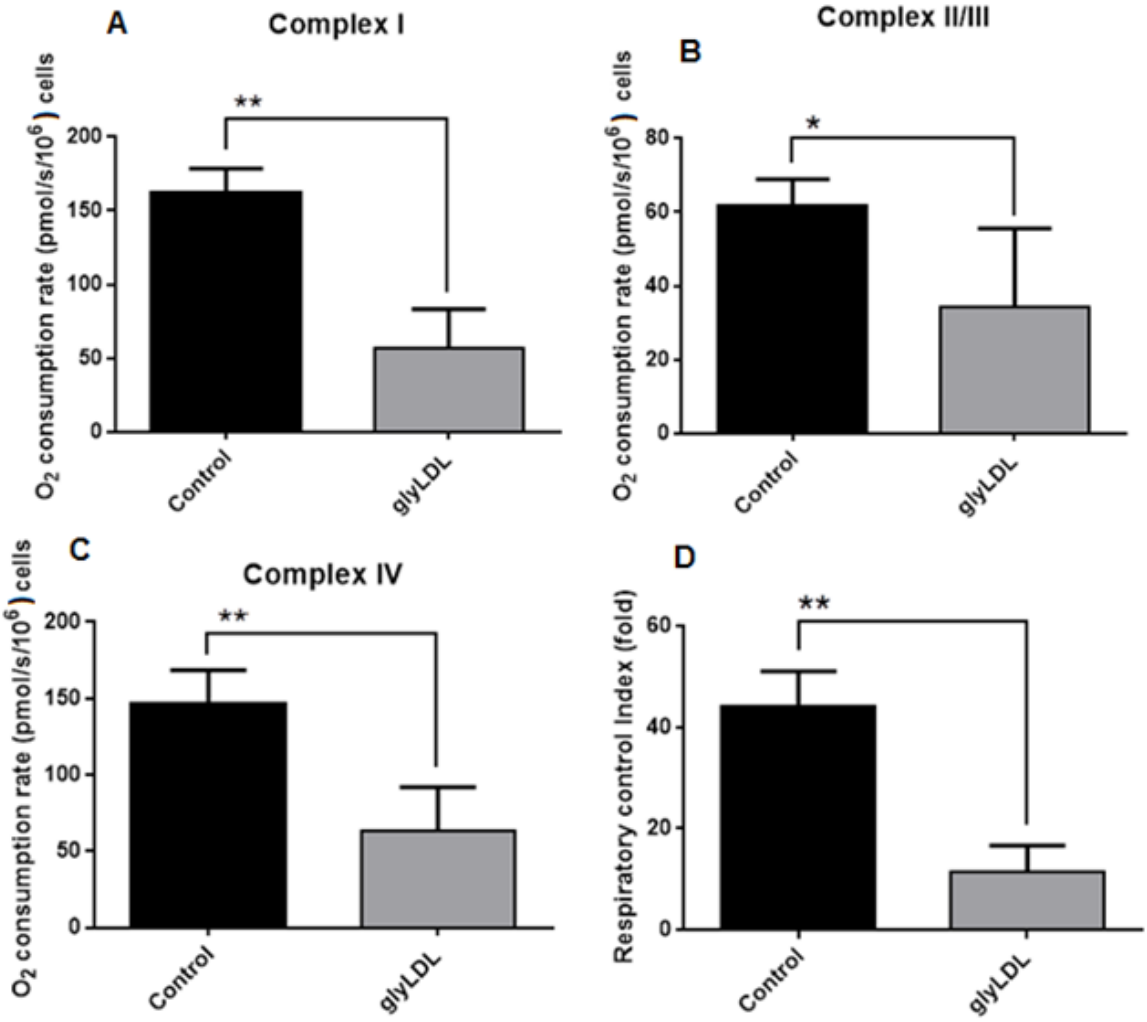

Figure 10: Effect of glyLDL on the mitochondrial respiratory chain complexes and respiratory control index (RCI) in permeabilized HUVEC mitochondria by Oxygraph-2k

Effect of glyLDL on O_2 consumption in Complex I, II + III, and IV in mitochondria of HUVEC was assessed using oxygraph-2k. HUVEC was treated with 100 µg/ml of glyLDL for 24 h. **Panel A:** Oxygen consumption in Complex I, evaluated in the presence of glutamate + malate + ADP followed by the addition of rotenone. **Panel B:** Complex II/III respiration assessed with succinate-coupled oxygen consumption followed by addition of antimycin A. **Panel C**: Complex

IV respiration evaluated by KCN-sensitive oxygen consumption induced by ascorbate + TMPD. **Panel D:** Respiratory Control Index was measured from oxygen consumption rate in HUVEC. RCI= ratio of state 3 and state 4 respiration. Integrated data were expressed in pmol O_2/s/10^6 cells after normalization with cell number (mean ± SD, n = 3 experiments) *, **; $p<0.05$ or 0.01 versus control.

Figure 11

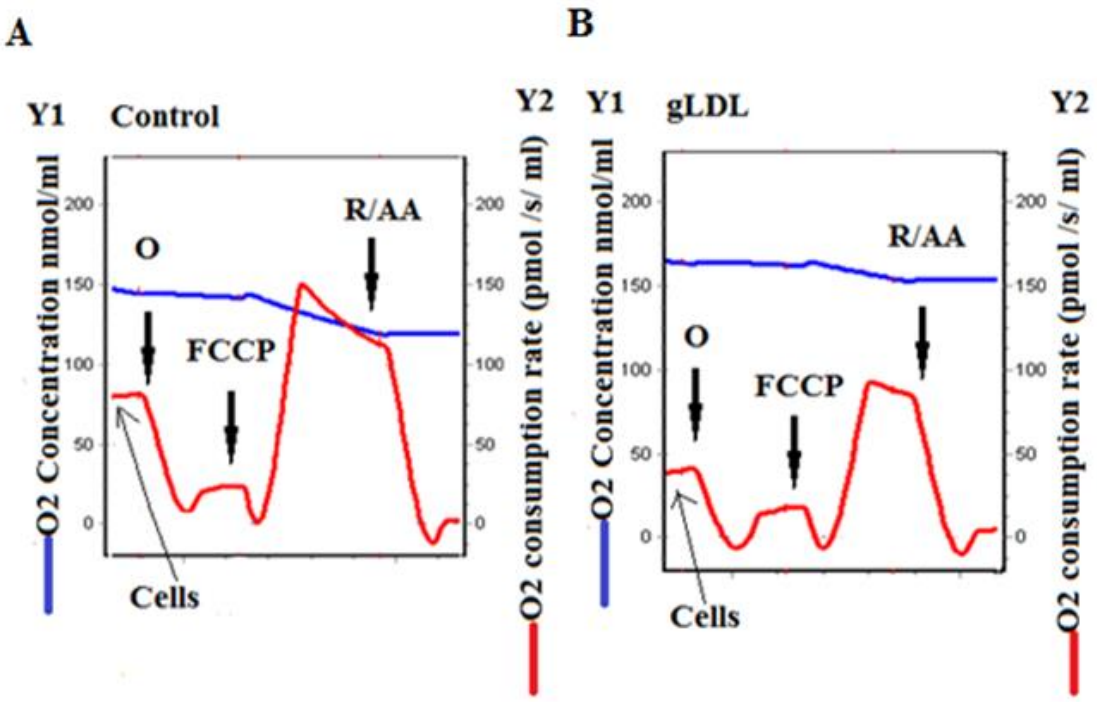

Figure 11: Representative Oxygraph tracings of altered mitochondrial bioenergetics profile in cultured HUVEC treated with control and glyLDL

HUVECs were incubated with 100 µg/ml of glyLDL or vehicle (control) for 24 h. Mitochondrial bioenergetics profile was assessed in HUVECs by measuring the oxygen consumption rate using oxygraph-2k. Arrows indicate addition of HUVEC at a concentration of 2.5 x 10^6 cells/ml and following substrates, uncoupler or inhibitors. O: oligomycin (1 µM); FCCP: carbonyl cyanide p-trifluoromethoxy phenylhydrazone (1 µM); AA: antimycin A (1 µg/mL) R: Rotenone (1 µM).

Figure 12

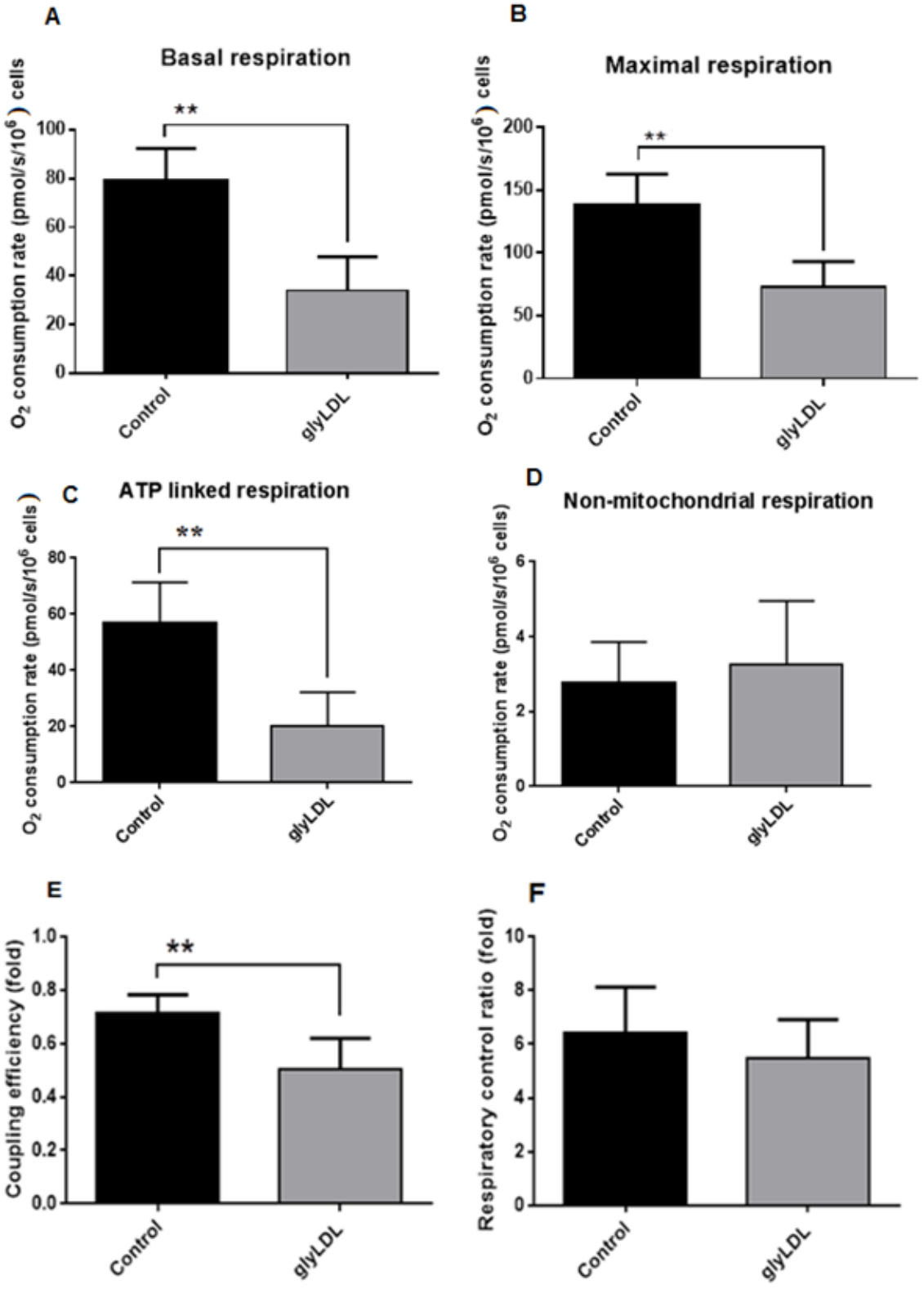
A
Basal respiration
O_2 consumption rate (pmol/s/10^6) cells
**
Control
glyLDL
B
Maximal respiration
O_2 consumption rate (pmol/s/10^6) cells
**
Control
glyLDL
C
ATP linked respiration
O_2 consumption rate (pmol/s/10^6 cells)
**
Control
glyLDL
D
Non-mitochondrial respiration
O_2 consumption rate (pmol/s/10^6 cells)
Control
glyLDL
E
Coupling efficiency (fold)
**
Control
glyLDL
F
Respiratory control ratio (fold)
Control
glyLDL

Figure 12

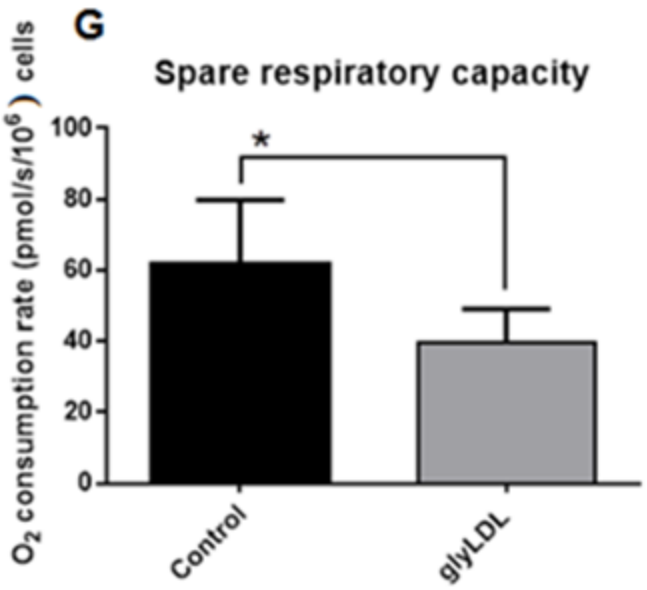

Figure 12: Effect of glyLDL on the mitochondrial bioenergetics profile in intact mitochondria of control and glyLDL-treated HUVEC

HUVECs were treated with 100 µg/ml of glyLDL and control (vehicle) for 24 h. The oxygen consumption rate in intact mitochondria of HUVECs was measured using Oxygraph-2k. Mitochondrial bioenergetics profile was assessed from the oxygen consumption rate values obtained from control versus glyLDL treated HUVEC. The mitochondrial bioenergetics profile including, basal respiration **(A)**, maximal respiration **(B)**, ATP-Linked respiration **(C)**, non-mitochondrial respiration **(D)**, coupling efficiency **(E)**, respiratory control ratio **(F)** and spare respiratory capacity **(G)** were determined after sequential addition of oligomycin, FCCP and rotenone combined with antimycin-A in HUVEC as represented as in **Figure 12.** Integrated data

were expressed in pmol O_2/s/10^6 cells after normalization with the cell number (mean ± SD, n = 3 experiments) *, **; $p<0.05$ or 0.01 versus control.

4.3 Platelet mitochondrial bioenergetics in healthy subjects

4.3.1 Assessment of mitochondrial bioenergetics profile in intact healthy human platelets

This study investigated the mitochondrial bioenergetics profile in intact non-permeabilized platelet mitochondria from healthy human donor by measuring the oxygen consumption rate using Oxygraph-2k. Platelets were freshly isolated from blood plasma of 48 healthy donors (after 12 h fasting) using centrifugation and counted on a hemocytometer. The platelets were incubated in Oxygraph chambers at a concentration of 100×10^6 platelets/ml. These were treated sequentially with oligomycin, FCCP and rotenone combined with antimycin-A as substrates and inhibitors as described in the Methods using similar parameters explained under **section 6.2.3.** Non-permeabilized cells can be used for determining the mitochondrial bioenergetics parameters as the substrates and inhibitors involved in these studies can easily access or cross through the cell membrane without permeabilizing using digitonin.

Forty-eight healthy donors were grouped based on their gender, age, body mass index (BMI) and family history of chronic metabolic diseases as shown in demographic data **(Table: 7)**. The healthy donors consist of 16 males and 32 females with an average age of 35.01 ±14.01 years and 41.21 ± 13.24 years respectively. The healthy donors were aged between 18-67 years with a mean age of 37.89 ± 13.63 yrs. The average BMI of the healthy donors was 24.81 ± 4.67 kg/m^2. The first-degree family history of diabetes was self-reported by eight donors; heart disease by seven donors, and no family history of diabetes or heart disease among 33 healthy donors. The mitochondrial bioenergetics profile in human platelets can be assessed from peripheral blood using Oxygraph-2k which is represented as in (**Figure 13)**. This study involves a non-surgical and minimal pain procedure for determination of mitochondrial function using

blood cells compared to the classical muscle biopsy, which requires a small surgical procedure. The assessment of mitochondrial function in platelets can be performed in clinical laboratory using peripheral blood samples from donors. Platelets can serve as excellent biomarkers for the determination of mitochondrial function in humans. Mitochondrial bioenergetics profile including basal respiration, maximal respiration, ATP linked respiration, non-mitochondrial respiration, coupling efficiency, respiratory control ratio and spare respiratory capacity were not significantly altered by variation in gender as represented in **(Figure 14, A-G)**, variation in age as represented in **(Figure 15, A-G)**, and variation in BMI as represented in **(Figure 16, A-G)**, among healthy subjects. However healthy donors with a first degree family history of diabetes have significantly impaired mitochondrial bioenergetics profile including basal respiration, maximal respiration, ATP linked respiration and non-mitochondrial respiration, but coupling efficiency, respiratory control ratio and spare respiratory capacity were not significantly different from healthy donors without a first degree family history of diabetes or heart disease (**Figure 17, A-G)**. These raw oxygen consumption rate (OCR) data is represented in (**Table: 8)** which indicates the significant impairment in platelet mitochondrial bioenergetics profile among healthy donors with a first degree family history of diabetes compared to healthy donors without any family history of chronic metabolic diseases.

Demographic Data - Healthy human donors	
	Average
Males (n=16)	35.01 ± 14.01 yrs.
Females (n=32)	41.21 ± 13.24 yrs.
Age (18-67 yrs.)	37.89 ± 13.63 yrs.
Mean BMI (kg/m^2)	24.81 ± 4.67
First-degree family history*	**Number of healthy donors**
Diabetes (male=4, female=4)	n=8
Heart disease (male=1, female=5)	n=6
No Family History (male=11, female=23)	n=34
Total healthy donors (male=16, female= 32)	n=48
* First-degree family history (self-reported), type 1 Diabetes was not excluded	

Table: 7 Demographic data including age, gender, body mass index and family history obtained from the healthy human donors.

Mitochondrial bioenergetics profile	**No family history** Mean oxygen consumption rate (OCR)	**Diabetes family history** Mean oxygen consumption rate (OCR)
Basal respiration	105.25 ± 25.25	65.82 ± 13.19**
Maximal respiration	129.81 ± 29.08	107.14 ± 30.01**
ATP- linked oxygen consumption	75.54 ± 35.94	45.64 ± 16.96**
Non-mitochondrial respiration	8.77 ± 3.44	11.37 ± 3.44**

Table: 8 The bioenergetics profiles (OCR) data obtained from healthy donors with and without family history of diabetes.

OCR from individual mitochondrial bioenergetics profile from healthy donors with family history of diabetes and without any family history of diabetes. Data are represented by mean ± SD,*, **; $p<0.05$ or 0.01 are considered significant. All values are expressed in pmol $O_2/s/10^6$ cells.

Figure 13

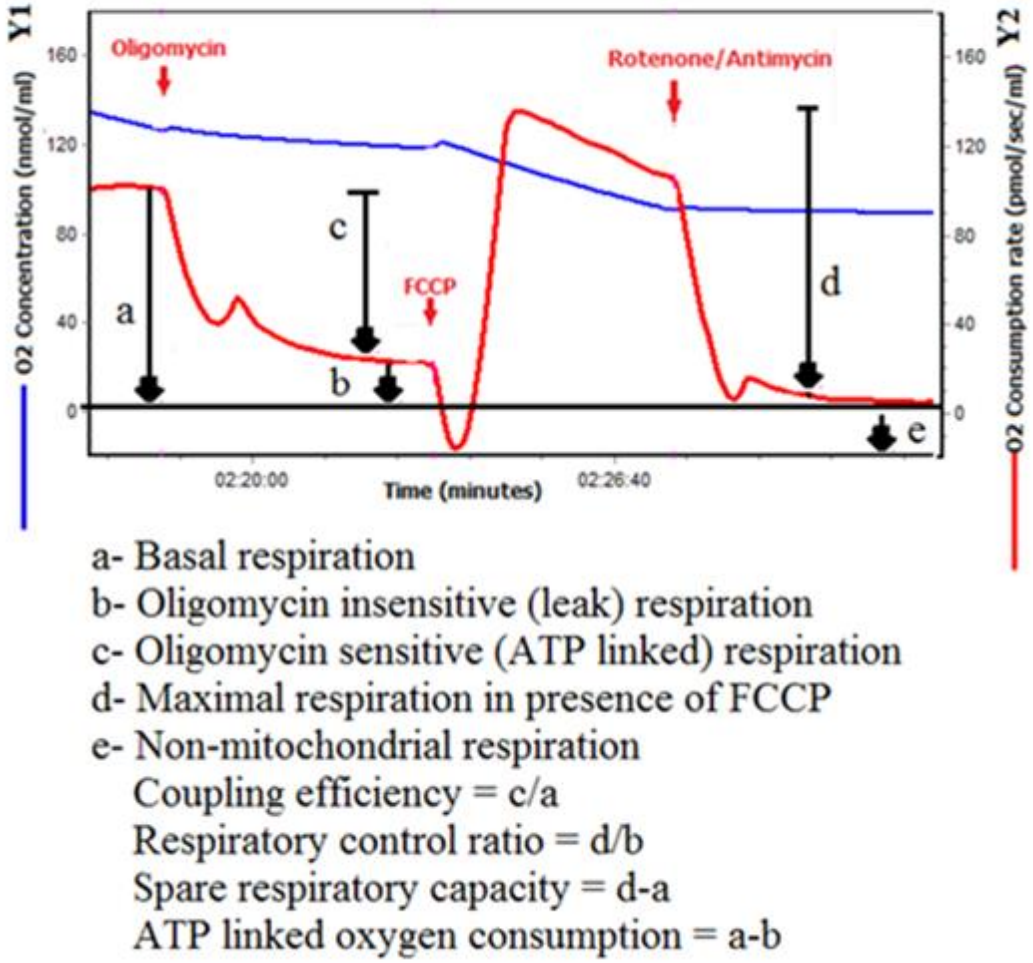

Figure 13: Representative Oxygraph tracing of mitochondrial bioenergetics profile in healthy human platelets

Platelets were freshly isolated and incubated in oxygraph-2k chambers in mitochondrial respiratory medium at a concentration of 100 x 10^6 platelets/ml for the determination of mitochondrial bioenergetics. Mitochondrial bioenergetics profile was assessed in platelets by measuring the oxygen consumption rate. Arrows indicate addition of following substrates,

uncoupler or inhibitors. O: oligomycin (1 µM); FCCP: carbonyl cyanide p-trifluoromethoxy phenylhydrazone (1 µM); AA: antimycin A (1 µg/mL) R: Rotenone (1 µM).

Figure 14

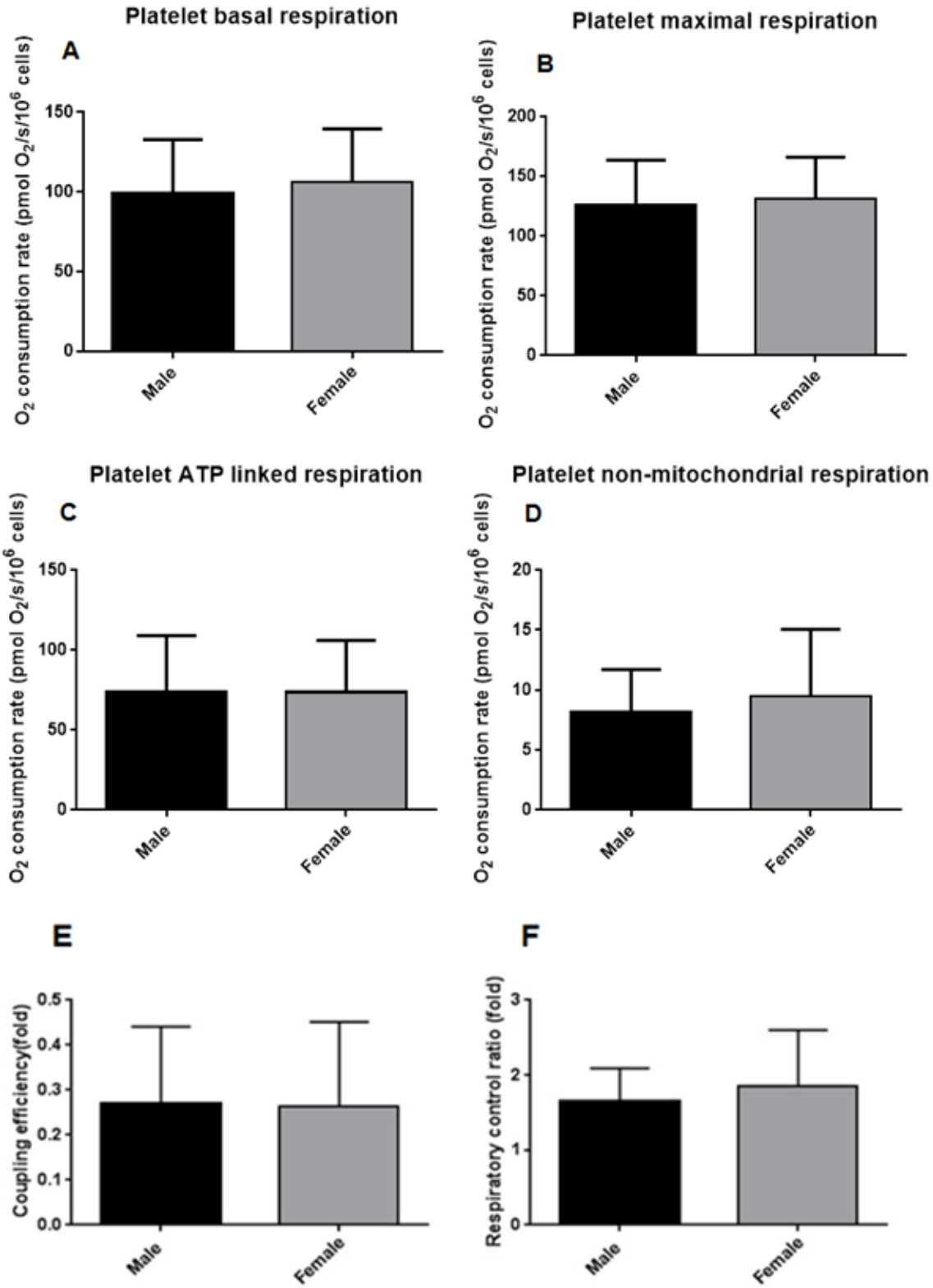
Platelet basal respiration
A
O_2 consumption rate (pmol O_2/s/10^6 cells)
150
100
50
0
Male
Female
Platelet maximal respiration
B
O_2 consumption rate (pmol O_2/s/10^6 cells)
200
150
100
50
0
Male
Female
Platelet ATP linked respiration
C
O_2 consumption rate (pmol O_2/s/10^6 cells)
150
100
50
0
Male
Female
Platelet non-mitochondrial respiration
D
O_2 consumption rate (pmol O_2/s/10^6 cells)
20
15
10
5
0
Male
Female
E
Coupling efficiency(fold)
0.5
0.4
0.3
0.2
0.1
0.0
Male
Female
F
Respiratory control ratio (fold)
3
2
1
0
Male
Female

Figure 14

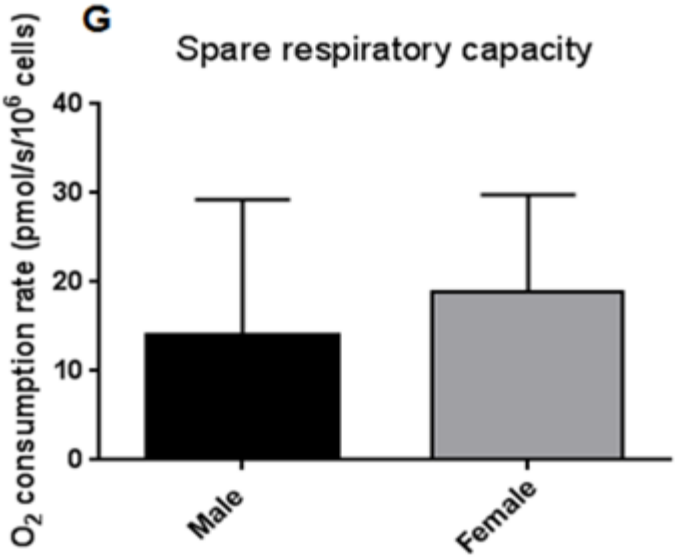

Figure 14: Gender variation and mitochondrial bioenergetics profile in intact mitochondria of platelets from healthy donors

The mitochondrial bioenergetics profile including basal respiration **(A)**, maximal respiration **(B)**, ATP-linked respiration **(C)**, non-mitochondrial respiration **(D)**, coupling efficiency **(E)**, respiratory control ratio **(F)** and spare respiratory capacity **(G)** were determined after sequential addition of oligomycin, FCCP and rotenone combined with antimycin-A on mitochondria of platelets from healthy donors. Integrated data were expressed in pmol O_2/s/10^6 cells after normalization with the cell number (mean ± SD).

Figure 15

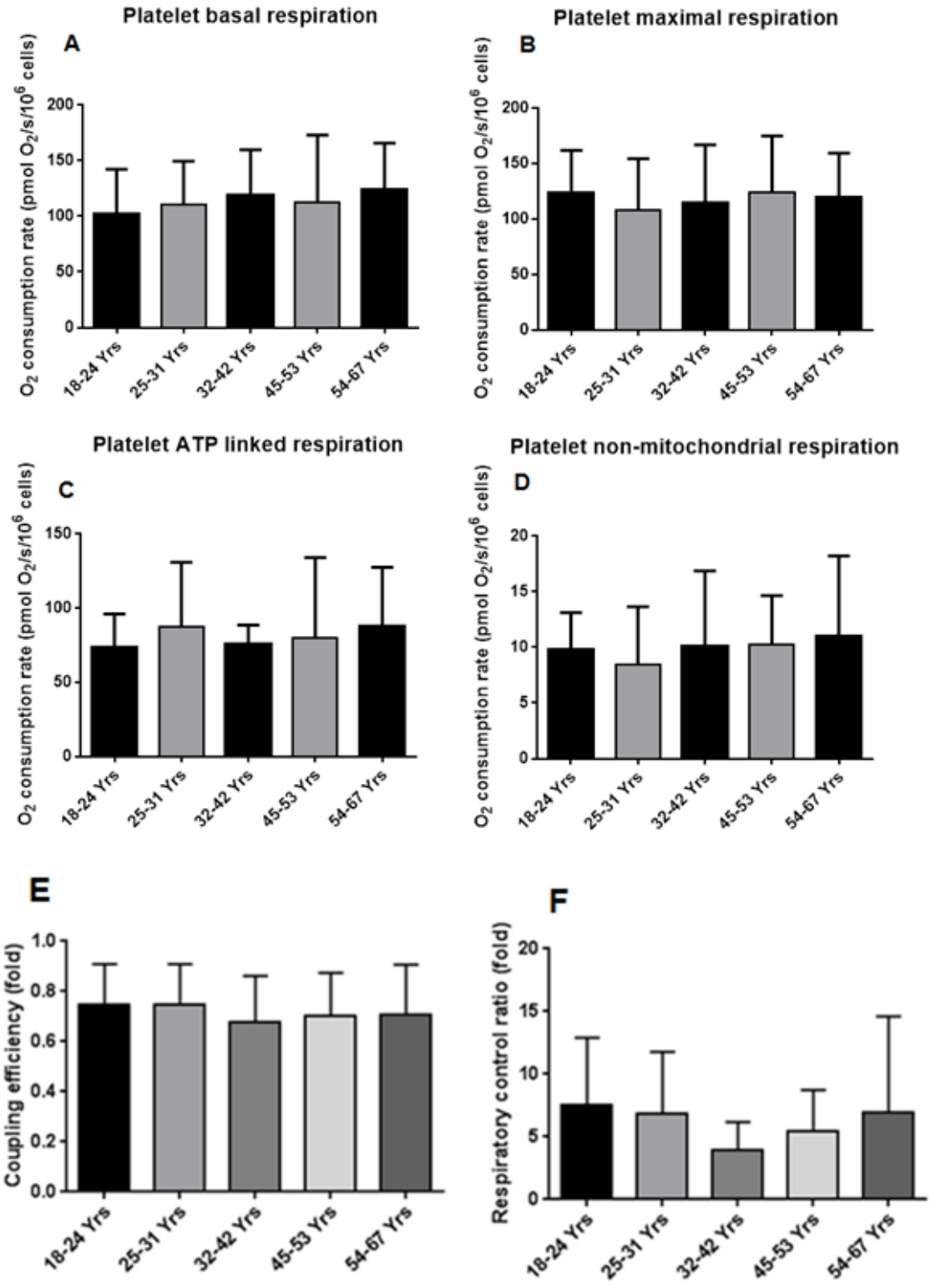
Platelet basal respiration
A
O_2 consumption rate (pmol O_2/s/10^6 cells)
200
150
100
50
0
18-24 Yrs
25-31 Yrs
32-42 Yrs
45-53 Yrs
54-67 Yrs
Platelet maximal respiration
B
O_2 consumption rate (pmol O_2/s/10^6 cells)
200
150
100
50
0
18-24 Yrs
25-31 Yrs
32-42 Yrs
45-53 Yrs
54-67 Yrs
Platelet ATP linked respiration
C
O_2 consumption rate (pmol O_2/s/10^6 cells)
150
100
50
0
18-24 Yrs
25-31 Yrs
32-42 Yrs
45-53 Yrs
54-67 Yrs
Platelet non-mitochondrial respiration
D
O_2 consumption rate (pmol O_2/s/10^6 cells)
20
15
10
5
0
18-24 Yrs
25-31 Yrs
32-42 Yrs
45-53 Yrs
54-67 Yrs
E
Coupling efficiency (fold)
1.0
0.8
0.6
0.4
0.2
0.0
18-24 Yrs
25-31 Yrs
32-42 Yrs
45-53 Yrs
54-67 Yrs
F
Respiratory control ratio (fold)
20
15
10
5
0
18-24 Yrs
25-31 Yrs
32-42 Yrs
45-53 Yrs
54-67 Yrs

Figure 15

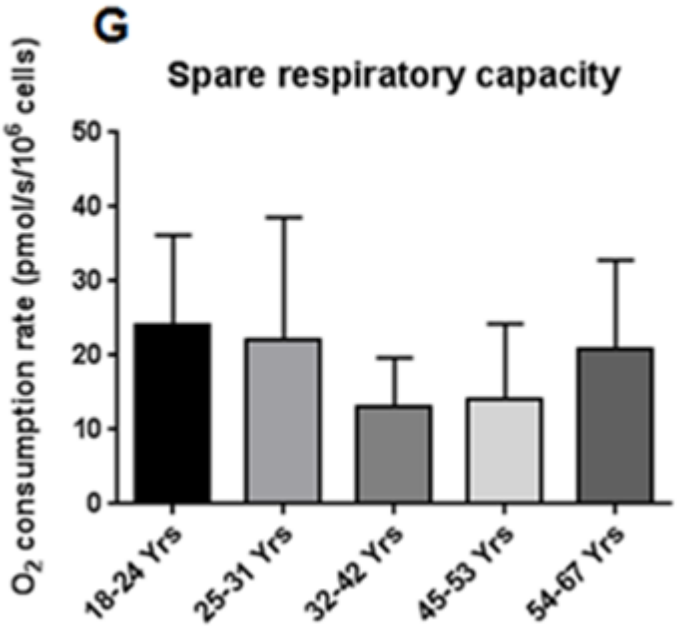

Figure 15: Age variation and mitochondrial bioenergetics profile in intact mitochondria of platelets from healthy donors

The mitochondrial bioenergetics profile including basal respiration **(A)**, maximal respiration **(B)**, ATP-linked respiration **(C)**, non-mitochondrial respiration **(D)**, coupling efficiency **(E)**, respiratory control ratio **(F)** and spare respiratory capacity **(G)** were determined after sequential addition of oligomycin, FCCP and rotenone combined with antimycin-A on mitochondria of platelets from healthy donors. Integrated data were expressed in pmol O_2/s/10^6 cells after normalization with the cell number (mean ± SD).

Figure 16

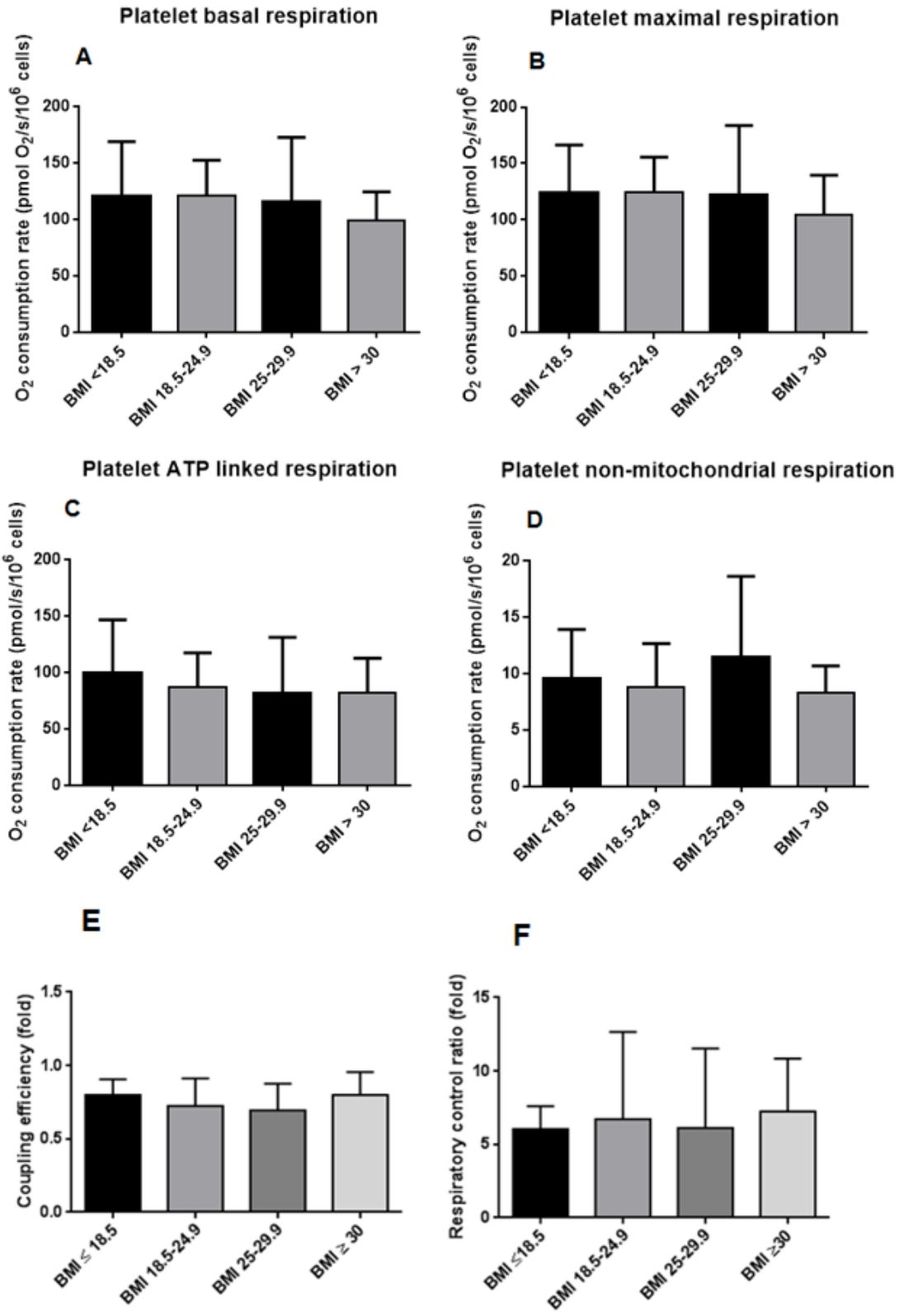
Platelet basal respiration
A
O_2 consumption rate (pmol O_2/s/10^6 cells)
200
150
100
50
0
BMI <18.5
BMI 18.5-24.9
BMI 25-29.9
BMI > 30
Platelet maximal respiration
B
O_2 consumption rate (pmol O_2/s/10^6 cells)
200
150
100
50
0
BMI <18.5
BMI 18.5-24.9
BMI 25-29.9
BMI > 30
Platelet ATP linked respiration
C
O_2 consumption rate (pmol/s/10^6 cells)
200
150
100
50
0
BMI <18.5
BMI 18.5-24.9
BMI 25-29.9
BMI > 30
Platelet non-mitochondrial respiration
D
O_2 consumption rate (pmol/s/10^6 cells)
20
15
10
5
0
BMI <18.5
BMI 18.5-24.9
BMI 25-29.9
BMI > 30
E
Coupling efficiency (fold)
1.5
1.0
0.5
0.0
BMI ≤ 18.5
BMI 18.5-24.9
BMI 25-29.9
BMI ≥ 30
F
Respiratory control ratio (fold)
15
10
5
0
BMI ≤18.5
BMI 18.5-24.9
BMI 25-29.9
BMI ≥30

Figure 16

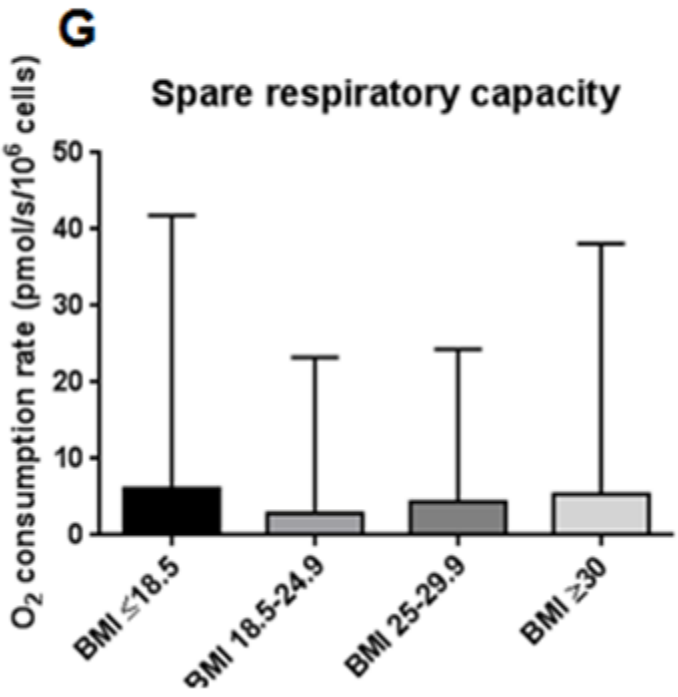

Figure 16: Body mass index variation and mitochondrial bioenergetics profile in intact mitochondria of platelets from healthy donors

The mitochondrial bioenergetics profile including basal respiration **(A)**, maximal respiration **(B)**, ATP-linked respiration **(C)**, non-mitochondrial respiration **(D)**, coupling efficiency **(E)**, respiratory control ratio **(F)** and spare respiratory capacity **(G)** were determined after sequential addition of oligomycin, FCCP and rotenone combined with antimycin-A on mitochondria of platelets from healthy donors. Integrated data were expressed in pmol O_2/s/10^6 cells after normalization with the cell number (mean ± SD).

Figure 17

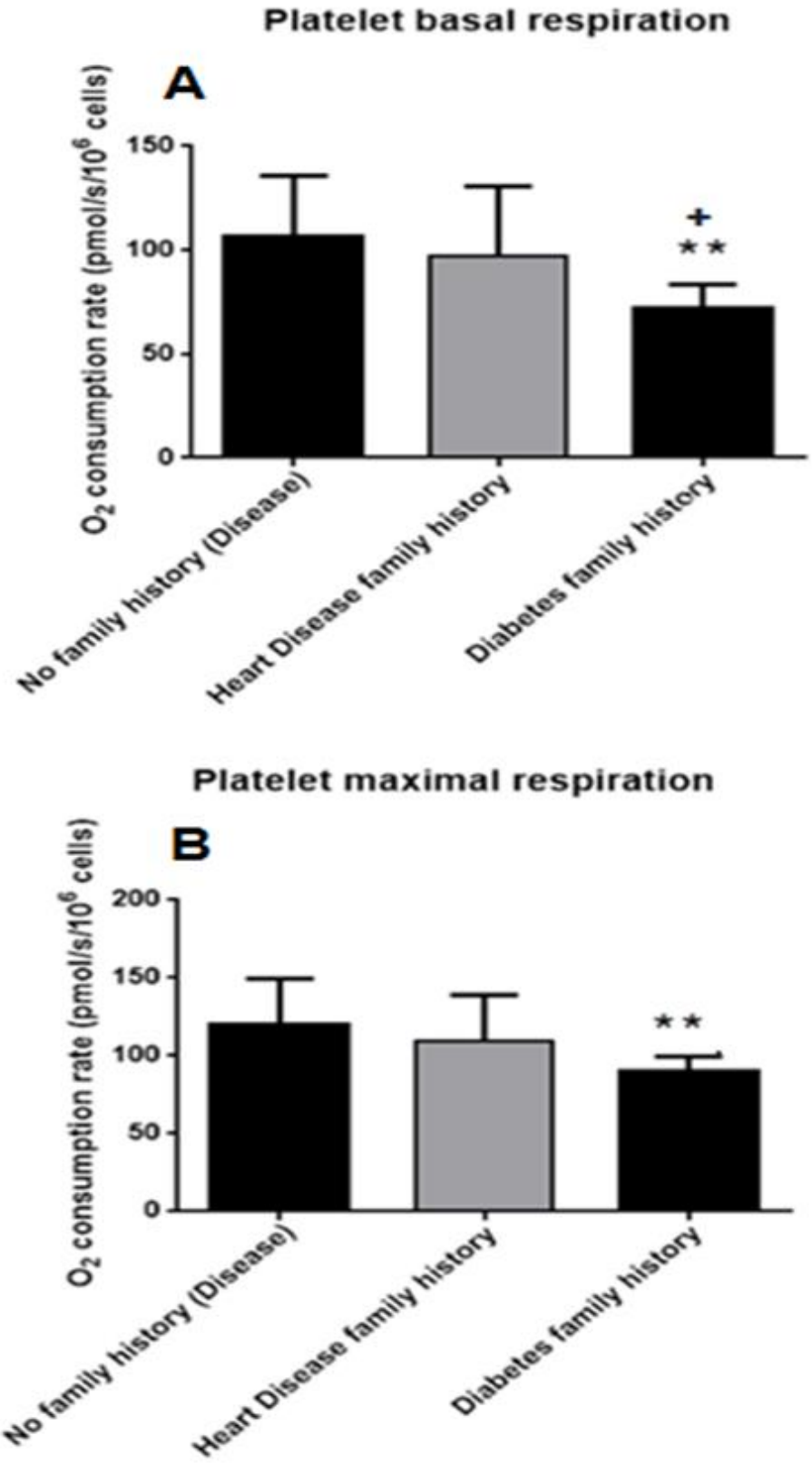
Platelet basal respiration
A
O_2 consumption rate (pmol/s/10^6 cells)
150
100
50
0
+
**
No family history (Disease)
Heart Disease family history
Diabetes family history
Platelet maximal respiration
B
O_2 consumption rate (pmol/s/10^6 cells)
200
150
100
50
0
**
No family history (Disease)
Heart Disease family history
Diabetes family history

Figure 17

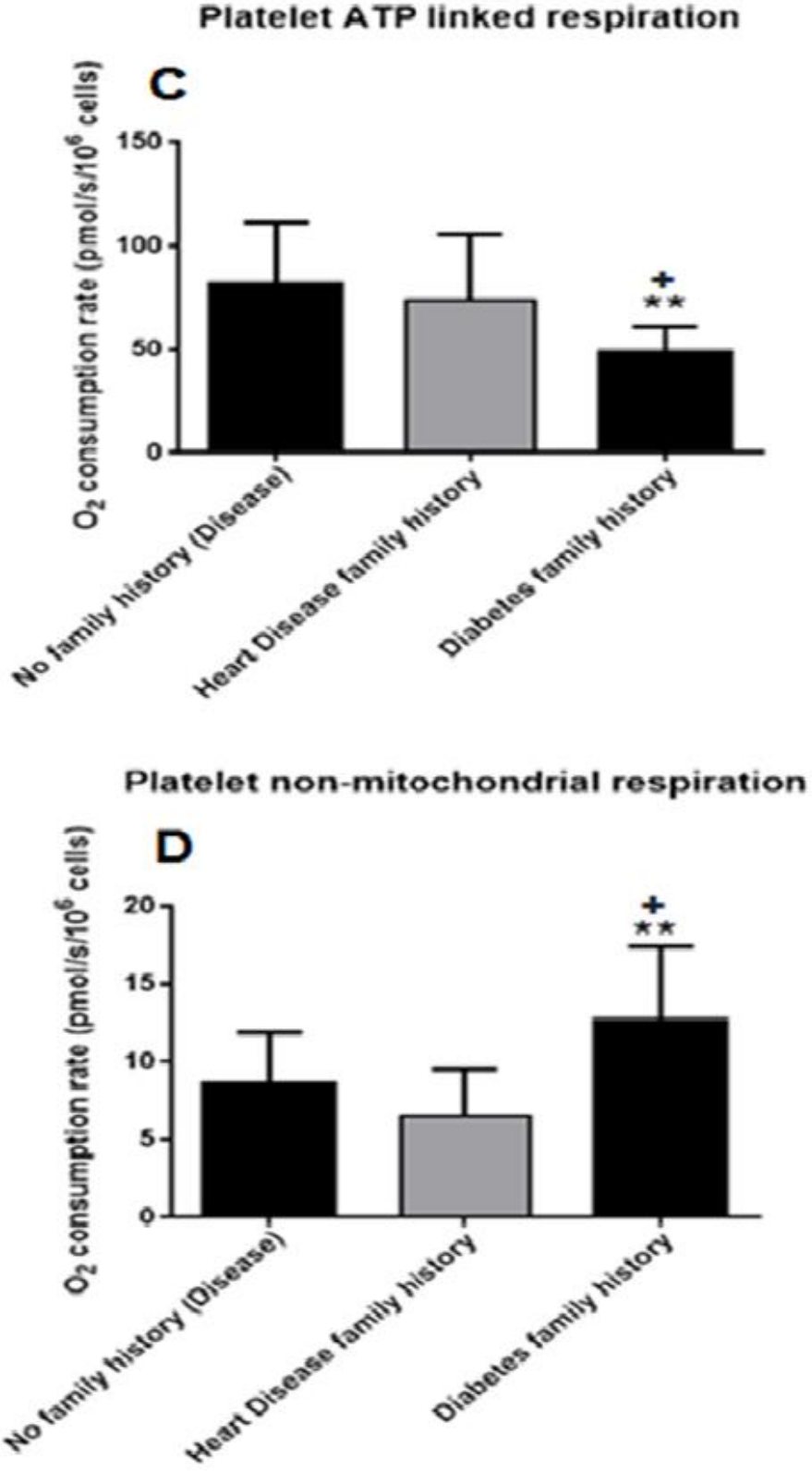
Platelet ATP linked respiration
C
O_2 consumption rate (pmol/s/10^6 cells)
150
100
50
0
+
**
No family history (Disease)
Heart Disease family history
Diabetes family history
Platelet non-mitochondrial respiration
D
O_2 consumption rate (pmol/s/10^6 cells)
20
15
10
5
0
+
**
No family history (Disease)
Heart Disease family history
Diabetes family history

Figure 17

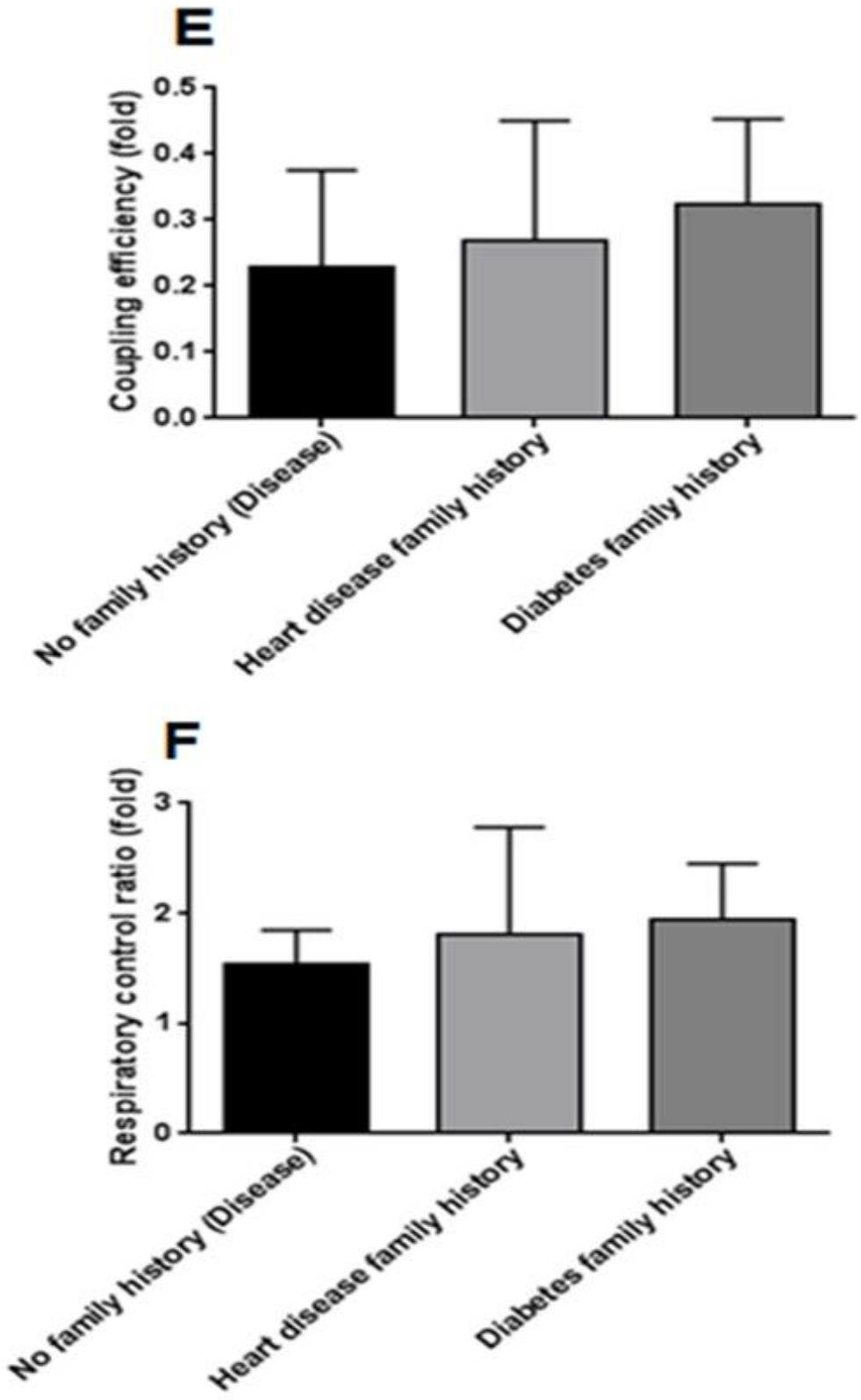
E
Coupling efficiency (fold)
0.5
0.4
0.3
0.2
0.1
0.0
No family history (Disease)
Heart disease family history
Diabetes family history
F
Respiratory control ratio (fold)
3
2
1
0
No family history (Disease)
Heart disease family history
Diabetes family history

Figure 17

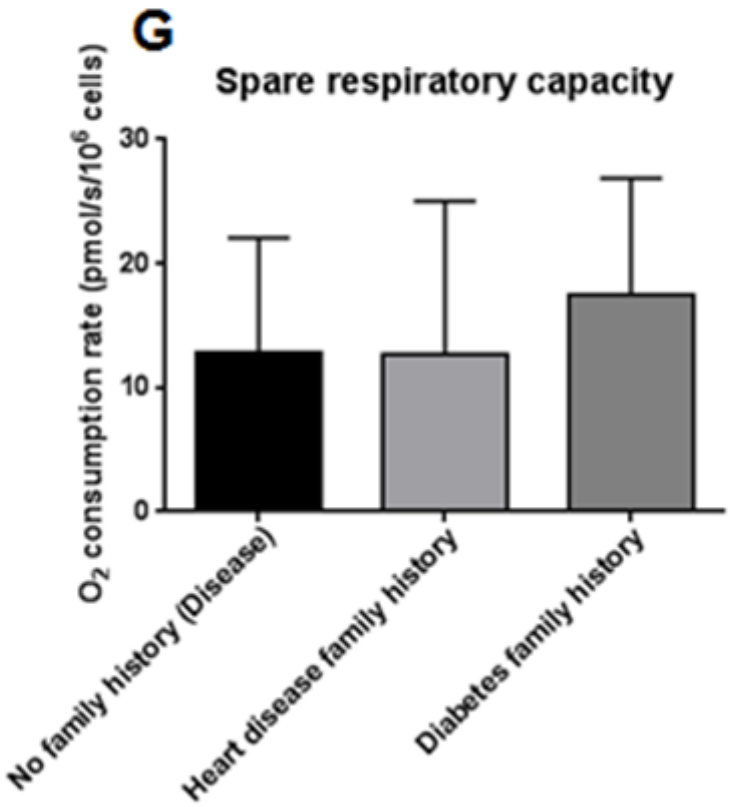

Figure 17: Family history and mitochondrial bioenergetics profile in intact mitochondria of platelets from healthy donors

The mitochondrial bioenergetics profile including basal respiration **(A)**, maximal respiration **(B)**, ATP-linked respiration **(C)**, non-mitochondrial respiration **(D)**, coupling efficiency **(E)**, respiratory control ratio **(F)** and spare respiratory capacity **(G)** were determined after sequential addition of oligomycin, FCCP and rotenone combined with antimycin-A on mitochondria of platelets from healthy donors.. Integrated data were expressed in pmol O_2/s/10^6 cells after normalization with the cell number (mean ± SD). *, **; p<0.05 or 0.01versus no family history; +, ++: p<0.05 or 0.01 versus heart disease family history.

Chapter 5

Discussion

The results from our studies observed the following significant novel findings:

1. Exposure to physiological concentrations of glyLDL decreased the protein, activity and mRNA of eNOS in cultured HUVEC.
2. RAGE/H-Ras pathway mediates the upstream signaling for glyLDL-induced inhibition of eNOS protein in EC.
3. GlyLDL treatment impaired the mitochondrial bioenergetics profile in cultured HUVEC.
4. Healthy donors with a first degree family history of diabetes have significantly impaired platelet mitochondrial bioenergetics profile compared to healthy subjects without a family history of heart disease or diabetes.

5.1 Effect of glyLDL on the eNOS production and transmembrane upstream signaling events in EC

Previous studies have identified that glycooxided LDL down regulated eNOS in human coronary artery EC (Napoli et al., 2002). Glyco-oxidized LDL attenuated endothelial function potently than oxLDL by impairment of endothelium-dependent dilation in rabbit aorta (Galle et al., 1998). GlyLDL reduced the shear stress-induced NO production and bioactivity in the porcine aortic EC due to increased release of superoxide (Posch et al., 1999). 'Heavily oxidized' glycated LDL (HOG-LDL) attenuated the eNOS protein in bovine aortic EC, without altering eNOS mRNA levels. Impaired acetylcholine-induced endothelium-dependent vasorelaxation was observed in isolated mouse aortas, and the activation of protease calpain impaired eNOS function by its degradation (Dong et al., 2009). OxLDL treatment in human saphenous vein reduced the

NOS activity and eNOS mRNA levels, which may result from early transcriptional inhibition or post-transcriptional mRNA destabilization (Liao et al., 1995). Glycation of collagen inhibited the actin fiber filament, eNOS activation, NO release and translocation in EC exposed to shear stress; moreover it impaired the mechanotransduction in EC (Kemeny et al., 2011). It has not been documented yet in the literature whether LDL modified by glycation alone without chemical oxidation altered eNOS protein, activity or gene expression.

The present study demonstrated the significant reduction of the eNOS protein, mRNA expression and activity in HUVEC treated with glyLDL compared to vehicle control or LDL. The down-regulation of eNOS protein and activity is likely due to decreased transcription of eNOS gene or an increased degradation of eNOS mRNA or both.

High glucose (25mM) also down-regulated the expression of eNOS protein in EC, which is consistent with the several studies favoring similar attenuation of eNOS in EC in increased glucose conditions (Chen et al., 2015; Srinivasan et al., 2004; Zhu et al., 2015). Glucose and glyLDL have distinct receptors for its entry into the EC. Glucose usually enters most cells through GLUT receptors, while glyLDL is identified to enter through the RAGE receptors from our previous lab studies in EC (Sangle, Zhao, et al., 2010). The effect of glucose in down-regulating the eNOS may also be a consequence of the formation of glycated albumin in the medium containing fetal bovine serum supplemented in EC. Glycated albumin, as it's a glycated protein use the similar RAGE pathway for its action in down-regulating the eNOS protein in EC (Collison et al., 2002). The eNOS downregulation in eNOS due to high glucose can be RAGE independent or dependent, which needs further investigation using RAGE specific siRNA or RAGE inhibitors to find out the exact mechanism behind it.

Studies done previously have demonstrated that the uptake of LDL by the LDLR is reduced by glycation that may lead to an increased level of glyLDL in circulation (Lyons, 1993).Studies conducted previously in our lab have shown that glyLDL increased the abundance of RAGE in vascular EC (Sangle, Zhao, et al., 2010). LDLR is the receptor that regulates the LDL uptake and glyLDL is poorly recognized by the LDLR, LDL-R related protein (LRP) and the scavenger receptor (SR). Lipoprotein lipase is identified to mediate the glyLDL in macrophages, fibroblast and EC. Glycation of LDL contribute to increased atherosclerotic risk for diabetes and hyperlipidemia patients (Zimmermann et al., 2001). Glycated LDL cause injury to retinal capillary EC and pericytes and it activates extracellular signal-regulated protein kinases 1 and 2, an early mitogenic signal (Nivoit et al., 2003). The receptors for AGEs include RAGE, AGE-1, AGE-2, and AGE-3, which are detected in monocytes, macrophages, and EC. AGEs-LDL was also observed to activate Toll-like receptors (TLR-4) (Hodgkinson et al., 2008). Blockage of RAGE may be considered as a therapeutic strategy for preventing glyLDL-induced decrease in eNOS expression and decline of endothelium-dependent vasodilation in diabetes.

The effect of glyLDL on the down-regulation of eNOS protein in HUVEC was inhibited by RAGE antibody in this study. The results indicate that transmembrane signaling in glyLDL-induced downregulation of eNOS protein in cultured HUVEC is medicated by RAGE.

Previous studies demonstrated that the farnesylation was necessary for the H-Ras protein translocation from cytosol to cell membrane (Zhang and Casey, 1996). The membrane translocation and H-Ras activation in human EC is increased by LDL (Zhu et al., 2001). Our lab studies have also demonstrated previously that oxLDL increased H-Ras protein translocation from cytosol to membrane in EC. (Sangle, Zhao, et al., 2010). H-Ras inhibitor, farnesyl transferase inhibitor, FTI-276 was used to verify the participation of H-Ras in glyLDL treated

HUVEC. FTI targets the protein farnesyltransferase and inhibits its downstream effector H-Ras and its function. FTI inhibits the post-translation lipid modification of the H-Ras and alternatively prenylated by geranylgeranyl transferase-1. FTI also prevents membrane localization and reverse cellular transformation (Basso et al., 2005).

Studies conducted previously in our lab and other group have shown that glyLDL-induced ROS production and reduced the anti-oxidant enzyme activity in EC (Zhao and Shen, 2005). The source of ROS in glyLDL-treated human EC was due the activation of NADPH oxidase or impaired mitochondrial respiratory chain enzymes (Sangle, Chowdhury, et al., 2010). ROS increased the H-Ras and its downstream effector interactions (Kowluru et al., 2004). H-Ras exist either in an inactive form (GDP-bound cytosolic form) or in an active form (GTP-bound membrane-associated form). H-Ras post-translationally modifies by farnesylation to translocate from cytosol to cell membrane (Zhang and Casey, 1996). High glucose exposure leads to increased H-Ras protein and mRNA levels in EC (Kowluru et al., 2004).

In the present study, FTI-276, farnesyltransferase inhibitor prevented the glyLDL-stimulated translocation of H-Ras and also prevented glyLDL induced eNOS downregulation (normalized the eNOS protein in HUVEC. The present study confirms the previous finding that the incubation of glyLDL with HUVEC increased the H-Ras translocation from cytosol to cell membrane (Sangle, Zhao, et al., 2010). These finding suggest that H-Ras plays a major role in the attenuation of eNOS in glyLDL-treated EC.

Increased H-Ras protein expression and translocation towards the cell membrane are ncessary for glyLDL-treated downregulation of eNOS protein in HUVEC. H-Ras may be considered as a therapeutic target for endothelium-dependent vasodilation under diabetic condition.

Vascular complication in diabetes was linked to ER stress in vascular cells. Previous studies inour lab have observed increased the accumulation of misfolded proteins as the elevation of thioflavin T intensity and increased the abundance of ER stress response mediators including GRP78/94, XBP-1 and CHOP in EC treated with glyLDL (CDA 2014 abstract) (Xie and Shen, 2014).

The present study demonstrated the involvement of ER stress in glyLDL-induced downregulation of eNOS in HUVEC by the fact that 4-PBA, an ER stress antagonist, prevented the glyLDL-induced attenuation of eNOS expression in HUVEC. This finding supports the hypothesis that ER stress is implicated in glyLDL-induced eNOS downregulation in vascular EC.

GlyLDL treatment (25-150 μg/ml for 24 h) used in the studies was within the normal physiological range as reported previously (Tames et al., 1992). GlyLDL preparations used were glycated in vitro (>30 % lysine residues were glycated). GlyLDL was observed to be pro-apoptotic after prolonged incubation. Treatment with 100 μg/ml glyLDL beyond 36 h reduced cell viability in HUVEC. However, no significant alteration in viability of cells was detected in HUVEC stimulated with glyLDL for 24 h or less, which was used throughout in our studies.

HUVECs are widely used as a model of cultured human EC in atherosclerosis studies. In addition to its feasibility, HUVEC is functionally similar to arterial EC than venous EC due to transport of oxygen and nutrient-rich blood to fetus in the umbilical vein (Ren et al., 1997), which makes it an appropriate cell line to use in our studies.

The findings from this section of the present studies indicate that glyLDL reduces eNOS mRNA, protein and activity in vascular EC. Transmembrane signaling mediators, RAGE and H-Ras regulate glyLDL-induced eNOS downregulation in cultured HUVEC, which provides an

insight on signaling pathway for diabetes-associated metabolic stress-induced cardiovascular complications and potenital therapeutic targets for the management and prevention of diabetic cardiovascular diseases.

5.2 Mitochondrial respiratory chain activity in HUVEC treated with glyLDL

Previous studies have identified decreased mitochondrial respiration in skeletal muscle of type 2 DM patients compared to age and BMI-matched control subjects. The lower mitochondrial respiration may be due to attenuated mitochondrial content (Rabol et al., 2009). Hyperglycemia increased ROS production, uncoupled electron transfer, increased superoxide and reduced ATP synthesis in diabetes (Green et al., 2004). The mitochondrial respiratory chain is a significant source of intracellular oxidative stress in pathological conditions. The imbalance between antioxidants and ROS production results in oxidative stress (Turrens, 2003). Hyperglycemia causes mitochondrial superoxide production in EC. In addition, mitochondrial derived reactive species activate NFκB, which further increases the VCAM-1 expression and other pro-inflammation mediators in early stage of atherosclerosis. Mitochondrial dysfunction in EC was involved both oxidative stress and reduced energy generation, which impaired vascular integrity (Ballinger, 2005).

Glyco-oxidized HDL induced apoptotic mechanisms in EC by increased mitochondrial apoptotic factors like Bad, Bax, and cytochrome *c* and activated caspase 9 and 3 (Matsunaga et al., 2001). Type 2 DM was characterized by age-related significant reduction of mitochondrial DNA, mitochondrial DNA gene transcription and translation, lower mitochondrial respiratory capacity and ATP production (Nile et al., 2014).

Mitochondrial dysfunction acts as the central contributor to β-cell failure in type 2 DM. ROS generated from mitochondria affects its structure and function. Moreover, ROS activated UCP-2, caused proton leak in the inner membrane, reduced ATP synthesis, oxidized mitochondrial cardiolipin, impaired membrane integrity and released cytochrome *c* leading to apoptosis (Ma et al., 2012). AGEs interaction with RAGE generates oxidative stress as well as

produces ROS in mitochondria, which induce mitochondrial damage and release cytochrome c from cells (Wang et al., 2015). This evidence suggests that diabetes-associated metabolic disorders potentially impair mitochondrial respiratory chain activity.

Impairment of respiratory chain activity in porcine aortic EC treated with glyLDL and extensively oxLDL have been prevously demonstrated in our lab (Roy Chowdhury et al., 2010; Sangle, Chowdhury, et al., 2010). We have shown in our present study that the glyLDL exposure significantly attenuated the mETC function in cultured HUVEC. GlyLDL significantly reduced the complex specific oxygen consumption rate of Complex I, II/III or IV in cultured HUVEC. These results support our hypothesis that diabetes-associated lipoprotein impairs mitochondrial respiratory chain function in cultured HUVEC. In addition, the study showed that glyLDL incubation significantly attenuated the ADP-induced oxygen uptake and respiratory control index (RCI) in cultured HUVEC. RCI is the ratio of state 3 (ADP excess) and state 4 (ADP limited) respiration (Brand and Nicholls, 2011).

NO interacts with superoxide to form peroxynitrite and also decrease the mETC and Complex I activity (Cassina and Radi, 1996). Complex I is the primary source of free radical production and the rate-limiting step in mETC. Inhibition of Complex I produces excess superoxide (Matsuzaki and Humphries, 2015). Decline in Complex I activity was observed in normal and high glucose conditions in mesangial cells exposed to AGEs (Coughlan et al., 2009). This evidence supports the present findings that glyLDL treatment significantly reduced oxygen consumption at Complex I.

Complex II is a vital enzyme complex in aerobic respiratory chain. The defects in Complex II are associated with mitochondrial diseases (Tomitsuka et al., 2003). High glucose exposure leads to ROS production and involvement of Complex II in EC (Nishikawa et al.,

2000), also generation of superoxide, mitochondrial attenuated ATP levels, partial inactivation of Complex III activity and hyperpolarization in normal rat renal proximal tubular cells. Mitochondrial superoxide generation is considered as a key early event in the development of mitochondrial dysfunction (Munusamy and MacMillan-Crow, 2009).

The present study also provide evidence that glyLDL impaired the activity of Complex II/III in EC as determined using succinate and antimycin-A sensitive oxygen consumption. EC exposed to laminar shear stress inactivated the mitochondrial Complexes I-IV, due to excessive generation of reactive nitrogen species and inhibiting electron flux at multiple ETC (Han et al., 2007). The present study also demonstrated impaired Complex IV activity in HUVEC exposed to glyLDL as determined from ascorbate/TMPD and KCN sensitive OCR. Since the decrease in the activity of oxygen consumption in any of mitochondrial respiration chain complex may cause excess ROS production (Shen, 2012), the impairment of the mitochondrial respiration chain complex enzyme activities in glyLDL-treated EC induce oxidative stress.

Mitochondrial dysfunction caused an increased ROS and decreased bioavailability of eNOS. EC with damaged mitochondria release high mobility group protein B1 (HMGB1), heat shock proteins, and S100 proteins that can induce inflammation by recruiting macrophages that encourage the atherosclerosis progression. eNOS has a significant part in the regulation of mitochondrial function and its biogenesis, and mitochondrial dysfunction modulate endothelial NO and superoxide production. Arterial blood flow is lowered in patients with systemic mitochondrial dysfunction (Lee and Shim, 2013), which may be consequence of lack of endothelium-dependant vasodilation.

Mitochondrial function is vital for the proper maintenance of cellular energy status (Matsuzaki and Humphries, 2015). Abnormal platelet membrane fluidity was observed in type 2

DM patients with macrovascular complications (Caimi et al., 1995). Higher ATP content and lower mitochondrial membrane potential was observed in platelets from type 2 DM (Guo et al., 2009). Uncoupled electron transfer and oxidative phosphorylation increased superoxide, and reduced ATP synthesis was found among diabetics (Mehta et al., 2006). Mitochondrial dysfunction was observed primarily due to reduced mitochondrial content and decreased function mitochondria in diabetes (Hojlund et al., 2008). However, one study evaluated oxygen consumption rate from freshly isolated PBMCs and further examined mitochondrial function in patients with diabetes mellitus. They have observed higher basal, maximal, and uncoupled oxygen consumption in the diabetic patients and increased mitochondrial ROS production (Hartman et al., 2014).

Our study have alos shown that exposure of glyLDL on HUVEC significantly reduced the bioenergetic profile, including basal respiration, maximal respiration, ATP-linked respiration, coupling efficiency and spare respiratory capacity. Addition of the mitochondrial uncoupler (FCCP) reduced the oxygen consumption rate in glyLDL treated cells than the control. The result of the present study suggests that a significant reduction of mitochondrial respiration in glyLDL-induced cells was due to dysfunction of mETC.

Mitochondrial dysfunction reduced energy generation and raised the mitochondrial stress and mitochondrial damage which are the risk factors for CVD (Ballinger, 2005). The results of the present study indicate that glyLDL simultaneously attenuates the energy generation (mitochondrial bioenergetics profile) and oxygen consumption (the complex-specific oxygen consumption) in HUVEC treated with glyLDL. These may increase mitochondrial and intracellular ROS production in HUVEC that has a vital role in the pathogenesis of diabetic macrovascular complications.

Increased mitochondrial superoxide, reduced mitochondrial mass, and mitochondrial hyperpolarization was detected in type 2 DM patients. The alterations in mitochondrial function were linked to impaired endothelium-dependent vasodilation. Mitochondrial ROS and mass is predictive for the *in-vivo* measurement of endothelial dysfunction. Excessive ROS can lead to endothelial inflammatory signaling activation, NF-κB, protein kinase-C and reduced NO bioavailability, Moreover increased mitochondrial superoxide was associated with the impaired endothelial function (Kizhakekuttu et al., 2012). Studies are required further to understand the relationship between the development of endothelial dysfunction and mitochondrial dysfunction.

Mitochondrial impairment and generation of ROS promotes endothelial damage in atherosclerotic vascular disease in diabetes. The results of the present study support our hypothesis that diabetes-associated lipoprotein impairs complex-specific oxygen consumption and energy production in mitochondria of HUVEC simultaneously. Estimation of mitochondrial function may be an early marker of the vascular endothelial function.

5.3 Platelet mitochondrial bioenergetics in healthy subjects

Previous studies have demonstrated the reduction in respiration rate, mitochondrial enzymatic activities and mitochondrial proteome expression in sensory neurons in diabetes. Impaired mitochondrial function in diabetic nerves in animals caused cellular energy depletion despite increased substrate availability (Roy Chowdhury et al., 2012).

Several evidences from the literature suggest the mitochondrial dysfunction in diabetes. The classical method for the assessment of mitochondrial respiratory chain activity or bioenergetics profile *in-vivo* requires tissue sampling via muscle biopsy, which requires a surgical procedure and may cause adverse effects. Peripheral blood platelets can be an appropriate alternative for detecting the mitochondrial bioenergetics profile since platelets have abundant functional mitochondria and primarily depends on oxidative metabolism (Garcia-Souza and Oliveira, 2014).

Previous studies have reported that, platelets from type 2 DM patients are observed with higher ATP content and lower membrane potential (Guo et al., 2009). Lower basal and maximal respiration was observed in platelets in diabetics. The assessment of metabolic function of blood cells for diagnosis and treatment is an important area of translational research (Kramer et al., 2014). The measurement of cellular bioenergetics in platelets may serve as index for mitochondrial function in several pathologies.

Platelets are sensitive markers of mitochondrial dysfunction and have detectable oxidative phosphorylation that can be studied using polarographic measurements. They are commonly used in bioenergetics studies in translational research. Sensitive assay protocols for determining cellular bioenergetics in platelets and leucocytes have been developed and characterized (Chacko et al., 2013; Kramer et al., 2014). Reduced ATP and mitochondrial

function are observed in insulin-resistant off-springs with familial type 2 DM (Petersen et al., 2004). Intrinsic mitochondrial dysfunction in the skeletal muscle biopsy of the type 2 DM patients were detected and interestingly showed tendency of mitochondrial dysfunction in the first degree relatives which were not significant when compared to the control subjects (Phielix et al., 2008). This study supports our findings, that family history has an impact on the mitochondrial function in healthy subjects. The bioenergetics profile was alone assessed, rather than any complex-specific studies in platelets due to the fact that, platelets function at near maximal energetic capacity under basal conditions, which is not the appropriate to measure the defects in Complexes I–IV in platelets as the reserve capacity is too small (Chacko et al., 2013).

Previous studies from different groups have investigated the mitochondrial bioenergetics or oxygen consumption in platelets of diabetic patients using Oxygraphy or Seahorse plate reader (Avila et al., 2012; Chacko et al., 2013; Phielix et al., 2008; Rabol et al., 2009). Study by Avila *et.al,* have identified that platelets isolated from diabetic patients have lower mitochondrial function compared to healthy subjects using the similar Oxygraph-2k (Avila et al., 2012). Phielix *et.al,* have compared the platelet mitochondrial bioenergetics in healthy subjects with and without first-degree family history of diabetes and detected no significant difference (Phielix et al., 2008). Our group has presently established the method for the assessment of platelet mitochondrial bioenergetics in 48 healthy subjects. We did not found gender; age or body mass index had a significant impact on platelet mitochondrial bioenergetics. Among healthy subjects with first-degree family history of diabetes but not heart disease had a significant decrease in mitochondrial bioenergetics profile compared to those without family history of diabetes or heart disease.

Measurement of oxygen consumption rate in the presence of uncoupler, (FCCP) determined the mETC (maximal respiration). The present study revealed significant attenuation of maximal respiration in platelets from healthy donors with family history of diabetes compared to that of healthy donors without any family history of chronic metabolic diseases. The family history of diabetes significantly reduced the basal respiration and ATP linked respiration, however, increased non-mitochondrial respiration was observed in healthy donors with family history of diabetes. The results from these bioenergetics profiles revealed a series of defects and alterations in platelet mitochondrial function in the platelets of healthy donors with a first-degree family history of diabetes, which may reflect the early abnormalities in mitochondrial respiration activities in human blood cells of healthy subjects with genetic defect which favors in the development of diabetes

Platelets serve as an excellent marker for understanding the human mitochondrial diseases due to satisfactory non-invasive, safe and, readily available source to investigate mitochondrial enzymatic activity (Sangiorgi et al., 1994). The classical method of muscle biopsy is quite invasive with higher risk for bleeding or infection than regular blood withdrawal. Alternative approaches to measuring the mitochondrial function using blood cells including platelets, have several advantages over the classical biopsy method (Garcia-Souza and Oliveira, 2014). Oxygen consumption was evaluated in PBMC from diabetic patients and control which observed contrary reports suggesting increased basal, maximal and uncoupled oxygen consumption in diabetic patients (Hartman et al., 2014). The mechanism for the difference in mitochondrial activity in platelets and PBMC in diabetic patients requires further investigation.

The limitations of the present clinical study could be the modest sample size, imbalanced gender ratio and self-reported medical history of donors. Further studies are needed to find out

the mechanisms and supporting evidence involved in the familial diabetes and early mitochondrial dysfunction in platelets. The measurement of oxygen consumption is necessary to be performed immediately after the platelet isolation as platelet activation, and aggregation is a common issue.

The relative disadvantages of Oxygraph over Seahorse plate reader are; the titrations and sequential injections of mitochondrial uncoupler, substrates and inhibitors are performed manually using separate micro-syringes and only two chambers are present in Oxygraph-2k which limits the experimentation of multiple samples simultaneously. The advantages of this method are it can be adopted in the clinics for the assessment of mitochondrial function from an acceptable volume of the blood sample (20-30 ml). The operational cost of Oxygraphy is affordable than Seahorse plate reader, which requires typical plates and reader for the detection and analysis.

Mitochondrial damage results in reduced energy generation and increased mitochondrial oxidative stress (Ballinger, 2005). The results from the mitochondrial bioenergetics studies in healthy human platelets suggest that first degree family history of diabetes has a significant impact on the platelet mitochondrial function in healthy subjects. Platelet mitochondrial dysfunction may reflect impaired mitochondrial activity in other types of cells in the body of diabetic patients. The findings may help to develop feasible and sensitive methods for non-surgical detection of mitochondrial activity in patients or people with risk for diabetes or other chronic diseases.

Chapter 6

Conclusion

1. The present study for the first time demonstrated an inhibitory effect of glyLDL on eNOS and NO production in cultured HUVEC. The RAGE/H-Ras pathway is implicated as the upstream signaling events in the glyLDL-induced eNOS downregulation in cultured EC.
2. Moreover, the impairment of mitochondrial complex-specific oxygen consumption and mitochondrial bioenergetics were detected in EC exposed to glyLDL.
3. In addition, we have demonstrated for the first time that, a significant impairment of mitochondrial bioenergetics in the platelets of healthy individuals with a first-degree family history of diabetes compared to that of healthy individuals without first degree family history of diabetes or heart disease.

Chapter 7

Reference List

Akhter, F., Khan, M. S., Shahab, U., Moinuddin, & S., A. (2013). Bio-physical characterization of ribose induced glycation: A mechanistic study on DNA perturbations. *Int J Biol Macromol, 58*, 206-210.

Alp, N. J., McAteer, M. A., Khoo, J., Choudhury, R. P., & Channon, K. M. (2004). Increased endothelial tetrahydrobiopterin synthesis by targeted transgenic GTP-cyclohydrolase I overexpression reduces endothelial dysfunction and atherosclerosis in ApoE-knockout mice. *Arterioscler Thromb Vasc Biol, 24*(3), 445-450.

Artwohl, M., Graier, W. F., Roden, M., Bischof, M., Freudenthaler, A., Waldha, W., & Baumgartner-Parzer, S. M. (2003). Diabetic LDL Triggers Apoptosis in Vascular Endothelial Cells. *Diabetes, 52*, 1240-1247.

Atamna, H., Liu, J., & Ames, B. N. (2001). Heme deficiency selectively interrupts assembly of mitochondrial complex IV in human fibroblasts: revelance to aging. *J Biol Chem, 276*(51), 48410-48416.

Avila, C., Huang, R. J., Stevens, M. V., Aponte, A. M., Tripodi, D., Kim, K. Y., & Sack, M. N. (2012). Platelet mitochondrial dysfunction is evident in type 2 diabetes in association with modifications of mitochondrial anti-oxidant stress proteins. *Exp Clin Endocrinol Diabetes, 120*(4), 248-251.

Bakker, W., Eringa, E. C., Sipkema, P., & van Hinsbergh, V. W. (2009). Endothelial dysfunction and diabetes: roles of hyperglycemia, impaired insulin signaling and obesity. *Cell Tissue Res, 335*(1), 165-189.

Ballinger, S. W. (2005). Mitochondrial dysfunction in cardiovascular disease. *Free Radic Biol Med, 38*(10), 1278-1295.

Ballinger, S. W., Patterson, C., Yan, C. N., Doan, R., Burow, D. L., Young, C. G., . . . Runge, M. S. (2000). Hydrogen peroxide-and peroxynitrite-induced mitochondrial DNA damage and dysfunction in vascular endothelial and smooth muscle cells. *Circulation Research, 86*(9), 960-966.

Banerjee, M., & Vats, P. (2013). Reactive metabolites and antioxidant gene polymorphisms in Type 2 diabetes mellitus. *Redox Biol, 2C*, 170-177.

Basha, B., Samuel, S. M., ;, Triggle, C. R., ;, & Ding, H. (2012). Endothelial dysfunction in diabetes mellitus: possible involvement of endoplasmic reticulum stress? *Exp Diabetes Res, 2012*, 481840.

Basso, A. D., Mirza, A., Liu, G., Long, B. J., Bishop, W. R., & Kirschmeier, P. (2005). The farnesyl transferase inhibitor (FTI) SCH66336 (lonafarnib) inhibits Rheb farnesylation and mTOR signaling. Role in FTI enhancement of taxane and tamoxifen anti-tumor activity. *J. Biol. Chem, 280*(35), 31101-31108.

Beckman, J. A., Creager, M. A., & Libby, P. (2002). Diabetes and Atherosclerosis Epidemiology, Pathophysiology, and Management. *JAMA, 287*, 2570-2581.

Bierman, E. L. (1992). George Lyman Duff Memorial Lecture-Atherogenesis in Diabetes. *Arterioscler Thromb Vasc Biol, 12*(6), 647-656.

Brand, M. D., & Nicholls, D. G. (2011). Assessing mitochondrial dysfunction in cells. *Biochemical Journal, 435*(2), 297-312.

Caimi, G., Presti, R. L., Montana, M., Canino, B., Ventimiglia, G., Romano, A., ;, . . . Sarno, A. (1995). Membrane fluidity, membrane lipid pattern, and cytosolic ca2+ content in platelets from a group of type 2 diabetic patients with macrovascular complications. *Diabetes Care, 18*(1), 60-64.

Cassina, A., & Radi, R. (1996). Differential inhibitory action of nitric oxide and peroxynitrite on mitochondrial electron transport. *Archives of Biochemistry and Biophysics, 328*(2), 309-316.

CDCP. (2011). National diabetes fact sheet: national estimates and general information on diabetes and prediabetes in the United States,. In D. o. H. a. H. Services (Ed.), *Centers for Disease Control and Prevention* (pp. 1-12). Atlanta, GA: U.S.

Chacko, B. K., Kramer, P. A., Ravi, S., Johnson, M. S., Hardy, R. W., Ballinger, S. W., & Darley-Usmar, V. M. (2013). Methods for defining distinct bioenergetic profiles in platelets, lymphocytes, monocytes, and neutrophils, and the oxidative burst from human blood. *Laboratory Investigation, 93*(6), 690-700.

Chen, Q., Dong, L., Wang, L., Kang, L., & Xu, B. (2009). Advanced glycation end products impair function of late endothelial progenitor cells through effects on protein kinase Akt and cyclooxygenase-2. *Biochem Biophys Res Commun, 381*(2), 192-197.

Chen, R., Peng, X., Du, W., Wu, Y., Huang, B., Xue, L., . . . Jiang, Q. (2015). Curcumin attenuates cardiomyocyte hypertrophy induced by high glucose and insulin via the PPARgamma/Akt/NO signaling pathway. *Diabetes Res Clin Pract.*

Chikani, G., Zhu, W., & Smart, E. J. (2004). Lipids: potential regulators of nitric oxide generation. *Am J Physiol Endocrinol Metab, 287*, E386-E389.

Cipollone, F., Iezzi, A., Fazia, M., Zucchelli, M., Pini, B., Cuccurullo, C., . . . Mezzetti, A. (2003). The receptor RAGE as a progression factor amplifying arachidonate-dependent inflammatory and proteolytic response in human atherosclerotic plaques: role of glycemic control. *Circulation, 108*(9), 1070-1077.

Collison, K. S., Parhar, R. S., Saleh, S. S., Meyer, B. F., Kwaasi, A. A., Hammami, M. M., . . . Al-Mohanna, F. A. (2002). RAGE-mediated neutrophil dysfunction is evoked by advanced glycation end products (AGEs). *J Leukoc Biol, 71*(3), 433-444.

Coughlan, M. T., Thorburn, D. R., Penfold, S. A., Laskowski, A., Harcourt, B. E., Sourris, K. C., . . . Forbes, J. M. (2009). RAGE-induced cytosolic ROS promote mitochondrial superoxide generation in diabetes. *J Am Soc Nephrol, 20*(4), 742-752.

de Nigris, F., Rienzo, M., Sessa, M., Infante, T., Cesario, E., Ignarro, L. J., . . . Napoli, C. (2012). Glycoxydation promotes vascular damage via MAPK-ERK/JNK pathways. *J Cell Physiol, 227*(11), 3639-3647.

Desler, C., Hansen, T. L., Frederiksen, J. B., Marcker, M. L., Singh, K. K., & Juel Rasmussen, L. (2012). Is there a link between mitochondrial reserve respiratory capacity and aging? *J Aging Res, 2012*, 192503.

Dong, Y., Wu, Y., Wu, M., Wang, S., Zhang, J., Xie, Z., . . . Zou, M. (2009). Activation of protease calpain by oxidized and glycated LDL increases the degradation of endothelial nitric oxide synthase. *J Cell Mol Med, 13*(9A), 2899-2910.

Duell, P. B., Oram, J. F., & Bierman, E. L. (1990). Nonenzymatic glycosylation of HDL resulting in inhibition of high-affinity binding to cultured human fibroblasts. *Diabetes, 39*(10), 1257-1263.

El-Remessy, A. B., Tawfik, H. E., Matragoon, S., Pillai, B., Caldwell, R. B., & Caldwell, R. W. (2010). Peroxynitrite mediates diabetes-induced endothelial dysfunction: possible role of Rho kinase activation. *Exp Diabetes Res, 2010*, 1-9.

Fonseca, S. G., Burcin, M., Gromada, J., & Urano, F. (2009). Endoplasmic reticulum stress in beta-cells and development of diabetes. *Curr Opin Pharmacol, 9*(6), 763-770.

Forstermann, U., & Munzel, T. (2006). Endothelial nitric oxide synthase in vascular disease: from marvel to menace. *Circulation, 113*(13), 1708-1714.

Fu.;, D., Wu.;, M., Zhang.;, J., Du.;, M., Yang.;, S., Hammad.;, S. M., . . . Lyons.;, T. J. (2012). Mechanisms of modified LDL-induced pericyte loss and retinal injury in diabetic retinopathy. *Diabetologia, 55*, 3128-3140.

Galle, J., Schneider, R., Winner, B., Lehmann-Bodem, C., Schinzel, R., Munch, G., . . . Wanner, C. (1998). Glyc-oxidized LDL impair endothelial function more potently than oxidized LDL: role of enhanced oxidative stress. *Atherosclerosis, 138*(1), 65-77.

Garcia-Souza, L. F., & Oliveira, M. F. (2014). Mitochondria: biological roles in platelet physiology and pathology. *Int J Biochem Cell Biol, 50*, 156-160.

Genest, J., McPherson, R., Frohlich, J., Anderson, T., Campbell, N., Carpentier, A., . . . Ur, E. (2009). 2009 Canadian Cardiovascular Society/Canadian guidelines for the diagnosis and treatment of dyslipidemia and prevention of cardiovascular disease in the adult-2009 recommendations. *Can J Cardiol, 25*(10), 567-579.

Green, K., Brand, M. D., & Murphy, M. P. (2004). Prevention of mitochondrial oxidative damage as a therapeutic strategy in diabetes. *Diabetes, 53 Suppl 1*, S110-118.

Guo, X., Wu, J., Du, J., Ran, J., & Xu, J. (2009). Platelets of type 2 diabetic patients are characterized by high ATP content and low mitochondrial membrane potential. *Platelets, 20*(8), 588-593.

Hadi, H. A., & Suwaidi, J. A. (2007). Endothelial dysfunction in diabetes mellitus. *Vasc Health Risk Manag, 3*(6), 853-876.

Hamuro, M., Polan, J., Natarajan, M., & Mohan, S. (2002). High glucose induced nuclear factor kappa B mediated inhibition of endothelial cell migration. *Atherosclerosis, 162*, 227-287.

Han, Z., Chen, Y. R., Jones, C. I., Meenakshisundaram, G., Zweier, J. L., & Alevriadou, B. R. (2007). Shear-induced reactive nitrogen species inhibit mitochondrial respiratory complex activities in cultured vascular endothelial cells. *Am J Physiol Cell Physiol, 292*(3), C1103-1112.

Hartman, M. L., Shirihai, O. S., Holbrook, M., Xu, G., Kocherla, M., Shah, A., . . . Vita, J. A. (2014). Relation of mitochondrial oxygen consumption in peripheral blood mononuclear cells to vascular function in type 2 diabetes mellitus. *Vascular Medicine, 19*(1), 67-74.

Heitzer, T., Krohn, K., Albers, S., & Meinertz, T. (2000). Tetrahydrobiopterin improves endothelium-dependent vasodilation by increasing nitric oxide activity in patients with Type II diabetes mellitus. *Diabetologia, 43*(11), 1435-1438.

Hodgkinson, C. P., Laxton, R. C., Patel, K., & Ye, S. (2008). Advanced glycation end-product of low density lipoprotein activates the toll-like 4 receptor pathway implications for diabetic atherosclerosis. *Arterioscler Thromb Vasc Biol, 28*(12), 2275-2281.

Hojlund, K., Mogensen, M., Sahlin, K., & Beck-Nielsen, H. (2008). Mitochondrial dysfunction in type 2 diabetes and obesity. *Endocrinol Metab Clin North Am, 37*(3), 713-731.

Hroudova, J., Fisar, Z., Kitzlerova, E., Zverova, M., & Raboch, J. (2013). Mitochondrial respiration in blood platelets of depressive patients. *Mitochondrion, 13*(6), 795-800.

Huang, P. L. (2009). eNOS, metabolic syndrome and cardiovascular disease. *Trends Endocrinol Metab, 20*(6), 295-302.

Ignarro, L. J. (1989). Endothelium-derived nitric oxide: actions and properties. *FASEB J, 3*(1), 31-36.

Jamaluddin, M. S., Liang, Z., Lu, J. M., Yao, Q., & Chen, C. (2014). Roles of cardiovascular risk factors in endothelial nitric oxide synthase regulation: an update. *Curr Pharm Des, 20*(22), 3563-3578.

Kemeny, S. F., Figueroa, D. S., Andrews, A. M., Barbee, K. A., & Clyne, A. M. (2011). Glycated collagen alters endothelial cell actin alignment and nitric oxide release in response to fluid shear stress. *J Biomech, 44*(10), 1927-1935.

Kizhakekuttu, T. J., Wang, J., Dharmashankar, K., Ying, R., Gutterman, D. D., Vita, J. A., & Widlansky, M. E. (2012). Adverse alterations in mitochondrial function contribute to type 2 diabetes mellitus-related endothelial dysfunction in humans. *Arterioscler Thromb Vasc Biol, 32*(10), 2531-2539.

Kowluru, R. A., Kowluru, A., Chakrabarti, S., & Khan, Z. (2004). Potential contributory role of H-Ras, a small G-protein, in the development of retinopathy in diabetic rats. *Diabetes, 53*(3), 775-783.

Kramer, P. A., Ravi, S., Chacko, B., Johnson, M. S., & Darley-Usmar, V. M. (2014). A review of the mitochondrial and glycolytic metabolism in human platelets and leukocytes: implications for their use as bioenergetic biomarkers. *Redox Biol, 2*, 206-210.

Kumar, A., Kumar, S., Vikram, A., Hoffman, T. A., Naqvi, A., Lewarchik, C. M., . . . Irani, K. (2013). Histone and DNA methylation-mediated epigenetic downregulation of endothelial Kruppel-like factor 2 by low-density lipoprotein cholesterol. *Arterioscler Thromb Vasc Biol, 33*(8), 1936-1942.

Lee, H. K., & Shim, E. B. (2013). Extension of the mitochondria dysfunction hypothesis of metabolic syndrome to atherosclerosis with emphasis on the endocrine-disrupting chemicals and biophysical laws. *J Diabetes Investig, 4*(1), 19-33.

Leem, J., & Koh, E. H. (2012). Interaction between mitochondria and the endoplasmic reticulum: implications for the pathogenesis of type 2 diabetes mellitus. *Exp Diabetes Res, 2012*,1-8.

Li, H., Horke, S., & Forstermann, U. (2014). Vascular oxidative stress, nitric oxide and atherosclerosis. *Atherosclerosis, 237*(1), 208-219.

Liao, J. K., Shin, W. S., Lee, W. Y., & L.;, C. S. (1995). Oxidized Low density lipoprotein decreases the expression of endothelial nitric oxide synthase *J Biol Chem, 270*(1), 319-324.

Liu, L., Liu, J., Huang, Z., Yu, X., Zhang, X., Dou, D., & Huang, Y. (2015). Berberine improves endothelial function by inhibiting endoplasmic reticulum stress in the carotid arteries of spontaneously hypertensive rats. *Biochem Biophys Res Commun, 458*(4), 796-801.

Liu, Y., Fiskum, G., & Schubert, D. (2002). Generation of reactive oxygen species by the mitochondrial electron transport chain. *J Neurochem, 80*(5), 780-787.

Luciano, C., Pasini, A. F., Garbin, U., Davoli, A., Tosetti, M. L., Campagnola, M., . . . Sawamura, T. (2000). Oxidized Low Density Lipoprotein (Ox-LDL) Binding To Ox-LDL Receptor-1 In Endothelial Cells Induces The Activation Of Nf-B Through An Increased Production Of Intracellular Reactive Oxygen Species. *J Biol Chem, 275*(17), 12633-12638.

Lyons, T. J. (1993). Glycation and Oxidation: A Role in the Pathogenesis of Atherosclerosis. *Am J Cardiol, 71*, 26B-31Bs.

Ma, Z. A., Zhao, Z., & Turk, J. (2012). Mitochondrial dysfunction and beta-cell failure in type 2 diabetes mellitus. *Exp Diabetes Res, 2012*, 1-11.

Madamanchi, N. R., & Runge, M. S. (2007). Mitochondrial dysfunction in atherosclerosis. *Circ Res, 100*(4), 460-473.

Madamanchi, N. R., Vendrov, A., & Runge, M. S. (2005). Oxidative stress and vascular disease. *Arterioscler Thromb Vasc Biol, 25*(1), 29-38.

Martínez-Fernández, L., Pons, Z., Margalef, M., Arola-Arnal, A., & Muguerza, B. (2014). Regulation of vascular endothelial genes by dietary flavonoids: structure-expression relationship studies and the role of the transcription factor KLF-2. *J Nutr Biochem, 26*(3), 277-284.

Matsunaga, T., Iguchi, K., Nakajima, T., Koyama, I., Miyazaki, T., Inoue, I., . . . Komoda, T. (2001). Glycated high-density lipoprotein induces apoptosis of endothelial cells via a mitochondrial dysfunction. *Biochem Biophys Res Commun, 287*, 714-720.

Matsuzaki, S., & Humphries, K. M. (2015). Selective inhibition of deactivated mitochondrial complex I by biguanides. *Biochemistry, 54*(11), 2011-2021.

Mehta, J. L., Rasouli, N., Sinha, A. K., & Molavi, B. (2006). Oxidative stress in diabetes: a mechanistic overview of its effects on atherogenesis and myocardial dysfunction. *Int J Biochem Cell Biol, 38*(5-6), 794-803.

Michel, T., & Vanhoutte, P. M. (2010). Cellular signaling and NO production. *Pflugers Arch, 459*(6), 807-816.

Morgan, E. P., Dean, R. T., & Davies, M. J. (2002). Inactivation of cellular enzymes by carbonyls and protein-bound glycation/glycoxidation products. *Arch Biochem Biophys, 403*, 259-269.

Munusamy, S., & MacMillan-Crow, L. A. (2009). Mitochondrial superoxide plays a crucial role in the development of mitochondrial dysfunction during high glucose exposure in rat renal proximal tubular cells. *Free Radic Biol Med, 46*(8), 1149-1157.

Napoli, C., Lerman, L. O., de Nigris, F., Loscalzo, J., & Ignarro, L. J. (2002). Glycoxidized low-density lipoprotein downregulates endothelial nitric oxide synthase in human coronary cells. *J Am Coll Cardiol, 40*(2), 1515-1522.

Neeper, M., Schmidt, A. M., Brett, J., Yan, S. D., Wang, F., Pan, Y. C., . . . Shaw, A. (1992). Cloning and expression of a cell surface receptor for advanced glycosylation end products of proteins. *J Biol Chem, 267*(21), 14998-15004.

Nguyen, K. H., Yao, X. H., Moulik, S., Mishra, S., & Nyomba, B. L. (2011). Human IGF binding protein-3 overexpression impairs glucose regulation in mice via an inhibition of insulin secretion. *Endocrinology, 152*(6), 2184-2196.

Nile, D. L., Brown, A. E., Kumaheri, M. A., Blair, H. R., Heggie, A., Miwa, S., . . . Walker, M. (2014). Age-Related Mitochondrial DNA Depletion and the Impact on Pancreatic Beta Cell Function. *PLoS One, 9*(12), 1-18.

Nishikawa, T., Edelstein, D., Du, X. L., Yamagishi, S., Matsumura, T., Kaneda, Y., . . . Brownlee, M. (2000). Normalizing mitochondrial superoxide production blocks three pathways of hyperglycaemic damage. *Nature, 404*(6779), 787-790.

Nivoit, P., Wiernsperger, N., Moulin, P., Lagarde, M., & Renaudin, C. (2003). Effect of glycated LDL on microvascular tone in mice: a comparative study with LDL modified in vitro or isolated from diabetic patients. *Diabetologia, 46*(11), 1550-1558.

Ohtsu, H., Suzuki, H., Nakashima, H., Dhobale, S., Frank, G. D., Motley, E. D., & Eguchi, S. (2006). Angiotensin II signal transduction through small GTP-binding proteins:

mechanism and significance in vascular smooth muscle cells. *Hypertension, 48*(4), 534-540.

Perry, C. G., Kane, D. A., Lanza, I. R., & Neufer, P. D. (2013). Methods for assessing mitochondrial function in diabetes. *Diabetes, 62*(4), 1041-1053.

Pesta, D., & Gnaiger, E. (2012). High-resolution respirometry: OXPHOS protocols for human cells and permeabilized fibers from small biopsies of human muscle. *Methods Mol Biol, 810*, 25-58.

Petersen, K. F., Dufour, S., Befroy, D., Garcia, R., & Shulman, G. I. (2004). Impaired mitochondrial activity in the insulin-resistant offspring of patients with type 2 diabetes. Petersen KF, Dufour S, Befroy D, Garcia R, Shulman GI. N Engl J Med 2004; 350: 664-71. *Vasc Med, 9*(3), 223-224.

Phielix, E., Schrauwen-Hinderling, V. B., Mensink, M., Lenaers, E., Meex, R., Hoeks, J., . . . Schrauwen, P. (2008). Lower intrinsic ADP-stimulated mitochondrial respiration underlies in vivo mitochondrial dysfunction in muscle of male type 2 diabetic patients. *Diabetes, 57*(11), 2943-2949.

Posch, K., Simecek, S., Wascher, T. C., Jürgens, G., Baumgartner-Parzer, S., Kostner, G. M., & Graier, W. F. (1999). Glycated Low-Density Lipoprotein Attenuates Shear Stress–Induced Nitric Oxide Synthesis by Inhibition of Shear Stress–Activated L- Arginine Uptake in Endothelial Cells. *Diabetes, 48*, 1331-1337.

Puddu, G. M., Cravero, E., Arnone, G., Muscari, A., & Puddu, P. (2005). Molecular aspects of atherogenesis: new insights and unsolved questions. *J Biomed Sci, 12*(6), 839-853.

Quyyumi, A. A. (1998). Endothelial function in health and disease: New insights into the genesis of cardiovascular disease. *Am J Med, 105 A*, 32S-39S.

Rabbani, N., Chittari, M. V., Bodmer, C. W., Zehnder, D., Ceriello, A., & Thornalley, P. J. (2010). Increased glycation and oxidative damage to apolipoprotein B100 of LDL cholesterol in patients with type 2 diabetes and effect of metformin. *Diabetes, 59*(4), 1038-1045.

Rabol, R., Hojberg, P. M., Almdal, T., Boushel, R., Haugaard, S. B., Madsbad, S., & Dela, F. (2009). Effect of hyperglycemia on mitochondrial respiration in type 2 diabetes. *J Clin Endocrinol Metab, 94*(4), 1372-1378.

Rafikov, R., Kumar, S., Aggarwal, S., Pardo, D., Fonseca, F. V., Ransom, J., . . . Black, S. M. (2014). Protein engineering to develop a redox insensitive endothelial nitric oxide synthase. *Redox Biol, 2C*, 156-164.

Ramasamy, R., Vannucci, S. J., Yan, S. S., Herold, K., Yan, S. F., & Schmidt, A. M. (2005). Advanced glycation end products and RAGE: a common thread in aging, diabetes, neurodegeneration, and inflammation. *Glycobiology, 15*(7), 16R-28R.

Ren, S., Lee, H., Hu, L., Lu, L., & Shen, G. X. (2002). Impact of diabetes-associated lipoproteins on generation of fibrinolytic regulators from vascular endothelial cells. *J Clin Endocrinol Metab, 87*(1), 286-291.

Ren, S., Man, R. Y. K., Angel, A., & Shen, G. X. (1997). Oxidative modification enhances lipoprotein(a)-induced overproduction of plasminogen activator inhibitor-1 in cultured vascular endothelial cells. *Atherosclerosis, 128*, 1-10.

Ren, S., & Shen, G. X. (2000). Impact of Antioxidants and HDL on Glycated LDL-Induced Generation of Fibrinolytic Regulators From Vascular Endothelial Cells. *Arterioscler Thromb Vasc Biol, 20*(6), 1688-1693.

Rogers, S. C., Zhang, X., Azhar, G., Luo, S., & Wei, J. Y. (2013). Exposure to high or low glucose levels accelerates the appearance of markers of endothelial cell senescence and induces dysregulation of nitric oxide synthase. *J Gerontol A Biol Sci Med Sci, 68*(12), 1469-1481.

Rolo, A.P., & Palmeira, C. M. (2006). Diabetes and mitochondrial function: role of hyperglycemia and oxidative stress. *Toxicol Appl Pharmacol, 212*(2), 167-178.

Roy Chowdhury, S., K.; , Smith, D. R., Saleh, A., Schapansky, J., Marquez, A., Gomes, S., . . . Fernyhough, P. (2012). Impaired adenosine monophosphate-activated protein kinase signalling in dorsal root ganglia neurons is linked to mitochondrial dysfunction and peripheral neuropathy in diabetes. *Brain, 135*(Pt 6), 1751-1766.

Roy Chowdhury, S. K., Sangle, G. V., Xie, X., Stelmack, G. L., Halayko, A. J., & Shen, G. X. (2010). Effects of extensively oxidized low-density lipoprotein on mitochondrial function and reactive oxygen species in porcine aortic endothelial cells. *Am J Physiol Endocrinol Metab, 298*(1), E89-98.

Ruiz-Velasco, N., Dominguez, A., & Vega, M. A. (2004). Statins upregulate CD36 expression in human monocytes, an effect strengthened when combined with PPAR-gamma ligands Putative contribution of Rho GTPases in statin-induced CD36 expression. *Biochem Pharmacol, 67*(2), 303-313.

Saluja, R., Jyoti, A., Chatterjee, M., Habib, S., Verma, A., Mitra, K., . . . Dikshit, M. (2011). Molecular and biochemical characterization of nitric oxide synthase isoforms and their intracellular distribution in human peripheral blood mononuclear cells. *Biochim Biophys Acta, 1813*(10), 1700-1707.

Sangiorgi, S., Mochi, M., Riva, R., Cortelli, P., Monari, L., Pierangeli, G., & Montagna, P. (1994). Abnormal platelet mitochondrial function in patients affected by migraine with and without aura. *Cephalalgia, 14*(1), 21-23.

Sangle, G. V., Chowdhury, S. K., Xie, X., Stelmack, G. L., Halayko, A. J., & Shen, G. X. (2010). Impairment of mitochondrial respiratory chain activity in aortic endothelial cells induced by glycated low-density lipoprotein. *Free Radic Biol Med, 48*(6), 781-790.

Sangle, G. V., Zhao, R., Mizuno, T. M., & Shen, G. X. (2010). Involvement of RAGE, NADPH oxidase, and Ras/Raf-1 pathway in glycated LDL-induced expression of heat shock factor-1 and plasminogen activator inhibitor-1 in vascular endothelial cells. *Endocrinology, 151*(9), 4455-4466.

Schalkwijk, C. G., & Stehouwer, C. D. A. (2005). Vascular complications in diabetes mellitus: the role of endothelial dysfunction. *Clinical Science, 109*, 143-159.

Schmidt, A. M., & Stern, D. (2000). Atherosclerosis and diabetes: the RAGE connection. *Curr Atheroscler Rep, 2*(5), 430-436.

Shen, C., Li, Q., Zhang, Y. C., Ma, G., Feng, Y., Zhu, Q., . . . Liu, N. (2010). Advanced glycation endproducts increase EPC apoptosis and decrease nitric oxide release via MAPK pathways. *Biomed Pharmacother, 64*(1), 35-43.

Shen, G. X. (2003). Dyslipoproteinemia And Fibrinolysis. In M. N. GN Pieree, P. Zahradka, and NS. Dhalla (Ed.), *Atherosclerosis, Hypertension And Diabetes.* (pp. 289-299). Boston: Kluwer Academic Publishers.

Shen, G. X. (2012). Mitochondrial dysfunction, oxidative stress and diabetic cardiovascular disorders. *Cardiovasc Hematol Disord Drug Targets, 12*(2), 106-112.

Sima, A., & Stancu, C. (2002). Modified lipoproteins accumulate in human coronary atheroma. *J Cell Mol Med, 6*(1), 110-111.

Sitia, S., Tomasoni, L., Atzeni, F., Ambrosio, G., Cordiano, C., Catapano, A., . . . Turiel, M. (2010). From endothelial dysfunction to atherosclerosis. *Autoimmun Rev, 9*(12), 830-834.

Sjovall, F., Ehinger, J. K., Marelsson, S. E., Morota, S., Frostner, E. A., Uchino, H., . . . Elmer, E. (2013). Mitochondrial respiration in human viable platelets--methodology and influence of gender, age and storage. *Mitochondrion, 13*(1), 7-14.

Sjovall, F., Morota, S., Hansson, M. J., Friberg, H., Gnaiger, E., & Elmer, E. (2010). Temporal increase of platelet mitochondrial respiration is negatively associated with clinical outcome in patients with sepsis. *Crit Care, 14*(6), R214.

Soran, H., & Durrington, P. N. (2011). Susceptibility of LDL and its subfractions to glycation. *Curr Opin Lipidol, 22*(4), 254-261.

Srinivasan, S., Hatley, M. E., Bolick, D. T., Palmer, L. A., Edelstein, D., Brownlee, M., & Hedrick, C. C. (2004). Hyperglycaemia-induced superoxide production decreases eNOS expression via AP-1 activation in aortic endothelial cells. *Diabetologia, 47*(10), 1727-1734.

Steinberg, D. (1987). Lipoproteins And The Pathogenesis Of Atherosclerosis. *Circulation, 76*(3), 508-514.

Stephens, E., Thureen, P. J., Goalstone, M. L., Anderson, M. S., Leitner, J. W., Hay, W. W. J., & Draznin, B. (2001). Fetal hyperinsulinemia increases farnesylation of p21 Ras in fetal tissues. *Am J Physiol Endocrinol Metab, 281*(2), E217-223.

Stern, D., Yan, S. D., Yan, S. F., & Schmidt, A. M. (2002). Receptor for advanced glycation endproducts: a multiligand receptor magnifying cell stress in diverse pathologic settings. *Adv Drug Deliv Rev, 54*(12), 1615-1625.

Stocker, R., & Keaney, J. F. (2004). Role of Oxidative Modifications in Atherosclerosis. *Physiological Reviews, 84*, 1381-1478.

Takai, Y., Sasaki, T., & Matozaki, T. (2001). Small GTP-binding proteins. *Physiol Rev, 81*(1), 153-208.

Tames, F. J., Mackness, M. I., Arrol, S., Laing, I., & Durrington, P. N. (1992). Non-enzymatic glycation of apolipoprotein B in the sera of diabetic and non-diabetic subjects. *Atherosclerosis, 93*(3), 237-244.

Toma, L., Stancu, C. S., Sanda, G. M., & Sima, A. V. (2011). Anti-oxidant and anti-inflammatory mechanisms of amlodipine action to improve endothelial cell dysfunction induced by irreversibly glycated LDL. *Biochem Biophys Res Commun, 411*(1), 202-207.

Tomitsuka, E., Hirawake, H., Goto, Y., Taniwaki, M., Harada, S., & Kita, K. (2003). Direct evidence for two distinct forms of the flavoprotein subunit of human mitochondrial complex ii (succinate-ubiquinone reductase). *J. Biochem, 134*(2), 191-195.

Tozer, E. C., & Carew, T. E. (1997). Residence time of low-density lipoprotein in the normal and atherosclerotic rabbit aorta. *Circulation Research, 80*(2), 208-218.

Turrens, J. F. (2003). Mitochondrial formation of reactive oxygen species. *J Physiol, 552*(Pt 2), 335-344.

Wang, X., Yu, S., Wang, C. Y., Wang, Y., Liu, H. X., Cui, Y., & Zhang, L. D. (2015). Advanced glycation end products induce oxidative stress and mitochondrial dysfunction in SH-SY5Y cells. *In Vitro Cell Dev Biol-Anim, 51*(2), 204-209.

Warboys, C. M., Amini, N., de Luca, A., & Evans, P. C. (2011). The role of blood flow in determining the sites of atherosclerotic plaques *F1000 Med Rep* (Vol. 3, pp. 5).

Wautier, J. L., & Schmidt, A. M. (2004). Protein glycation: a firm link to endothelial cell dysfunction. *Circ Res, 95*(3), 233-238.

Wautier, M. P., Chappey, O., Corda, S., Stern, D. M., Schmidt, A. M., & Wautier, J. L. (2001). Activation of NADPH oxidase by AGE links oxidant stress to altered gene expression via RAGE. *Am J Physiol Endocrinol Metab, 280*, E685-E694.

White, J., Guerin, T., Swanson, H., Post, S., Zhu, H., Gong, M., . . . Smart, E. J. (2008). Diabetic HDL-associated myristic acid inhibits acetylcholine-induced nitric oxide generation by preventing the association of endothelial nitric oxide synthase with calmodulin. *Am J Physiol Cell Physiol, 294*(1), C295-305.

WHO. (2011). Cardiovascular diseases *Fact sheet N°317* (pp. 1-4). Geneva: WHO Media centre.

Wiley, J. C., Meabon, J. S., Frankowski, H., Smith, E. A., Schecterson, L. C., Bothwell, M., & Ladiges, W. C. (2010). Phenylbutyric acid rescues endoplasmic reticulum stress-induced suppression of APP proteolysis and prevents apoptosis in neuronal cells. *PLoS One, 5*(2), e9135.

Wu, K. K. (2002). Regulation of Endothelial Nitric Oxide Synthase Activity and Gene Expression. *Ann. N.Y. Acad. Sci., 962*, 122-130.

Xie, X., Chowdhury, S. R., Sangle, G. V., & Shen, G. X. (2010). Impact of diabetes-associated lipoproteins on oxygen consumption and mitochondrial enzymes in porcine aortic endothelial cells. *Acta Biochimica Polonica, 57*(4), 393-398.

Xie, X., & Shen, G. X. (2014). Impact of glycated low-density lipoprotein and anthocyanins on endoplasmic reticulum stress in vascular endothelial cells. *Can J Diabetes, 38*(5), S60.

Yetik-Anacak, G., & Catravas, J. D. (2006). Nitric oxide and the endothelium: history and impact on cardiovascular disease. *Vascul Pharmacol, 45*(5), 268-276.

Younis, N., Charlton-Menys, V., Sharma, R., Soran, H., & Durrington, P. N. (2009). Glycation of LDL in non-diabetic people: Small dense LDL is preferentially glycated both in vivo and in vitro. *Atherosclerosis, 202*(1), 162-168.

Zhang, F. L., & Casey, P. J. (1996). Protein prenylation: molecular mechanisms and functional consequences. *Annu Rev Biochem, 65*, 241-269.

Zhang, J., Ren, S., Sun, D., & Shen, G. X. (1998). Influence of Glycation on LDL-Induced Generation of Fibrinolytic Regulators in Vascular Endothelial Cells. *Arterioscler Thromb Vasc Biol, 18*(7), 1140-1148.

Zhao, R., Ma, X., Xie, X., & Shen, G. X. (2009). Involvement of NADPH oxidase in oxidized LDL-induced upregulation of heat shock factor-1 and plasminogen activator inhibitor-1 in vascular endothelial cells. *Am J Physiol Endocrinol Metab, 297*(1), E104-111.

Zhao, R., & Shen, G. X. (2005). Functional modulation of antioxidant enzymes in vascular endothelial cells by glycated LDL. *Atherosclerosis, 179*(2), 277-284.

Zhu, M., Wen, M., Sun, X., Chen, W., Chen, J., & Miao, C. (2015). Propofol protects against high glucose-induced endothelial apoptosis and dysfunction in human umbilical vein endothelial cells. *Anesth Analg, 120*(4), 781-789.

Zhu, Y., Liao, H., Wang, N., Ma, K. S., Verna, L. K., Shyy, J. Y., . . . Stemerman, M. B. (2001). LDL-activated p38 in endothelial cells is mediated by Ras. *Arterioscler Thromb Vasc Biol, 21*(7), 1159-1164.

Zimmermann, R., Panzenbock, U., Wintersperger, A., Levak-Frank, S., Graier, W., Glatter, O., Zechner, R. (2001). Lipoprotein lipase mediates the uptake of glycated LDL in fibroblasts, endothelial cells, and macrophages. *Diabetes, 50*(7), 1643-1653.